



Universiteit
Leiden
The Netherlands

Bioorthogonal Antigens

Pawlak, J.B.

Citation

Pawlak, J. B. (2017, November 14). *Bioorthogonal Antigens*. Retrieved from <https://hdl.handle.net/1887/55262>

Version: Not Applicable (or Unknown)

License: [Licence agreement concerning inclusion of doctoral thesis in the Institutional Repository of the University of Leiden](#)

Downloaded from: <https://hdl.handle.net/1887/55262>

Note: To cite this publication please use the final published version (if applicable).

Cover Page



Universiteit Leiden



The handle <http://hdl.handle.net/1887/55262> holds various files of this Leiden University dissertation.

Author: Pawlak, J.B.

Title: Bioorthogonal Antigens

Issue Date: 2017-11-14

Bioorthogonal Antigens

PROEFSCHRIFT

ter verkrijging van

de graad van Doctor aan de Universiteit Leiden,

op gezag van Rector Magnificus prof. mr. C. J. J. M. Stolker,

volgens besluit van het College voor Promoties

te verdedigen op dinsdag 14 november 2017

klokke 15:00 uur

door

Joanna Barbara Pawlak

Geboren te Olsztyn, Polen in 1983

Promotiecommissie

Promotor: Prof. dr. H. S. Overkleeft

Co-promotor: Dr. S.I. van Kasteren

Overige leden: Prof. dr. M.H.M. Noteborn (LU)

Prof. dr. J. Brouwer (LU)

Prof. dr. J.J. Neefjes (LUMC)

Prof. dr. H. L. Ploegh (Children's Hospital Boston and Harvard Medical School)

Dr. I. Berlin (LUMC)

Dr. M. van der Stelt (LU)

Printed by Ridderprint B.V.

All rights reserved. No part of this book may be reproduced in any manner or by any means without permission.

Dla Taty

"It always seems impossible until it's done."

- Nelson Mandela

Table of Contents

Chapter 1	5
General introduction	
Chapter 2	15
Tools for studying antigen processing and cross-presentation	
Chapter 3	31
The optimization of bioorthogonal epitope ligation within MHC-I complexes	
Chapter 4	59
Towards imaging of bioorthogonal antigens throughout antigen cross-presentation	
Chapter 5	77
Bioorthogonal deprotection on the dendritic cell surface allows chemical control of antigen cross-presentation	
Chapter 6	93
Summary and future prospects	
Streszczenie	101
List of Publications	104
Curriculum Vitae	105

1

General introduction

Published as part of: Joanna B. Pawlak and Sander I. van Kasteren. eLS. 2017, in press.

1.1 Introduction

The human immune system has developed to defend us from infection by a diverse array of pathogens, ranging from nanometer-sized viruses to metazoans many centimeters in length^[1]. To achieve such a feat – especially in the face of species capable of far more rapid evolution than ourselves – it has adapted a series of defense mechanisms that can match this evolutionary prowess pound-for-pound. This defense system can crudely be divided into two parts^[2]: an innate part, which recognizes and responds to evolutionary conserved molecular patterns for which evolution is very slow (as well as to other conserved signs of damage and danger); and an adaptive part, which has the ability to react to particular molecular patterns on specific pathogens and can tailor the response against them. It has also the intrinsic ability to continually adjust the immune response against the microorganisms even over the course of an infection. Strikingly, the adaptive immune system retains memory of previous infections and thus can prevent disease upon multiple exposures to a pathogen.

These two branches of the immune system are in intimate interplay: the detection of danger by innate receptors and cells helps shape the response formed by the adaptive immune system through information transfer resulting from activation of

receptors that recognize *pathogen and danger associated molecular patterns* (PAMPs and DAMPs)^[3]. This results in the release of signaling molecules that attract and activate the appropriate cell types for a given immune response. A second key information transfer event between the innate and adaptive immune system is the process by which phagocytic immune cells capture, process and present antigens and peptides from the pathogenic proteome to the body's diverse population of T cells^[4]. Recognition of these peptides by specific T cells results in their activation and not in the activation of T cells incapable of recognizing the pathogenic peptides^[5]. This leads to the T cell activating and adopting its role as orchestrator/executioner in the anti-pathogen response^[6].

In 1985, it was discovered that the unit of information were processed peptides^[7] presented on molecules called *major histocompatibility complexes* (MHC). Two types of MHC molecules were identified: MHC class I (MHC-I) and MHC class II (MHC-II)^[8]. The most important difference between these two classes is the source of antigenic peptides they present and the type of T cells they activate^[9]. The implication was that dendritic cells – the major cell type responsible for T cell activation^[10] – had to kill and degrade the pathogens in a controlled manner to produce peptides of sufficient length for MHC-loading and presentation.

Interestingly, the diversity of both MHCs themselves within the human population and peptide repertoires they can present is enormous^[11]. In humans, over 2000 different MHC-alleles are known^[12].

1.2 The source of MHC-I and MHC-II restricted peptides

MHC-I and –II complexes present peptides from different sources. MHC-I complexes, in general, present peptides derived from cytosolic self-proteins and MHC-II present peptides from material taken up by endo, macro, pino- and phagocytosis. Nearly all peptides capable of MHC-binding are part of proteins and proteolysis is therefore required to liberate them. This is a complex event. For example, over 17 proteases in the endo-lysosomal environment alone have been implicated in the liberation of peptides from protein antigens^[13]. These proteases themselves vary in specificity and activity in a particular cell – and even in an explicit vesicle as it matures – meaning that the precise nature of the repertoire of peptides that can be produced from a specific protein can be highly variable^[14]. The different antigen presentation routes will now be discussed in more detail.

1.3 MHC class I antigen presentation pathway

MHC-I molecules are expressed on the surface of all nucleated cells^[15] and display peptides derived from cytosolic proteins of self, tumor or viral origin for recognition by CD8⁺ cytotoxic T lymphocytes (CTLs)^[16]. The cytosolic proteins are degraded by the

proteasome and cytosolic proteases into peptides, which are then transported through the transporter associated with antigen processing (TAP) complex into the endoplasmic reticulum (ER)^[17]. Here they are further trimmed by ER aminopeptidases (ERAPs) to generate peptides consisting of 8-10 amino acids^[9b, 18]. To be presented at the cell surface of antigen presenting cells (APCs), produced peptides and MHC-I molecules have to be properly assembled in the ER. This assembly of the peptide with the two subunits of the MHC-I (pMHC-I) is coordinated by the peptide-loading complex (PLC) in the ER^[19]. The PLC is composed of a disulfide-linked dimer of tapasin and the thiol oxidoreductase ERp57, lectin chaperone calreticulin (CRT) and TAP transporter molecules^[8, 19a]. Tapasin is the principle protein in the PLC that facilitates exchange of low affinity for high affinity peptides ('peptide editing')^[20] and ensures

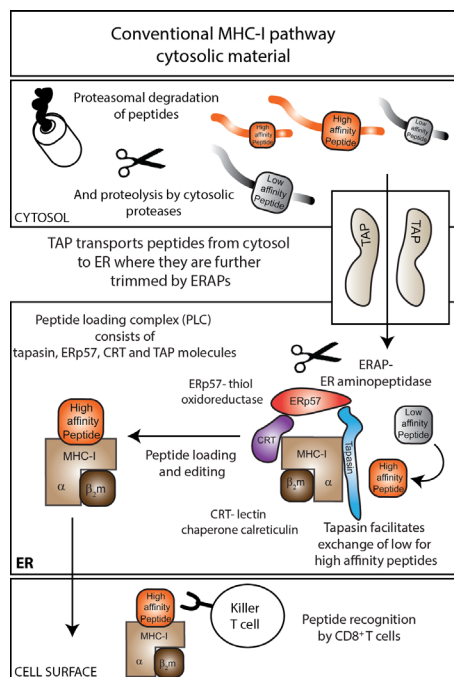


Figure 1. Schematic representation of antigen processing (peptide editing and loading), routing and presentation during MHC class I antigen presentation pathway.

that MHC-I molecules do not leave the ER unless they carry high affinity peptides^[21]. After editing, MHC-I molecules that contain optimal peptides are transported to the cell surface for presentation of their antigenic cargo to CD8⁺ T cells^[19b] (Figure 1). If an activated CD8⁺ T cell recognizes its cognate peptide presented by a cell, it will initiate the killing of the target cell. As self-reactive T cells have been eliminated in the thymus during development, this is a potent method for recognizing and eliminating cells that have become genetically altered such as tumor cells and virus-infected cells by virtue of these cells presenting non-self peptides (of viral origin; or having arisen from the expression of genetic mutations in the cancer cells).

To achieve broad binding and to protect the population against viral infections, the repertoire of self and foreign peptides that have the ability to bind to even a single class of MHC-I must be enormous^[22]. This is indeed the case resulting from a very promiscuous binding mode of the MHC to the peptide and a very high diversity in the haplotypes of the receptor. The peptide-binding region of the MHC-I consists of a beta-sheet 'floor' on which two alpha-helices define a closed peptide binding groove^[23], and most polymorphic positions line this binding groove^[24]. These positions define binding pockets (of which usually two dominate^[22]), lend certain MHC

molecules their specificity for anchor residues of antigenic peptide. The mouse MHC-I molecule H2-K^b, for example, binds peptides through a deep hydrophobic primary anchor pocket selective for aromatic residues at position 5 in the peptide binding sequence and a second hydrophobic pocket specific for alkyl side chains at position P8/9^[25] (Figure 2; primary anchor residues depicted in red). The peptide side chains of P4, P6, and P7 are T cell receptor binding determinants and contribute minimally to the binding to MHC-I and display the highest tolerance to amino acid variability^[26] (Figure 2).

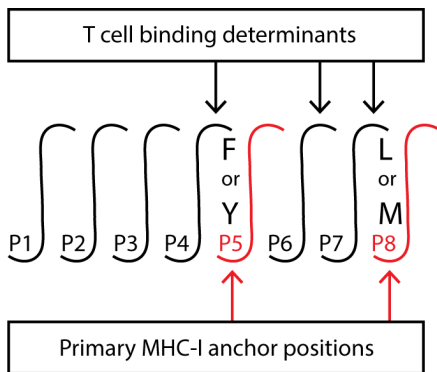


Figure 2. Certain positions are key for anchoring to MHC-I and others are key to T cell recognition. Two dominant H2-K^b anchor positions: phenylalanine (F) or tyrosine (Y) at position 5 (P5) and leucine (L) or methionine (M) at position 8 (P8). Whereas positions 4, 6 and 7 are T cell binding determinants.

The precise affinities of peptides for H2-K^b were studied in detail using a large peptide library randomized at each of the 8 positions^[27] and shown to correlate best with the size and hydrophobicity of individual side chains. For example, the primary anchor residue bound most strongly to phenylalanine and tyrosine, as this pocket shows extensive π -stacking capacity with these amino acids^[23].

1.4 MHC class II antigen presentation pathway

Unlike MHC class I, which is expressed on all nucleated cells, MHC class II (MHC-II) expression is restricted to professional antigen presenting cells including dendritic cells (DCs), macrophages and B cells. Like MHC-I complexes, these protein complexes also display peptide fragments of proteins but with the main difference being that the peptides displayed are not from the cytosolic pool, but from exogenous proteins taken up by the APC through phagocytosis. These peptides serve to activate CD4⁺ helper T lymphocytes, which in turn affect the function of cells displaying the given peptide-MHC-II complex. These cells can, for instance, assist in clearance of intracellular pathogens, induce tolerance, or unlock advanced functions in B cell development such as class switching and memory B cell development^[9a, 28].

Exogenous proteins from which MHC-II peptides are derived are taken up by the APC through endocytosis, phagocytosis or macropinocytosis^[29]. Once inside endosomal confines, vesicles mature to a special subclass of late endosomes to which MHC-IIs in complex with a protein called the invariant chain are delivered. The invariant chain

sits across the peptide binding groove of MHC-II to prevent inappropriate loading of peptides outside the endo-lysosomal vesicles. Once delivered to the late endo-/lysosomes, the invariant chain is degraded by a variety of endo-lysosomal proteases^[8, 9b], resulting in only a minimal peptide called the class II-associated invariant chain peptide (CLIP)^[30]. This CLIP-peptide has sufficiently low affinity for MHC-II and it can be exchanged for higher affinity peptides present in the endo-lysosome with the help of the accessory protein HLA-DM^[31].

MHC-II binds peptides in a different manner than MHC-I. In general, MHC-II molecules have four major anchor pockets, designated P1, P4, P6 and P9^[32]. The binding pockets are much shallower than the one of MHC-I, which results in broader tolerance of peptides they can bind. Moreover, they are also open-ended and have the capacity to bind larger peptides (10-30 amino acids in length)^[33], a feature that results in a presence of flanking residues of peptide's N- and C- termini and the appearance of 'nested' peptides: peptides with the same core binding motif, but with different N- and C-terminal extensions^[34].

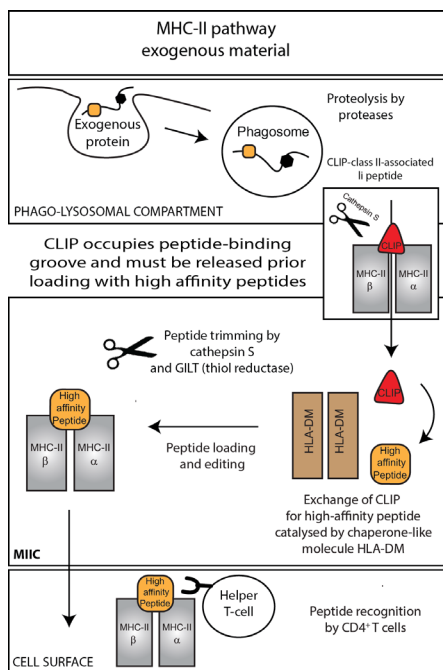


Figure 3. Schematic representation of antigen processing (peptide editing and loading), routing and presentation during MHC class II antigen presentation pathway.

Before this loading of peptides can take place, the exogenous material – whether from host cellular source, vaccine, or pathogen – has to be killed (if needed) and degraded so that peptides of the appropriate length can be produced. This is done by the same family of endolysosomal proteases that degrade the invariant chain, including the cysteine cathepsins^[35], asparagine endopeptidase^[30a], and aspartyl cathepsins. The exchange of CLIP for a high affinity peptide is catalyzed by the chaperone-like molecule called HLA-DM which fulfills the peptide editing role^[13] in this compartment. Once loaded with high affinity peptides, MHC-II complexes are transported to the cell surface for presentation to CD4⁺ helper T cells. Helper T cells typically do not kill infected cells themselves^[9a], but are rather pivotal in activation of other immune cells proficient at killing (Figure 3).

1.5 MHC class II to I cross-presentation pathway

There is also cross-talk between MHC-II and MHC-I pathways termed antigen cross-presentation^[36]. This pathway requires extracellular materials to be endocytosed by APCs (usually dendritic cells) via the phago-lysosomal system and to 'cross' into the pathway typically reserved for presentation of antigens derived from the cytosol^[18b, 37]. The reverse can also occur – the cytosolic proteins can be trafficked into the phago-lysosomal system via autophagy for subsequent processing and presentation by MHC-II molecules^[38].

Uptake and cross presentation of peptides by dendritic cells (DCs) expressing appropriate co-stimulatory molecules stimulates naïve CD8⁺ T cells to become efficient killers of tumors or infected cells^[39]. Antigen cross-presentation thus leverages clearance of cancers, pathogenic infections of cells other than DCs and also vaccinations with protein antigens that, analogous to tumor or infected cells, must be cross-presented to activate CTLs^[40].

Importantly, different cellular routes for cross-presented antigens have been proposed^[41]. However, molecular mechanisms that regulate intracellular trafficking during this process, and the rates at which they occur, are still poorly understood^[42]. As those molecular mechanisms for cross-presentation are the topic of the chemistry developed in this thesis, they will be discussed in more detail in chapter 2.

1.6 Aim and outline of this thesis

The research described in this thesis aims at the exploration and development of bioorthogonal chemistry to study aspects of cross-presentation. Specifically, the aim is to use unnatural amino acids in epitope peptides that are stable to the conditions found under physiological conditions and at the same time have a group that survives the cross-presentation pathway(s), has a minimal impact on cross-presentation, and at the same time can be used to detect the peptide even after proteolysis.

Chapter 2 provides a comprehensive overview of cross presentation mechanisms, as well as the available molecular tools to monitor antigen processing and cross-presentation. A few examples of strategies that are employed to study antigen uptake, intracellular trafficking and presentation during cross-presentation are described and their strengths and limitations are discussed.

Chapter 3 explores the use of bioorthogonal chemistry to quantify specific peptide–MHC-I complexes (pMHC-I) on cells. The work in this chapter reveals that modification of epitope peptides with bioorthogonal groups in surface accessible positions generates epitope peptides that are capable of binding MHC-I with wild-type-like affinities. Furthermore, these groups can be used in a Cu(I)-catalyzed

Huisgen cycloaddition reaction, to visualize them with fluorophores. The optimization, applications and limitations of this approach are discussed in this chapter. Finally, the preliminary efforts to apply stochastic optical resolution microscopy (STORM) to the imaging of peptides in MHC-complexes are described with the aim of developing a method that allows the on-surface visualization of individual peptides using this technique.

In **chapter 4** the research attempting the translation of the above methodology to the analysis of surface appearance of peptides after antigen uptake and cross-presentation is described. The first steps towards a technique that allows the on-surface visualization of peptides within MHC-I complexes after cross-presentation are described, as well as the pitfalls and limitations of such an approach.

Chapter 5 describes a different use of the bioorthogonal group, the azide. Instead of using it as a ligation handle, its application as a bioorthogonal protecting group is explored. Using Staudinger reduction chemistry, chemical control over T cell activation is obtained by allowing the switching of a non-T cell recognized variant of the antigen to the cognate form on the surface of a dendritic cell.

Chapter 6 provides a summary of this thesis and future implications, strategies and directions towards imaging the entire antigen cross-presentation process.

1.7 References

- [1] E. S. Trombetta, I. Mellman, *Annu Rev Immunol* **2005**, *23*, 975-1028.
- [2] E. Vivier, B. Malissen, *Nat Immunol* **2005**, *6*, 17-21.
- [3] aS.-Y. Seong, P. Matzinger, *Nat Rev Immunol* **2004**, *4*, 469-478; bC. Janeway, *Immunology today* **1989**, *10*, 283-286; cS. Akira, K. Takeda, *Nat Rev Immunol* **2004**, *4*, 499-511.
- [4] F. M. Cruz, J. D. Colbert, E. Merino, B. A. Kriegsmann, K. L. Rock, *Annu Rev Immunol* **2017**.
- [5] N. van Montfoort, E. van der Aa, A. M. Woltman, *Front Immunol* **2014**, *5*, 182.
- [6] A. Lanzavecchia, *Nature* **1998**, *393*, 413-414.
- [7] B. P. Babbitt, P. M. Allen, G. Matsueda, E. Haber, E. R. Unanue, *Nature* **1985**, *317*, 359-361.
- [8] J. S. Blum, P. A. Wearsch, P. Cresswell, *Annu Rev Immunol* **2013**, *31*, 443-473.
- [9] aJ. Neefjes, M. L. Jongsma, P. Paul, O. Bakke, *Nat Rev Immunol* **2011**, *11*, 823-836; bK. L. Rock, E. Reits, J. Neefjes, *Trends Immunol* **2016**.
- [10] R. M. Steinman, Z. A. Cohn, *Journal of Experimental Medicine* **1973**, *137*, 1142-1162.
- [11] P. Parham, C. E. Lomen, D. A. Lawlor, J. P. Ways, N. Holmes, H. L. Coppin, R. D. Salter, A. M. Wan, P. D. Ennis, *Proceedings of the National Academy of Sciences of the United States of America* **1988**, *85*, 4005-4009.
- [12] N. Blanchard, N. Shastri, *Curr Opin Immunol* **2008**, *20*, 82-88.
- [13] E. R. Unanue, V. Turk, J. Neefjes, *Annu Rev Immunol* **2016**, *34*, 265-297.
- [14] S. I. van Kasteren, H. S. Overkleeft, *Current opinion in chemical biology* **2014**, *23*, 8-15.
- [15] J. D. Comber, R. Philip, *Ther Adv Vaccines* **2014**, *2*, 77-89.
- [16] M. H. Andersen, D. Schrama, P. thor Straten, J. C. Becker, *Journal of Investigative Dermatology* **2006**, *126*, 32-41.
- [17] J. E. Grotzke, D. Sengupta, Q. Lu, P. Cresswell, *Curr Opin Immunol* **2017**, *46*, 89-96.
- [18] aS. I. van Kasteren, H. Overkleeft, H. Ovaa, J. Neefjes, *Curr Opin Immunol* **2014**, *26*, 21-31; bA. L. Ackerman, P. Cresswell, *Nat Immunol* **2004**, *5*, 678-684; cT. Serwold, F. Gonzalez, J. Kim, R. Jacob, N. Shastri, *Nature* **2002**, *419*, 480-483.
- [19] aP. Cresswell, N. Bangia, T. Dick, G. Diedrich, *Immunol Rev* **1999**, *172*, 21-28; bC. Scholz, R. Tampe, *Biol Chem* **2009**, *390*, 783-794.
- [20] P. A. Wearsch, P. Cresswell, *Nat Immunol* **2007**, *8*, 873-881.
- [21] G. Dong, P. A. Wearsch, D. R. Peaper, P. Cresswell, K. M. Reinisch, *Immunity* **2009**, *30*, 21-32.
- [22] H. G. Rammensee, K. Falk, O. Rotzschke, *Annu Rev Immunol* **1993**, *11*, 213-244.
- [23] D. H. Fremont, M. Matsumura, E. A. Stura, P. A. Peterson, I. A. Wilson, *Science* **1992**, *257*, 919-927.
- [24] aP. J. Bjorkman, M. A. Saper, B. Samraoui, W. S. Bennett, J. L. Strominger, D. C. Wiley, *J Immunol* **2005**, *174*, 6-19; bP. J. Bjorkman, M. A. Saper, B. Samraoui, W. S. Bennett, J. L. Strominger, D. C. Wiley, *Nature* **1987**, *329*, 512-518.
- [25] T. E. Johansen, K. McCullough, B. Catipovic, X. M. Su, M. Amzel, J. P. Schneck, *Scand J Immunol* **1997**, *46*, 137-146.
- [26] K. Udaka, K. H. Wiesmuller, S. Kienle, G. Jung, P. Walden, *J Biol Chem* **1995**, *270*, 24130-24134.
- [27] K. Udaka, K. H. Wiesmuller, S. Kienle, G. Jung, P. Walden, *Journal of Biological Chemistry* **1995**, *270*, 24130-24134.
- [28] P. A. Roche, K. Furuta, *Nat Rev Immunol* **2015**, *15*, 203-216.

-
- [29] aM. A. West, R. P. A. Wallin, S. P. Matthews, H. G. Svensson, R. Zaru, H. G. Ljunggren, A. R. Prescott, C. Watts, *Science* **2004**, *305*, 1153-1157; bG. J. Doherty, H. T. McMahon, *Annual Review of Biochemistry* **2009**, *78*, 857-902.
- [30] aB. Manoury, D. Mazzeo, D. T. N. Li, J. Billson, K. Loak, P. Benaroch, C. Watts, *Immunity* **2003**, *18*, 489-498; bR. J. Riese, P. R. Wolf, D. Bromme, L. R. Natkin, J. A. Villadangos, H. L. Ploegh, H. A. Chapman, *Immunity* **1996**, *4*, 357-366; cG. P. Shi, R. A. R. Bryant, R. Riese, S. Verhelst, C. Driessen, Z. Q. Li, D. Bromme, H. L. Ploegh, H. A. Chapman, *Journal of Experimental Medicine* **2000**, *191*, 1177-1185.
- [31] K. S. Kobayashi, P. J. van den Elsen, *Nat Rev Immunol* **2012**, *12*, 813-820.
- [32] E. Y. Jones, L. Fugger, J. L. Strominger, C. Siebold, *Nat Rev Immunol* **2006**, *6*, 271-282.
- [33] F. A. Chaves, K. A. Richards, A. Torelli, J. Wedekind, A. J. Sant, *Biochemistry* **2006**, *45*, 6426-6433.
- [34] L. Bozzacco, H. Yu, H. A. Zebroski, J. Dengiel, H. Deng, S. Mojsov, R. M. Steinman, *Journal of Proteome Research* **2011**, *10*, 5016-5030.
- [35] aK. L. Rock, D. J. Farfan-Arribas, L. Shen, *J Immunol* **2010**, *184*, 9-15; bR. Singh, P. Cresswell, *Science* **2010**, *328*, 1394-1398.
- [36] K. L. Rock, L. Shen, *Immunol Rev* **2005**, *207*, 166-183.
- [37] C. M. Fehres, W. W. Unger, J. J. Garcia-Vallejo, Y. van Kooyk, *Front Immunol* **2014**, *5*, 149.
- [38] aC. Watts, *Biochim Biophys Acta* **2012**, *1824*, 14-21; bV. Kondylis, H. E. van Nispen Tot Pannerden, S. van Dijk, T. Ten Broeke, R. Wubbolts, W. J. Geerts, C. Seinen, T. Mutis, H. F. Heijnen, *Autophagy* **2013**, *9*, 861-880.
- [39] W. Ma, Y. Zhang, N. Vigneron, V. Stroobant, K. Thielemans, P. van der Bruggen, B. J. Van den Eynde, *J Immunol* **2016**, *196*, 1711-1720.
- [40] aO. P. Joffre, E. Segura, A. Savina, S. Amigorena, *Nat Rev Immunol* **2012**, *12*, 557-569; bC. Kurts, B. W. Robinson, P. A. Knolle, *Nat Rev Immunol* **2010**, *10*, 403-414.
- [41] O. P. Joffre, E. Segura, A. Savina, S. Amigorena, *Nat Rev Immunol* **2012**, *12*, 557-569.
- [42] aJ. M. Vyas, A. G. Van der Veen, H. L. Ploegh, *Nat Rev Immunol* **2008**, *8*, 607-618; bC. S. Wagner, J. E. Grotzke, P. Cresswell, *Front Immunol* **2012**, *3*, 138.

2

Tools for studying antigen processing and cross-presentation

Published as part of: Joanna B. Pawlak and Sander I. van Kasteren. eLS. 2017, in press.

2.1 Introduction

The adaptive immune system is the branch of the immune system that has evolved to mount a tailored immune response against specific antigens. The subset of adaptive immune cells called cytotoxic CD8⁺ T lymphocytes (CTLs) are arguably the key mediator in eliminating two specific diseases, namely viral infections and cancers. Despite their apparent different origin (although some cancers are caused by viruses), they share a feature that renders them susceptible to attack by CTLs: both the genetic alterations that are a hallmark of cancer^[1] and the extensive transcription program induced by a virus infection using host cell ribosomes, result in the presence of mutated proteins in the cytosol, which in turn can be processed in the MHC-I pathway to result in the appearance of *neoepitopes* on the cell surface. Unlike the peptides that are present during health, the CTLs capable of recognizing these neoepitopes have not been eliminated through central tolerance mechanisms and, once activated, could kill the virus infected or tumor cell upon recognizing its cognate neoepitope.

However, herein lies the conundrum of cross-presentation: the CTL has to be activated by an antigen presenting cell (likely a subset of dendritic cell, called the CD8⁺ DC) which, especially in the case of tumors, does not produce the same neoepitope as the tumor cell. These cells must thus acquire the mutated proteome

from the tumor exogenously and present it on its own MHC-I, which are normally reserved for the presentation of peptides from cytosolic sources. This process called antigen cross-presentation – discovered over 40 years ago^[2] – presents a complex trafficking problem that can be summarized as follows: “how does antigen that has been taken up and compartmentalized into the endo-lysosomal system encounter the MHC-I loading machinery that resides in the endoplasmic reticulum?”.

2.2 Pathways of antigen cross-presentation

Due to the pivotal importance of cross-presentation in the anti-viral and anti-tumor immune responses, it has been the subject of intensive research and different solutions to the above problem have been presented in the literature since its inception. At present, a spectrum of potential routes has been reported that are bookended by two suggested general paths: the cytosolic and vacuolar pathways of antigen cross-presentation^[3].

The key feature of the cytosolic pathway is that following uptake, antigen is routed via the cytosol where it intersects with the conventional MHC-I peptide processing and loading pathway: internalized exogenous antigens are exported from the phagosome to the cytosol early after uptake, where they are degraded into short peptides by the proteasome and transported into the endoplasmic reticulum (ER) by transporter associated with antigen processing 1 (TAP1) where they are loaded on MHC-I molecules and finally transported to the cell surface^[4]. However, the identity of molecular mechanism responsible for antigen export from endosomes and phagosomes to the cytosol still remains to be fully elucidated. A few possible models for antigen export to the cytosol have been proposed by different groups. One of these models describes a direct fusion of phagosomes with the ER membrane (ER-phagosome fusion) allowing for the ER-proteins to merge into phagosomes. This offers a possible explanation for a presence of the ER-resident proteins in phagosomes. Subsequently, it is believed that these ER-associated proteins such as Sec61 and p97 act as an antigen translocon into the cytosol^[4c, 5]. As an alternative to this model, involvement of Derlin-1 known as degradation in ER protein 1 instead of Sec61 in the ER-phagosome fusion model has been proposed^[6] (Figure 1, left panel). Yet another variant of the cytosolic pathway has been proposed: after proteasomal proteolysis the antigens are imported back into the phagosome via TAP1 transporters residing on the phagosomal surface rather than the ER, where they are recruited by the ER-derived molecule - SNARE-protein Sec22b^[7]. Back in the phagosome the peptides are loaded onto MHC-I molecules by a yet unidentified loading machinery and ultimately transported to the cell surface for sampling by the CD8⁺ T cells^[8] (Figure 1, left panel).

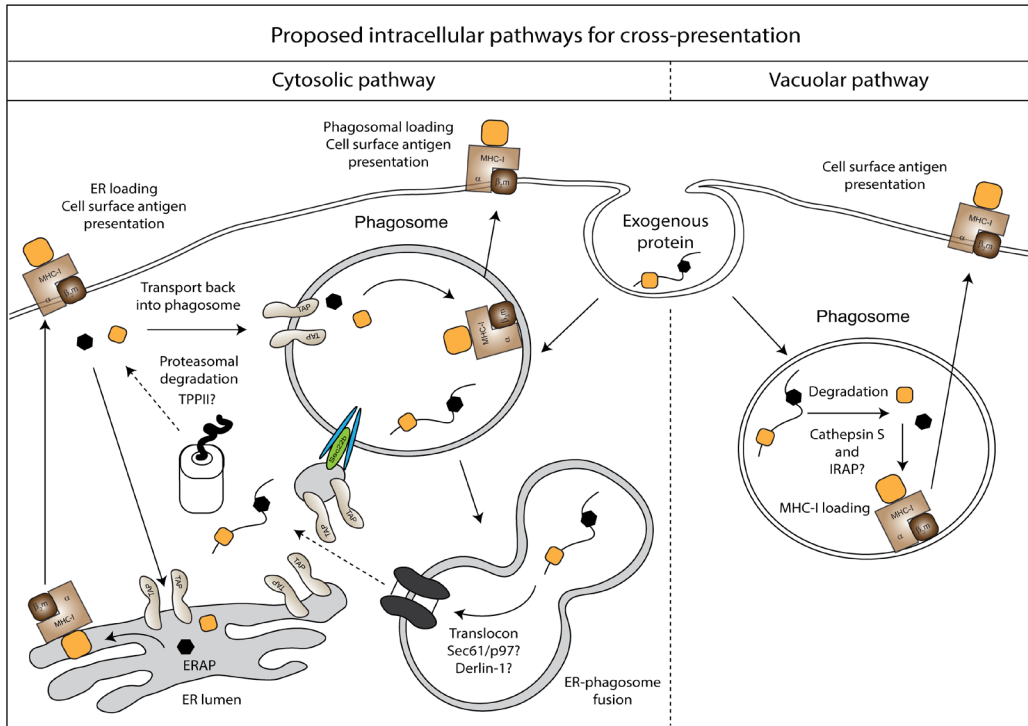


Figure 1. Schematic representation of the intracellular pathways operating throughout the cytosolic and vacuolar cross-presentation pathways (gap junctions mediated peptide transfer not shown).

Within the cytosolic pathway(s), it is generally believed that the proteolytic steps required for the liberation of the epitope peptides takes place outside the phagosome in which they have been taken up. It has, for example, been shown that raising the endosomal pH using chloroquine (which is postulated to lower protease activity in this compartment)^[9] enhanced the export of antigen into the cytosol. Instead, the key cleavages of peptides are believed to be executed by the constitutive proteasome^[10] or immunoproteasome^[11], the latter of which is expressed mainly in dendritic cells and it is induced by proinflammatory cytokines^[12]. Further trimming of the precursor peptides (peptides with *N*-terminal extensions) usually takes places after the peptides are transported to the ER but can also occur in the cytosol by cytosolic aminopeptidases such as tripeptidyl peptidase II (TPPII)^[13]. TPPII has both endo and exopeptidase activity and unlike most other aminopeptidases it can trim long (>14 amino acids) as well as short peptides (<14 aa)^[14]. There are many other cytosolic aminopeptidases such as leucine aminopeptidase (LAP)^[15], bleomycin hydrolase (BH) and pyromycin-sensitive aminopeptidase (PSA)^[16] however it is not known which ones other than TPPII contribute to antigen cross-presentation^[17].

Aminopeptidases present in the ER are referred to as ER aminopeptidases (ERAP) or ER-associated aminopeptidase (ERAAP)^[18]. ERAP trims peptides from the *N*-terminus

until they reach a size of 9 or 8 amino acids^[19]. It has been hypothesized that ERAP may also be able to trim the peptides that are already bound to MHC-I however limited evidence exists to prove or disprove this hypothesis^[19a].

In contrast, the evidence for the vacuolar route suggests that internalized exogenous antigens do not necessarily require departure from their initial uptake vesicle. Instead, antigens are directly degraded into peptides in the phagosomes and loaded onto MHC-I_s, which have either been actively recruited or co-internalized from the cell surface during uptake^[20] (Figure 1, right panel). After this loading has taken place, the MHC-I_s containing new cross-presented peptides are recycled to the cell surface^[21]. In this latter case, as well as in the hybrid pathway in which peptides are transported back into the cytosol, the machinery responsible for peptide editing remains poorly understood: how peptides are chosen for MHC-I loading in an environment more acidic than the ER is not known^[4b, 22]. One potential protein capable of peptide editing *in vitro*^[23] is TAPBPR, a homologue of tapasin^[24] which was found to be highly expressed in purified phagosomes of cross-presenting cells. Importantly, unlike tapasin, TAPBPR does not bind any conventional ER-based peptide loading proteins, nor is it retained in the ER (the principal compartment for conventional MHC-I peptide loading)^[23c]. Taken together these findings imply that TAPBPR could be one of the peptide editors in vacuolar antigen cross-presentation.

In the vacuolar pathway, the epitope peptides are generated in the phagosome itself however by which proteases is not fully known and understood. It is hypothesized that the cysteine proteases, such as cathepsin S and insulin-regulated aminopeptidase (IRAP) are the key proteases involved in a generation of these peptides^[25]. IRAP is a homologue of ERAP, it also trims peptides from the *N*-terminus but it does not stop when they reach size of 9 or 8 amino acids but instead can generate peptides shorter than 8-mer^[19c, 26]. Unlike other cathepsins which are active at the acidic pH, cathepsin S is strongly active at the neutral pH which is believed to be present in cross-presenting vacuoles implying that it could be able to generate 8-9mers peptides in that particular environment^[27]. Protease activity is thus crucial for generating an appropriate peptide length necessary for an efficient binding to MHC molecules^[28]. On the other hand an over-activity may be responsible for a too rapid degradation of peptides before it can be loaded on MHC molecules, or can escape the endo-lysosomal system for cross-presentation^[29].

An alternative mechanism for antigen cross-presentation: gap junction mediated peptide transfer has been presented where peptides can be transferred from the cytosol of one cell into the cytosol of its neighbor through gap junctions^[30]. Gap junctions are non-specific intercellular channels that allow passive diffusion of molecules (MW~1800). Once transferred, the peptides enter the MHC-I antigen

presentation pathway that results in cytotoxic T cell recognition of these innocent neighboring cells. That would mean that the cells can be recognized and killed by the CTL before the actual infection would take a place and thus prevent the spread of the infection itself.

As all of the above proposed models of intracellular cross-presentation may indicate, the biology of cross-presentation is still likely incompletely understood. This chapter focuses on two main topics in regard to the availability of molecular tools/assays for studying intracellular antigen trafficking and presentation.

2.3 Approaches for studying antigen presentation

The stalwart reagent for measuring cross-presentation activity has been the use of genetic techniques and the use of epitope-specific T cells and T cell clones. These very sensitive cells – capable of recognizing as few as 1-3 peptide-MHC-I complexes per target cell^[31] – allow the facile quantification of specific peptides on the cell surface^[32], as their activation is likely dependent on the concentration of presented peptide on the APC-surface.

Most commonly used are T cells directed towards the dominant epitope of the ovalbumin protein spanning residues 257-264 (SIINFEKL) in the context of H2-K^b^[33]. The development of transgenic mice producing only T cells against this epitope allowed the isolation of large numbers of primary T cells capable of *in vitro* detection of this specific epitope. The use of these cells is very widespread in the study of cross-presentation. It has allowed for the identification of potential contributing proteins and factors to the cross-presentation pathway. For example, the essential role of the proteasome in cross-presentation was discovered by Rock and co-workers when they used these OT-I cells in combination with proteasome inhibitors to show that inhibition of the proteasome abolished cross-presentation, but not MHC-II restricted presentation^[20d, 34].

Similarly, also TCR transgenic mice (OT-II) that produce MHC-II restricted, ovalbumin residues 323-339 (ISQAVHAAHAEINEAGR), specific CD4⁺ T cells (OT-II), are available and used for MHC-II antigen presentation studies^[35].

The on-surface quantification of specific peptides in MHC-complexes received a further boost by the development of immortal T cell clones – especially those that had incorporated β -galactosidase under the IL-2 promoter. The Shastri group produced immortal T cell hybridomas specific for SIINFEKL-MHC-I complex (OVA₂₅₇₋₂₆₄-H2-K^b) to quantify as a measurement of T cell response, the amount of generated SIINFEKL epitopes at the cell surface after ovalbumin processing by the APCs^[36]. The T cell hybridomas (B3Z) were generated by transfecting a bacterial β -galactosidase gene (*lacZ*)-inducible cell line (Z.8) with the nuclear factor of activated T cells (NFAT)-

element of the human interleukin 2 (IL-2) enhancer-*lacZ* reporter construct and subsequently by fusing the Z.8 with B3 cells (cytotoxic T cell clone specific for OVA/MHC-I ligand)^[32, 37]. Those B3Z T cells hybridomas will thus when activated not only produce *lacZ* but also secrete the IL-2. The generated SIINFEKL-MHC-I complexes can be evaluated in the context of T cell activation (*lacZ* assay) through monitoring of β -galactosidase mediated conversion of a fluorogenic or chromogenic substrates or by measuring the IL-2 secretion by colorimetric assays^[38]. The advantages of these cells were the quick read out and the sustained *in vitro* growth of these cells, eliminating the need for maintaining. The B3Zs were shown to be capable of detecting pMHC-I complexes after incubation with 20pM of peptide^[39], which – whilst two orders of magnitude less than that for the OT-I cells, is still very sensitive. This approach has thus been translated to the development of many other *lacZ* inducible T cell hybridomas specific for other pMHC-I complexes and are available against, for example, virus infected cells or tumor antigens^[37, 40]. A very recent boost to the field has been the reverse determination of a TCR-ligand. Using the known specificities for given MHCs and peptides from a large number of TCRs, Glanville *et al.* could find paratope hotspots that would allow the identification of TCR-specificity^[41]. In the future this may assist in the rational design of TCRs without the need to invoke and isolate T cells with a given affinity.

A reductionist approach (not requiring T cells or hybridoma) has also been developed, namely in the form of T cell receptor (TCR)-like antibodies specific for a given pMHC-I complex^[42]. Porgador *et al.* produced a monoclonal antibody specific for MHC-I bound to ovalbumin peptide OVA₂₅₇₋₂₆₄ (SIINFEKL) complex (25-D1.16) with a limit detection approaching that of T cells (approximately 20pm peptide)^[43]. This antibody conjugated to a fluorophore allows for direct quantification of SIINFEKL-MHC-I at the cell surface (direct binding of SIINFEKL and after ovalbumin processing) using flow cytometry as well as visualization of intracellular trafficking of this complex using confocal microscopy. Moreover the antibody can serve as a reporter to identify the *in situ* localization of antigen presenting cells bearing SIINFEKL-MHC-I complexes.

There are, however, two major limitations to the use of T cell-based reagents in the study of cross-presentation. The first one is that – by virtue of only the final stages of the process being detected – the underlying mechanisms can only be revealed indirectly. The second problem is that of bias: only those epitopes against which T cells have been identified and cultured can be detected but no information is given on other epitopes.

Evidence for the diversity of peptides capable of binding MHC-I came from the pioneering work by Rammensee and co-workers who provided insight into the properties of the MHC-I 'ligandome' using an approach based on elucidation and identification^[44]. Using a workflow that initially consisted of the immuno-precipitation

of MHC-complexes (from 10 billion cells) followed by Edman-degradation of the peptides, it was found that all positions of the bound peptide were highly varied^[45] at all positions, except the two anchor residues. At these points, very few amino acid types were identified using this approach, confirming the importance of these anchors to MHC-I binding. The advent of mass spectrometry added to the richness of the approach: rather than using Edman degradation for peptide identification and sequencing, LC-MS-MS did allow identification of specific MHC-I-bound peptides^[46] from a tumor cell line (SW1116). By this approach, sensitivities <10 fM could be achieved, which corresponded to the detection of peptides carrying 8 copies per cell. However, 3 billion cells were needed to achieve this, which is beyond the growth range of many cell lines. However, with the advent of more sensitive MS-MS techniques, the cell numbers needed to provide full coverage have dropped and the approach has now been used, for example, to quantify the number of spliced peptides on the MHC-I ligandome (made from the proteasome catalyzed re-ligation of peptide fragments)^[47], to show the contribution of peptides of non-canonical reading frames to antigen presentation^[48], and the role of specific proteases, such as ERAAP, to the peptidome^[49]. The diversity of the MHC-I-bound peptides over the course of a developing cancer has even recently been reported and the changes in these peptides longitudinally have shown the potential for T cell mediated clearance – even that based on non-neoepitopes^[50]. It was also discovered using this approach that post-translationally modified peptides (for example those modified with O-GlcNAc) were presented by cells providing a potential added layer of the complexity of the immune surveillance. The limitations of the technique lie in that, even with ever advancing mass spectrometry, the underlying immunoprecipitation means that it cannot be readily determined from where in the cell the peptide-MHCs have originated, nor can it be excluded that by disrupting the membranes in the cell peptides are exchanged in the MHC-I during the isolation process. Cell-surface acid elution of peptides can prevent this, but does require more cells. Despite these limitations, the use of mass spectrometry has provided major new insights into the peptides and proteins that are presented on cells in health and disease and are beginning to give us a molecular understanding of T cell recognition.

2.4 Approaches for studying intracellular antigen routing

The mechanistic elucidation of cross-presentation has proven difficult, especially due to the complex nature of intracellular routing the antigen can take. Some elegant approaches have been reported to study this subcellular routing, especially in combination with genetic techniques. Two that will be highlighted here are reporter proteins and fluorophore modified antigens.

The reporter proteins rely on intrinsic enzyme (or fluorescence) functionality to detect their presence in subcellular fractions. For example, horseradish peroxidase (HRP) was used by Watts and colleagues^[51] to show that the internalized antigens were released into cytosol^[52] by using fluorogenic substrates to detect intact protein in the cytosol after macropinocytosis^[52a, 53]. One downside to the use of HRP turned out to be that it stimulated its own uptake, because of which skewing of these results could not be excluded^[52a, 54].

Ackerman *et al.* used a luciferase enzyme to study cytosolic entry of protein^[4c]. Luciferases make up a class of oxidative enzymes that catalyze the oxidation of luciferin in the presence of ATP and oxygen to produce bioluminescence^[55], making them one of the most sensitive reporter proteins available. The luciferase reporter assay has, for example been used to study antigen retranslocation into phagosomes^[56] using a latex-bead retrieval approach. Isolated phagosomes were incubated with the cytosolic fraction of a cell either in absence or with presence of ATP and luciferase activity was observed only in the phagosomes that were incubated with ATP - containing cytosols and it served as an indication of a successful export of internalized antigen from phagosomes.

Lin *et al.*^[57] used a 'reporter protein' in a different manner: to detect cells capable of cross-presentation *in vivo*, horse cytochrome c protein was used as a model antigen. Cytochrome c (cyt c) is an oxidase enzyme found in the mitochondrion of eukaryotes^[58]. It is relatively small (~12 kDa) and soluble, features that make the cytosolic transfer in cells possible^[59]. Cyt c when released from mitochondrion can evoke programmed cell death (apoptosis)^[60]. Lin *et al.* exploited the fact that only the cytochrome c from higher eukaryotic organisms can initiate apoptosis in mammalian cells^[61]. They injected mice with either horse or yeast cyt c and observed apoptosis only in cells that were exposed to horse cyt c and that were capable of cyt c uptake and cytosolic transfer. Using flow cytometry they were able to quantify the relative proportion and numbers of various types of splenic cells that survived the cyt c exposure and hence, by negative difference, could determine which splenic DC cell subtypes are the most efficient in cytosolic transfer.

This assay was also used by Cebrian *et al.*^[62] to compare cross-presentation efficiency via the cytosolic route in two cell lines (DCs derived from wildtype mice and from Sec22b knockdowns). They showed that Sec22b as a vesicle trafficking protein is required for efficient export of antigens to the cytosol by measuring the amount of apoptosis in cells that have been incubated with cyt c. It was shown that apoptosis was decreased in cells lacking the Sec22b indicating that it is crucial for reporter export to the cytosol. The same group also generated mice bearing a conditional DC-specific mutation in the Sec22b gene and showed that Sec22b-dependent cross-presentation in DCs is required to induce anti-tumor immune responses *in vivo*^[63].

Cebrian *et al.*^[62] also developed, a new method which they adapted from Ray *et al.*^[64] to measure the cytosolic export of antigens. They used coumarin-cephalosporin-fluorescein (4)-acetoxymethyl (CCF4-AM) substrate that is lipophilic and readily cell permeable^[7]. When taken up by cells the substrate is converted into its negatively charged form (CCF4) which accumulates in the cytosol. CCF4 is also a Fluorescence Resonance Energy Transfer (FRET) substrate that consists of a cephalosporin core linking 7-hydroxycoumarin to fluorescein which together act as fluorescent probes/reporters for FRET assay. Cebrian *et al.*^[62] measured antigen export from endocytic compartment into cytosol as follows first dendritic cells (DCs) were loaded with FRET substrate of β -lactamase (CCF) that after cellular uptake accumulates in the endosome. Then the cells were exposed to β -lactamase which when transported to cytosol cleaves CCF4 resulting in decreased ratio of fluorescein (acceptor fluorophore) over coumarin (donor fluorophore)^[65]. Thus, a loss of FRET signal at 535 nm and increased signal at 450 nm (Figure 2). Finally, the β -lactamase serves as a model antigen and its export to the cytosol can be detected by calculating ratiometric values between the 450 and 535 signals (450:535) using flow cytometry^[65b, 66]. The bigger the ratio values the more increased export of the β -lactamase to the cytosol.

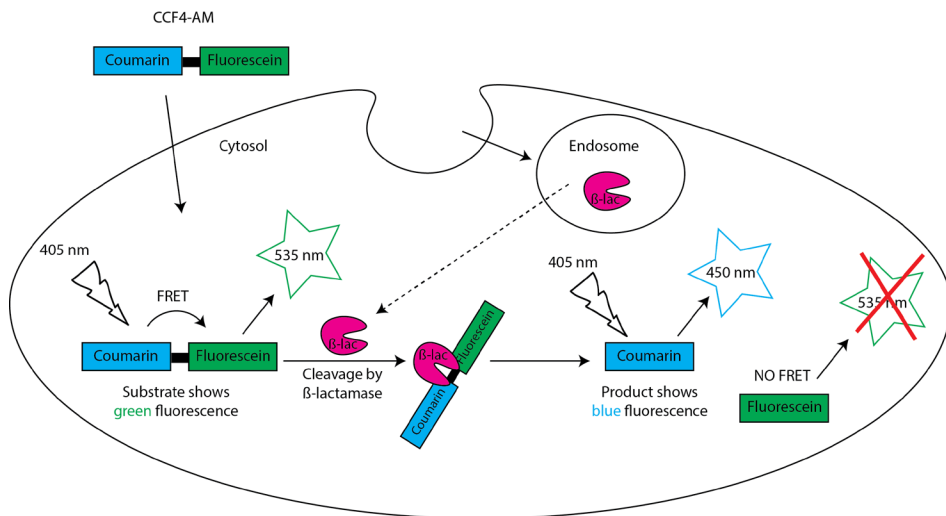


Figure 2. Schematic representation of the FRET based- β -lactamase assay used to evaluate endosomal export to the cytosol.

Recently, another assay available for measuring antigen export to cytosol but based on galectin-3 was presented by the van den Bogaart group. Galectin-3 (Gal-3) belongs to a family of beta-galactoside-binding proteins that have an affinity for beta-galactosides^[67]. Dingjan *et al.*^[68] have transfected cells with galectin-3 conjugated with the fluorescent protein mAzami^[69] which is evenly distributed in the cytosol and clusters only when exposed to β -galactoside residues present on glycosylated

proteins^[70]. Because these β -galactoside residues are located on glycosylated proteins in the luminal and not the cytosolic side of the endosomal membranes, the recruitment of Gal-3 to these β -galactoside residues could be established only upon endosomal rupture^[64]. By co-incubating the cells with OVA-conjugated to Alexa Fluor-647 as an endosomal marker the recruitment of Gal-3-mAzami to OVA-positive endosomes was measured using fluorescence microscopy^[71].

Fluorophore-modified antigens have also proven to be valuable reagents for the study of antigen uptake and routing^[72]. Ossendorp and colleagues studied kinetics of cross-presentation by conjugating Alexa Fluor-dyes to ovalbumin and presenting it to DCs as either the free, soluble antigen, or in immune complexes with anti-OVA antibodies^[72]. Using confocal microscopy and flow cytometry they were able not only to conclude that the antibody bound Alexa Fluor-ovalbumin was taken up much more efficiently than the 'free' OVA but also discovered that this antibody bound exogenous antigen can be conserved for several days within mature dendritic cells in the lysosome-like compartments.

The use of fluorescent protein-antigen fusions such as influenza nucleoprotein (NP) fused with SIINFEKL peptide and enhanced green fluorescence protein (GFP) termed NP-SIINFEKL-EGFP as reported by Princiotta *et al.*^[73] to study endogenous antigen processing is however also fraught with danger: fluorescent protein-antigen fusions which can undergo a premature proteolytic degradation and by the very nature of antigen processing – are cleaved from the antigen and can thus only be studied for early events in the process. Chemical fluorophores are relatively large and mostly hydrophobic organic molecules that can alter the properties of the antigen's routing, processing and MHC-loading abilities to the degree that the antigen cannot be found on the cell surface after presentation.

The aim of this thesis is to explore the use of bioorthogonal epitopes to study antigen cross-presentation^[74], which in future may provide clearer results to the study of cross-presentation. These are antigens carrying bioorthogonal groups in specific amino acid positions within the epitope region of the antigen that can be reacted selectively within/on the cell using bioorthogonal ligation strategies^[75]. Incorporation of bioorthogonal groups into antigens has the advantage over other methods because most of the groups are stable to proteolysis^[76] and are small enough to have a minimal impact on routing and loading onto MHC-I molecules^[74b, 77]. In the future, these antigens have potential to be applied for imaging of the entire cross-presentation pathway using a single bioorthogonal handle.

2.5 Conclusion

Peptide processing and cross-presentation on MHC-I and –II complexes represent one of the most complex problems in biology. Understanding the manner in which – with a surprising degree of fidelity – peptides are degraded, routed and presented by APCs and host cells remains to be completely understood and an improved understanding of this would lead to the ability to better design vaccines, especially those geared towards the induction tumor/virus targeting CD8 T cells.

2.6 References

- [1] D. Hanahan, R. A. Weinberg, *Cell* **2011**, *144*, 646-674.
- [2] *The Journal of Experimental Medicine* **1976**, *143*, 1283-1288.
- [3] O. P. Joffre, E. Segura, A. Savina, S. Amigorena, *Nat Rev Immunol* **2012**, *12*, 557-569.
- [4] aJ. E. Grotzke, A. C. Siler, D. A. Lewinsohn, D. M. Lewinsohn, *J Immunol* **2010**, *185*, 4336-4343; bA. L. Ackerman, P. Cresswell, *Nat Immunol* **2004**, *5*, 678-684; cA. L. Ackerman, A. Giodini, P. Cresswell, *Immunity* **2006**, *25*, 607-617.
- [5] E. Gagnon, S. Duclos, C. Rondeau, E. Chevet, P. H. Cameron, O. Steele-Mortimer, J. Paiement, J. J. M. Bergeron, M. Desjardins, *Cell* **2002**, *110*, 119-131.
- [6] aB. N. Lilley, H. L. Ploegh, *Nature* **2004**, *429*, 834-840; bY. Ye, Y. Shibata, C. Yun, D. Ron, T. A. Rapoport, *Nature* **2004**, *429*, 841-847.
- [7] M. Zehner, A. L. Marschall, E. Bos, J. G. Schloetel, C. Kreer, D. Fehrenschild, A. Limmer, F. Ossendorp, T. Lang, A. J. Koster, S. Dubel, S. Burgdorf, *Immunity* **2015**, *42*, 850-863.
- [8] aC. M. Fehres, W. W. Unger, J. J. Garcia-Vallejo, Y. van Kooyk, *Front Immunol* **2014**, *5*, 149; bJ. S. Blum, P. A. Wearsch, P. Cresswell, *Annu Rev Immunol* **2013**, *31*, 443-473.
- [9] D. Accapezzato, V. Visco, V. Francavilla, C. Molette, T. Donato, M. Paroli, M. U. Mondelli, M. Doria, M. R. Torrisi, V. Barnaba, *The Journal of experimental medicine* **2005**, *202*, 817-828.
- [10] M. Kovacovics-Bankowski, K. L. Rock, *Science* **1995**, *267*, 243-246.
- [11] M. J. Palmowski, U. Gileadi, M. Salio, A. Gallimore, M. Millrain, E. James, C. Addey, D. Scott, J. Dyson, E. Simpson, V. Cerundolo, *J Immunol* **2006**, *177*, 983-990.
- [12] aP. Cascio, C. Hilton, A. F. Kisselev, K. L. Rock, A. L. Goldberg, *EMBO J* **2001**, *20*, 2357-2366; bA. F. Kisselev, T. N. Akopian, K. M. Woo, A. L. Goldberg, *J Biol Chem* **1999**, *274*, 3363-3371.
- [13] N. Brouwenstijn, T. Serwold, N. Shastri, *Immunity* **2001**, *15*, 95-104.
- [14] M. Kawahara, I. A. York, A. Hearn, D. Farfan, K. L. Rock, *J Immunol* **2009**, *183*, 6069-6077.
- [15] C. F. Towne, I. A. York, J. Neijssen, M. L. Karow, A. J. Murphy, D. M. Valenzuela, G. D. Yancopoulos, J. J. Neefjes, K. L. Rock, *J Immunol* **2008**, *180*, 1704-1712.
- [16] L. Stoltze, M. Schirle, G. Schwarz, C. Schroter, M. W. Thompson, L. B. Hersh, H. Kalbacher, S. Stevanovic, H. G. Rammensee, H. Schild, *Nat Immunol* **2000**, *1*, 413-418.
- [17] I. A. York, N. Bhutani, S. Zendzian, A. L. Goldberg, K. L. Rock, *J Immunol* **2006**, *177*, 1434-1443.
- [18] G. E. Hammer, F. Gonzalez, M. Champsaur, D. Cado, N. Shastri, *Nat Immunol* **2006**, *7*, 103-112.
- [19] aT. Kanaseki, N. Blanchard, G. E. Hammer, F. Gonzalez, N. Shastri, *Immunity* **2006**, *25*, 795-806; bT. Serwold, F. Gonzalez, J. Kim, R. Jacob, N. Shastri, *Nature* **2002**, *419*, 480-483; cK. L. Rock, D. J. Farfan-Arribas, L. Shen, *J Immunol* **2010**, *184*, 9-15.
- [20] aM. Houde, S. Bertholet, E. Gagnon, S. Brunet, G. Goyette, A. Laplante, M. F. Princiotta, P. Thibault, D. Sacks, M. Desjardins, *Nature* **2003**, *425*, 402-406; bA. L. Ackerman, C. Kyritsis, R. Tampe, P. Cresswell, *Proc Natl Acad Sci U S A* **2003**, *100*, 12889-12894; cP. Guermonprez, L. Saveanu, M. Kleijmeer, J. Davoust, P. Van Endert, S. Amigorena, *Nature* **2003**, *425*, 397-402; dM. Kovacovics-Bankowski, K. L. Rock, *Science* **1995**, *267*, 243-246; eE. Segura, J. A. Villadangos, *Traffic* **2011**, *12*, 1677-1685.
- [21] S. Nierkens, J. Tel, E. Janssen, G. J. Adema, *Trends Immunol* **2013**, *34*, 361-370.

- [22] T. Kanaseki, K. C. Lind, H. Escobar, N. Nagarajan, E. Reyes-Vargas, B. Rudd, A. L. Rockwood, L. Van Kaer, N. Sato, J. C. Delgado, N. Shastri, *J Immunol* **2013**, *191*, 1547-1555.
- [23] aC. Hermann, L. M. Strittmatter, J. E. Deane, L. H. Boyle, *J Immunol* **2013**, *191*, 5743-5750; bC. Hermann, J. Trowsdale, L. H. Boyle, *Tissue Antigens* **2015**, *85*, 155-166; cG. I. Morozov, H. Zhao, M. G. Mage, L. F. Boyd, J. Jiang, M. A. Dolan, R. Venna, M. A. Norcross, C. P. McMurtrey, W. Hildebrand, P. Schuck, K. Natarajan, D. H. Margulies, *Proc Natl Acad Sci U S A* **2016**, *113*, E1006-1015.
- [24] P. V. Praveen, R. Yaneva, H. Kalbacher, S. Springer, *Eur J Immunol* **2010**, *40*, 214-224.
- [25] aL. Saveanu, O. Carroll, M. Weimershaus, P. Guermonprez, E. Firat, V. Lindo, F. Greer, J. Davoust, R. Kratzer, S. R. Keller, G. Niedermann, P. van Endert, *Science* **2009**, *325*, 213-217; bL. Shen, L. J. Sigal, M. Boes, K. L. Rock, *Immunity* **2004**, *21*, 155-165; cC. Watts, *Biochim Biophys Acta* **2012**, *1824*, 14-21.
- [26] L. Saveanu, P. van Endert, *Front Immunol* **2012**, *3*, 57.
- [27] R. Belizaire, E. R. Unanue, *Proc Natl Acad Sci U S A* **2009**, *106*, 17463-17468.
- [28] S. I. van Kasteren, H. S. Overkleeft, *Curr Opin Chem Biol* **2014**, *23*, 8-15.
- [29] R. D. Wilkinson, R. Williams, C. J. Scott, R. E. Burden, *Biol Chem* **2015**, *396*, 867-882.
- [30] aJ. Neijssen, C. Herberts, J. W. Drijfhout, E. Reits, L. Janssen, J. Neefjes, *Nature* **2005**, *434*, 83-88; bA. Handel, A. Yates, S. S. Pilyugin, R. Antia, *Trends Immunol* **2007**, *28*, 463-466.
- [31] J. W. Yewdell, E. Reits, J. Neefjes, *Nat Rev Immunol* **2003**, *3*, 952-961.
- [32] J. Karttunen, N. Shastri, *Proc Natl Acad Sci U S A* **1991**, *88*, 3972-3976.
- [33] aK. A. Hogquist, S. C. Jameson, W. R. Heath, J. L. Howard, M. J. Bevan, F. R. Carbone, *Cell* **1994**, *76*, 17-27; bS. R. Clarke, M. Barnden, C. Kurts, F. R. Carbone, J. F. Miller, W. R. Heath, *Immunol Cell Biol* **2000**, *78*, 110-117.
- [34] aK. L. Rock, S. Gamble, L. Rothstein, *Science* **1990**, *249*, 918-921; bK. L. Rock, L. Rothstein, S. Gamble, C. Fleischacker, *J Immunol* **1993**, *150*, 438-446.
- [35] aJ. M. Robertson, P. E. Jensen, B. D. Evavold, *J Immunol* **2000**, *164*, 4706-4712; bK. M. Murphy, A. B. Heimberger, D. Y. Loh, *Science* **1990**, *250*, 1720-1723.
- [36] J. Karttunen, S. Sanderson, N. Shastri, *Proc. Natl. Acad. Sci. U. S. A.* **1992**, *89*, 6020-6024.
- [37] G. Cafri, A. Sharbi-Yunger, E. Tzehoval, L. Eisenbach, *PLoS ONE* **2013**, *8*, e55583.
- [38] aG. P. Nolan, S. Fiering, J. F. Nicolas, L. A. Herzenberg, *Proc. Natl. Acad. Sci. U. S. A.* **1988**, *85*, 2603-2607; bJ. R. Sanes, J. L. Rubenstein, J. F. Nicolas, *The EMBO Journal* **1986**, *5*, 3133-3142.
- [39] N. Shastri, F. Gonzalez, *J Immunol* **1993**, *150*, 2724-2736.
- [40] S. N. Mueller, C. M. Jones, C. M. Smith, W. R. Heath, F. R. Carbone, *J Exp Med* **2002**, *195*, 651-656.
- [41] J. Glanville, H. Huang, A. Nau, O. Hatton, L. E. Wagar, F. Rubelt, X. Ji, A. Han, S. M. Krams, C. Pettus, N. Haas, C. S. L. Arlehamn, A. Sette, S. D. Boyd, T. J. Scriba, O. M. Martinez, M. M. Davis, *Nature* **2017**, *advance online publication*.
- [42] A. Porgador, J. W. Yewdell, Y. Deng, J. R. Bennink, R. N. Germain, *Immunity* **1997**, *6*, 715-726.
- [43] aO. Rotzschke, K. Falk, S. Stevanovic, G. Jung, P. Walden, H. G. Rammensee, *Eur J Immunol* **1991**, *21*, 2891-2894; bD. H. Fremont, E. A. Stura, M. Matsumura, P. A. Peterson, I. A. Wilson, *Proc Natl Acad Sci U S A* **1995**, *92*, 2479-2483; cA. Porgador, J. W. Yewdell, Y. Deng, J. R. Bennink, R. N. Germain, *Immunity* **1997**, *6*, 715-726.
- [44] H G Rammensee, a. K Falk, O. Röttschke, *Annu Rev Immunol* **1993**, *11*, 213-244.

- [45] K. Falk, O. Rotzschke, S. Stevanovic, G. Jung, H. G. Rammensee, *Nature* **1991**, *351*, 290-296.
- [46] M. Schirle, W. Keilholz, B. Weber, C. Gouttefangeas, T. Dumrese, H. D. Becker, S. Stevanović, H.-G. Rammensee, *European Journal of Immunology* **2000**, *30*, 2216-2225.
- [47] J. Liepe, F. Marino, J. Sidney, A. Jeko, D. E. Bunting, A. Sette, P. M. Kloetzel, M. P. H. Stumpf, A. J. R. Heck, M. Mishto, *Science* **2016**, *354*, 354-358.
- [48] C. M. Laumont, T. Daouda, J. P. Laverdure, E. Bonneil, O. Caron-Lizotte, M. P. Hardy, D. P. Granados, C. Durette, S. Lemieux, P. Thibault, C. Perreault, *Nat Commun* **2016**, *7*, 10238.
- [49] N. A. Nagarajan, D. A. de Verteuil, D. Sriranganadane, W. Yahyaoui, P. Thibault, C. Perreault, N. Shastri, *Journal of immunology (Baltimore, Md. : 1950)* **2016**, *197*, 1035-1043.
- [50] D. J. Kowalewski, H. Schuster, L. Backert, C. Berlin, S. Kahn, L. Kanz, H. R. Salih, H.-G. Rammensee, S. Stevanovic, J. S. Stickel, *Proceedings of the National Academy of Sciences of the United States of America* **2015**, *112*, E166-E175.
- [51] A. R. Mantegazza, J. G. Magalhaes, S. Amigorena, M. S. Marks, *Traffic* **2013**, *14*, 135-152.
- [52] aC. C. Norbury, L. J. Hewlett, A. R. Prescott, N. Shastri, C. Watts, *Immunity* **1995**, *3*, 783-791; bC. Watts, *Annu Rev Immunol* **1997**, *15*, 821-850.
- [53] J. A. Swanson, C. Watts, *Trends Cell Biol* **1995**, *5*, 424-428.
- [54] J. A. Swanson, B. D. Yirinec, S. C. Silverstein, *J Cell Biol* **1985**, *100*, 851-859.
- [55] aJ. C. Dunlap, J. W. Hastings, O. Shimomura, *Proc Natl Acad Sci U S A* **1980**, *77*, 1394-1397; bJ. W. Hastings, *Journal of Molecular Evolution* **1983**, *19*, 309-321.
- [56] S. T. Smale, *Cold Spring Harb Protoc* **2010**, *2010*, pdb prot5421.
- [57] M. L. Lin, Y. Zhan, A. I. Proietto, S. Prato, L. Wu, W. R. Heath, J. A. Villadangos, A. M. Lew, *Proc Natl Acad Sci U S A* **2008**, *105*, 3029-3034.
- [58] T. Tsukihara, H. Aoyama, E. Yamashita, T. Tomizaki, H. Yamaguchi, K. Shinzawa-Itoh, R. Nakashima, R. Yaono, S. Yoshikawa, *Science* **1995**, *269*, 1069-1074.
- [59] T. G. Frey, *Microsc Res Tech* **1994**, *27*, 319-332.
- [60] J. Cai, J. Yang, D. Jones, *Biochimica et Biophysica Acta (BBA) - Bioenergetics* **1998**, *1366*, 139-149.
- [61] R. M. Kluck, L. M. Ellerby, H. M. Ellerby, S. Naiem, M. P. Yaffe, E. Margoliash, D. Bredesen, A. G. Mauk, F. Sherman, D. D. Newmeyer, *J Biol Chem* **2000**, *275*, 16127-16133.
- [62] I. Cebrian, G. Visentin, N. Blanchard, M. Jouve, A. Bobard, C. Moita, J. Enninga, L. F. Moita, S. Amigorena, A. Savina, *Cell* **2011**, *147*, 1355-1368.
- [63] A. Alloatti, D. C. Rookhuizen, L. Joannas, J.-M. Carpier, S. Iborra, J. G. Magalhaes, N. Yatim, P. Kozik, D. Sancho, M. L. Albert, S. Amigorena, *The Journal of Experimental Medicine* **2017**.
- [64] K. Ray, A. Bobard, A. Danckaert, I. Paz-Haftel, C. Clair, S. Ehsani, C. Tang, P. Sansonetti, G. V. Tran, J. Enninga, *Cell Microbiol* **2010**, *12*, 545-556.
- [65] aD. M. Jones, S. Padilla-Parra, *Sensors (Basel)* **2016**, *16*; bJ. Kouznetsova, W. Sun, C. Martinez-Romero, G. Tawa, P. Shinn, C. Z. Chen, A. Schimmer, P. Sanderson, J. C. McKew, W. Zheng, A. Garcia-Sastre, *Emerg Microbes Infect* **2014**, *3*, e84.
- [66] G. Zlokarnik, P. A. Negulescu, T. E. Knapp, L. Mere, N. Burres, L. Feng, M. Whitney, K. Roemer, R. Y. Tsien, *Science* **1998**, *279*, 84-88.
- [67] I. Paz, M. Sachse, N. Dupont, J. Mounier, C. Cederfur, J. Enninga, H. Leffler, F. Poirier, M. C. Prevost, F. Lafont, P. Sansonetti, *Cell Microbiol* **2010**, *12*, 530-544.

- [68] I. Dingjan, D. R. Verboogen, L. M. Paardekooper, N. H. Revelo, S. P. Sittig, L. J. Visser, G. F. Mollard, S. S. Henriët, C. G. Figdor, M. Ter Beest, G. van den Bogaart, *Sci Rep* **2016**, *6*, 22064.
- [69] R. N. Day, M. W. Davidson, *Chemical Society reviews* **2009**, *38*, 2887-2921.
- [70] D. S. D'Astolfo, R. J. Pagliero, A. Pras, W. R. Karthaus, H. Clevers, V. Prasad, R. J. Lebbink, H. Rehmann, N. Geijsen, *Cell* **2015**, *161*, 674-690.
- [71] N. Schaft, B. Lankiewicz, J. W. Gratama, R. L. Bolhuis, R. Debets, *J Immunol Methods* **2003**, *280*, 13-24.
- [72] N. van Montfoort, M. G. Camps, S. Khan, D. V. Filippov, J. J. Weterings, J. M. Griffith, H. J. Geuze, T. van Hall, J. S. Verbeek, C. J. Melief, F. Ossendorp, *Proc Natl Acad Sci U S A* **2009**, *106*, 6730-6735.
- [73] M. F. Princiotta, D. Finzi, S. B. Qian, J. Gibbs, S. Schuchmann, F. Buttgereit, J. R. Bennink, J. W. Yewdell, *Immunity* **2003**, *18*, 343-354.
- [74] aJ. B. Pawlak, B. J. Hos, M. J. van de Graaff, O. A. Megantari, N. Meeuwenoord, H. S. Overkleeft, D. V. Filippov, F. Ossendorp, S. I. van Kasteren, *ACS chemical biology* **2016**, *11*, 3172-3178; bJ. B. Pawlak, G. P. Gential, T. J. Ruckwardt, J. S. Bremmers, N. J. Meeuwenoord, F. A. Ossendorp, H. S. Overkleeft, D. V. Filippov, S. I. van Kasteren, *Angewandte Chemie (International ed. in English)* **2015**, *54*, 5628-5631.
- [75] aE. M. Sletten, C. R. Bertozzi, *Angewandte Chemie (International ed. in English)* **2009**, *48*, 6974-6998; bC. P. Ramil, Q. Lin, *Chem Commun* **2013**, *49*, 11007-11022; cK. Lang, J. W. Chin, *ACS chemical biology* **2014**, *9*, 16-20.
- [76] J. C. M. Van Hest, K. L. Kiick, D. A. Tirrell, *Journal of the American Chemical Society* **2000**, *122*, 1282-1288.
- [77] aJ. B. Pawlak, G. P. Gential, T. J. Ruckwardt, J. S. Bremmers, N. J. Meeuwenoord, F. A. Ossendorp, H. S. Overkleeft, D. V. Filippov, S. I. van Kasteren, *Angew Chem Int Ed Engl* **2015**, *54*, 5628-5631; bJ. B. Pawlak, B. J. Hos, M. J. van de Graaff, O. A. Megantari, N. Meeuwenoord, H. S. Overkleeft, D. V. Filippov, F. Ossendorp, S. I. van Kasteren, *ACS Chem Biol* **2016**.

3

The optimization of bioorthogonal epitope ligation within MHC-I complexes

Published as part of: Joanna B. Pawlak, Brett J. Hos, Michel J. van de Graaff, Otty A. Megantari, Nico J. Meeuwenoord, Herman S. Overkleef, Dmitri V. Filippov, Ferry A. Ossendorp and Sander I. van Kasteren.

ACS Chemical Biology, 2016, 11(11): 3172-3178.

Silvia Pujals Riato and Lorenzo Albertazzi also contributed to the work described in this chapter.

3.1 Introduction

The first step of determining whether bioorthogonal antigens could serve as a method for studying the entirety of the cross-presentation pathway, was to determine what the parameters were under which bioorthogonal ligations could be performed on the surface of the cell. If successful, bioorthogonal variants of antigens could then be used to allow the quantification of epitope peptides, independent of T cell reagents. At present, reagents are mostly available for the study of known specific peptides, for example by using T cells specific for particular peptide-MHC-I (pMHC-I)^[1], recombinant T cell receptors (TCRs)^[2], or TCR-like antibodies specific for a given pMHC-I^[3].

It was hypothesized that bioorthogonal peptides would allow the quantification of the surface concentration in MHC-I complexes by specifically incorporating bioorthogonal functional groups in tolerated positions in epitopes, followed by an on-cell ligation reaction with a non-cell permeable reporter. This would mean, the epitope could be quantified independent of T cell-based reagents, which would for example greatly facilitate the study of pMHC-I for which TCR-based reagents are not available. Unlike larger detectable groups, bioorthogonal groups are small enough not to affect MHC

loading. Furthermore, their *in vivo* stability^[4] makes them potentially suited to the study of pMHC-I complexes on the surface of the cell^[5].

Quantification of the bioorthogonal antigens can be achieved by ligation of a complementary fluorophore to the bioorthogonal amino acid side chain at the end of the experiment. That is however quite challenging, due to the low numbers of specific pMHC-I molecules available on the cell surface. Typically, only 10^5 - 10^6 MHC-I molecules are present per cell^[6] which are loaded with multiple different self-peptides. The detection of a specific subset of peptide loaded MHC-I molecules would thus require sensitive and selective ligation of these peptides. Furthermore, these ligations have to be done on peptides within MHC-I complexes, adding to the experimental stringency.

This chapter reports the optimization of the bioorthogonal quantification of peptides loaded on MHC-I complexes. The binding and ligation parameters that allow the quantification of exogenous bioorthogonal epitopes within a pMHC-I complex were established. The effect of bioorthogonal modification of epitopes on MHC-I binding, TCR-recognition and bioorthogonal reaction efficiency in various possible ligation reactions to facilitate further translation to the quantification and imaging of the antigen presentation pathway was optimized and assessed.

3.2 Results and discussion

The first requirement for bioorthogonal epitopes to be of use in the study of pMHC-I is that the modification itself must not negate binding to MHC-I. Once bound to MHC-I, the steric hindrance should be sufficiently small to allow on-surface ligation of the bioorthogonal group to allow the quantification of the pMHC-I preferably below MHC-I saturation levels.

Bioorthogonal modification and pMHC-I stability

It was first determined whether bioorthogonal chemical functionalities could be incorporated into minimal MHC-I epitopes without affecting binding to the MHC-I. Initial focus was on the two smallest available bioorthogonal groups with the lowest side-reactivity: the alkyne and azide^[7]. Both minimally impact structure due to their small size and bioorthogonality, and are readily incorporated into peptides^[8] and proteins^[9] in the side-chain modified amino acids azidohomoalanine (Aha, **1**, Figure 1) and propargylglycine (Pg, **2**, Figure 1). Furthermore, they have exceptional stability profiles as only very few biological sequestration reactions of alkynes^[10] and azides^[11] have been reported.

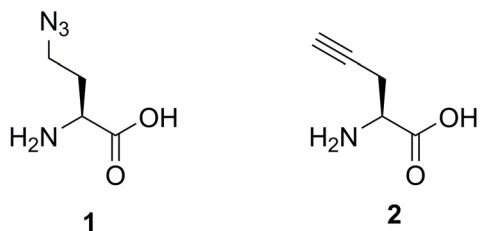


Figure 1. Structures of Aha (1), Pg (2).

To test MHC-I binding and to establish the constraints of performing bioorthogonal ligations within the MHC-I complex, a library of 16 bioorthogonal analogues of the major epitope peptide spanning residues 257-264 of the model antigen ovalbumin (OVA₂₅₇₋₂₆₄; SIINFEKL, Figure 2A) modified with either Aha or Pg at each of the positions within the epitope (P1-P8) was synthesized (Table S1). The binding of these 16 bioorthogonal peptides to the MHC-I molecule H2-K^b was compared against the affinity of the parent epitope, SIINFEKL. Binding was measured using the TAP-deficient RMA-S cell line, which expresses a large fraction of its 10⁵ MHC-I molecules with low affinity peptides, when incubated at 26 °C^[12]. These low affinity peptides rapidly dissociate when the temperature is raised to 37 °C, resulting in the internalization and degradation of the empty MHC-I complexes. These can, however, be stabilized by co-incubation with a high affinity peptide. Quantification of MHC-I at the cell surface with an anti MHC-I-antibody after incubation at 37 °C for 4 hours thus provides an indirect quantification of MHC-I binding affinity of a particular peptide. This assay revealed that Aha-substitutions were tolerated in terms of H2-K^b binding at all positions, except the primary anchor residue Phe-5^[13] (Figure 2B). Even modifications of P8 and the secondary anchor residues (P2 and P3) were well-tolerated^[14]. Pg substitutions in SIINFEKL were tolerated less broadly^[15], but still non-anchor positions could be substituted without loss of affinity (Figure 2B)^[16].

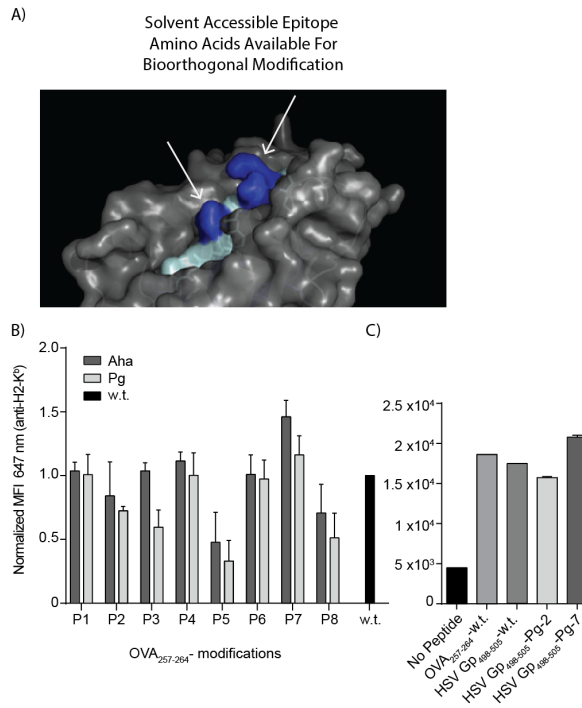


Figure 2. Bioorthogonal Antigens. A) Crystal structure of epitopes within MHC-I complexes allow the prediction of solvent accessible residues available for bioorthogonal modification. Here OVA₂₅₇₋₂₆₄ in H2-K^b with solvent accessible positions 4 and 7 highlighted in blue. B) H2-K^b-rescue by bioorthogonal analogues of SIINFEKL: peptides were exogenously loaded on RMA-S with 1 μ M of the indicated bioorthogonal rescue peptides at 37 °C for 4h to allow affinity- dependent stabilization of MHC-I. Positions 1, 4, 6, and 7 can be modified with both azides and alkynes without affecting MHC-I binding affinity and additionally positions 2, 3 and 8 also tolerated azide substitutions. Data obtained from experiments were normalized to the corresponding control of each sample, where the control values were set to equal 1 to account for batch-to-batch variation of MHC-expression on RMA-S cells. All error bars represent the SD of the mean from 3 independent experiments. C) MHC-I stabilization on RMA-S cells of the non-ligatable and ligatable variants of HSV-Gp₄₉₈₋₅₀₅ modified with Pg at the indicated positions: binding of these epitopes is similar to that of the wildtype epitope.

None of the modified antigens were recognized by the SIINFEKL cognate T cell clone B3Z except for Pg-8 (Figure 3). Binding of the TCR-like antibody that is specific for the peptide SIINFEKL in complex with H2-K^b (antibody 25-D1.16^[3]) was observed and found to be in alignment with the known contact sites from the crystal structure of the complex^[17]: modifications of P1-P4 (known not to interact with the antibody) were tolerated, whereas modifications of the antibody contact positions P5-P8 abolished 25-D1.16-binding (Figure 4). This discrepancy between B3Z and 25-D1.16 binding highlights the difference in fine specificity between antibody and TCR^[17].

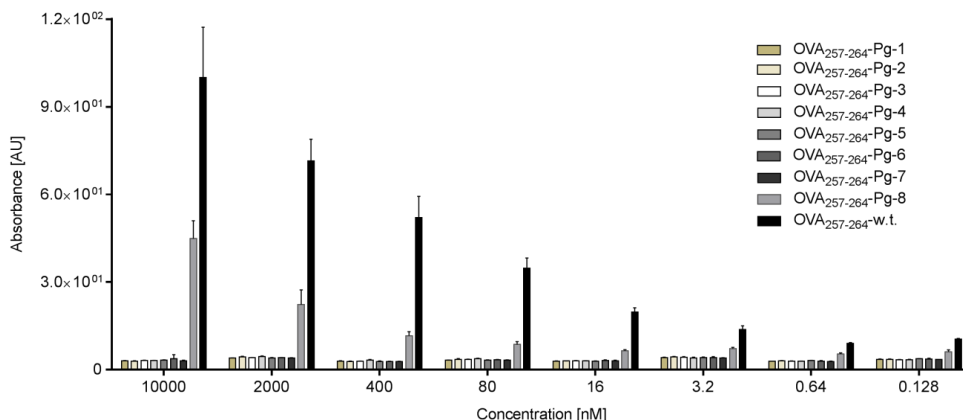


Figure 3. Reactivity of biorthogonal antigens with the SIINFEKL-specific T cell clone B3Z in T cell assay of Pg-modified SIINFEKL. Peptides were serially diluted 1:5 from 10 μ M and incubated with B3Z using standard conditions^[2]. Pg-modified SIINFEKL on the anchor position P8 showed a T cell response, but no other position did.

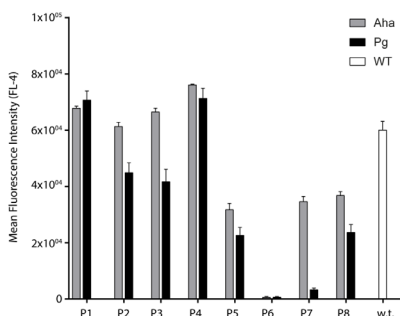


Figure 4. Binding of complex-specific antibody 25-D1.16 to H-2K^b-bound SIINFEKL analogues (1 μ M) on RMA-S cells. Modifications of P1-P4 were tolerated, whereas modifications of the antibody contact positions P5-P8 abolished 25-D1.16-binding.

Optimizing on-surface ligation chemistry

Having shown that positions 1, 4, 6 and 7 can be substituted to Aha and Pg without loss of affinity for H2-K^b, it was next determined whether the bioorthogonal epitopes could be ligated when bound to MHC-I. The suitability of the available azide- and alkyne-reactive bioorthogonal ligation reaction chemistries^[7] was tested by comparing the reactivity of unmodified SIINFEKL and the epitopes modified with either azides or alkynes at the solvent-accessible position P7. First, RMA-S cells were pulsed with the different peptides, then ligated to complementary bioorthogonal fluorophores

under various conditions and analyzed by flow cytometry for the increase in mean fluorescence intensity upon ligation. In these experiments, none of the attempted modifications of azide-containing epitopes, such as the strain-promoted azide-alkyne cycloaddition reactions (SPAAC; Figure 5), Staudinger ligations and copper(I)-catalyzed Huisgen cycloaddition-reactions (cChc; Figure 5) gave statistically significant signal-to-noise ratios using the Alexa Fluors.

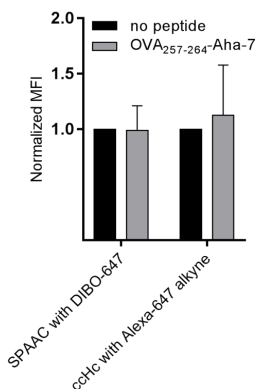


Figure 5. Normalized mean fluorescence intensity (MFI) in FL-4 channel (647 nm) of the strain-promoted azide-alkyne cycloaddition (SPAAC) with Alexa Fluor-647 DIBO alkyne (DIBO-647) and copper(I)-catalyzed azide-alkyne Huisgen cycloaddition (ccHc) with Alexa Fluor-647-alkyne. Both reactions were performed with OVA₂₅₇₋₂₆₄-Aha-7 and no peptide as control. Data obtained from experiments were normalized to the corresponding control of each sample, where the control equals 1. All error bars represent the SD of the mean from at least 2 independent experiments.

It was not until the fluorogenic azide-reactive CalFluor-488 was reported^[18] and applied during these experiments that significant signal-to-noise ratios were obtained. CF-488 is an alkyne reactive fluorophore that has two properties favorable for these experiments, namely a fluorescence quantum yield that increases of 250-fold upon ccHc-ligation and a zwitterionic head group that likely minimizes cell permeability and a-specific binding (**3**, Figure 6A). One downside of this fluorophore is that the fluorophore core is fluorescein-based, which renders it susceptible to quenching upon prolonged exposure to laser-light and makes it less stable to some conditions found in the cell^[19]. This makes it less suitable for microscopy, but readily combined with flow cytometry.

The switch to **3**, in combination with a modified ccHc-reaction protocol in which the cells were first fixed mildly (0.5% paraformaldehyde in PBS) and extensively blocked with 1% BSA and 1% w/v fish gelatin before and after the click-reaction proved optimal to imaging these rare on-cell events. (Figure

6B/D, Figure S1). This did mean that bioorthogonal antigens carrying alkynes in their epitopes were required as the azide-based CalFluors are exclusively alkyne reactive.

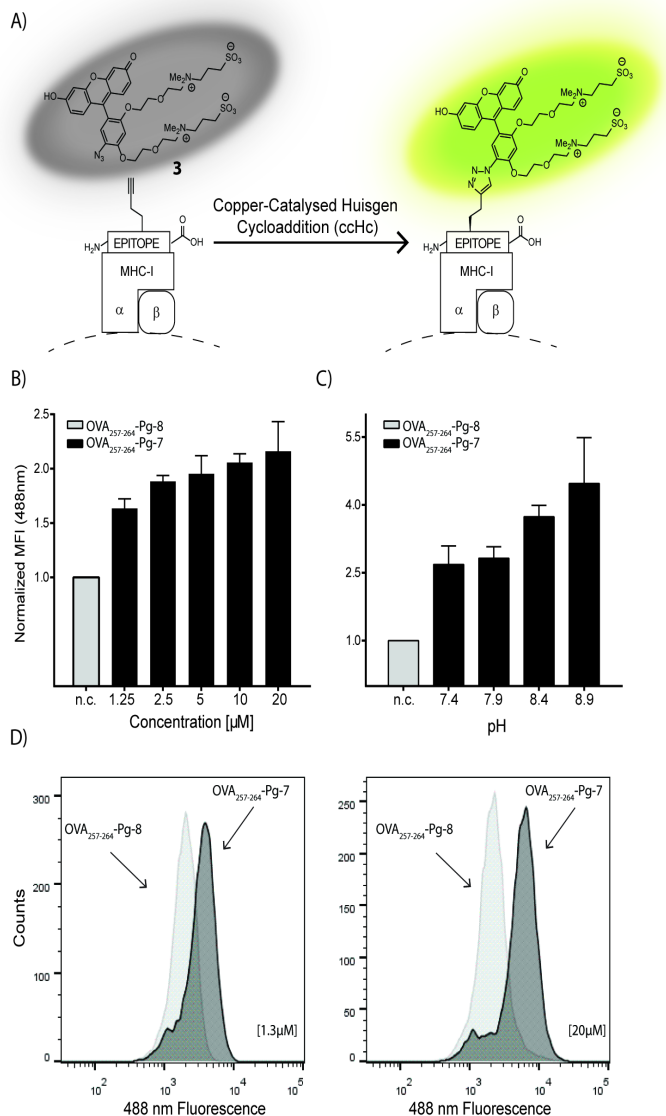


Figure 6. Bioorthogonal Ligation Strategy A) MHC-I loaded bioorthogonal epitopes can be modified using the fluorogenic CalFluor-488 dye after MHC-I loading. B) Serial dilution of a solvent accessible OVA₂₅₇₋₂₆₄-Pg-7 analogue compared to an inaccessible bioorthogonal modification Pg-8 highlights the importance of solvent accessibility in the ligation reaction. C) pH dependence of the CalFluor-ligations: after incubation with 10 µM of epitope peptide and ligation at different pH-values, a dependence of ligation on pH was observed. D) Histograms comparing P7 vs. P8 labeling at 1,3 µM and 20 µM. Data from both experiments were again normalized to the corresponding control of each samples, where the control equals 1. All error bars represent the SD of the mean from 2 independent experiments. n.c.- normalized control.

The ligation reaction showed a strong dependence on solvent accessibility of the amino acid side chain as determined from the reported crystal structure of OVA₂₅₇₋₂₆₄ presented on H2-K^b[²⁰]: OVA₂₅₇₋₂₆₄-Pg-8 (of which the Pg-sidechain likely resides in a hydrophobic pocket; Figure 8A) showed no labeling even at very high peptide

concentrations (up to 20 μM). This contrasts with OVA₂₅₇₋₂₆₄-Pg-7, which carries the bioorthogonal sidechain in a solvent exposed area. This epitope showed concentration dependent ligation efficiency (Figure 6B). This supports the hypothesis that the bioorthogonal peptides indeed react whilst bound to H2-K^b, rather than come out of the binding groove, react, and reenter the binding groove. The reaction also showed an increase in reactivity with an increase in pH (Figure 6C), likely due to the reported increased stability of CalFluor at higher pH-values^[18].

To assess whether fixation conditions used for the cChc permeabilized the cells, resulting in labeling of intracellular pMHC-complexes undergoing recycling^[21], the modification reaction on unfixed live cells was executed. Using short reaction times, similar labeling for live cell and fixed cell labeling was obtained, suggesting that the contribution of intracellular labeling of recycling pMHC-complexes does not contribute to the overall signal observed in these experiments (Figure 7).

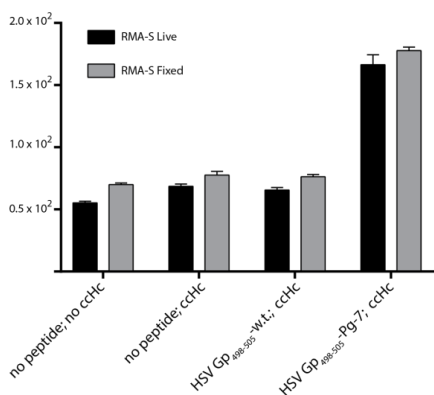


Figure 7. Comparison of cChc conditions on cells fixed with 0.5% PFA to cChc reaction performed on live cells (for these reactions the reaction time was reduced to 15 minutes to prevent permeabilization due to cell death). Cells were loaded with HSV Gp₄₉₈₋₅₀₅-Pg-7 (10 μM) and HSV Gp₄₉₈₋₅₀₅-w.t. (10 μM) and either fixed before cChc, or used under live cell cChc-conditions. Assay was set up in triplicate with all error bars correspond to SD of the mean.

also be ligated, the focus went on epitopes for which crystal structures are known and found. The nucleoprotein₅₂₋₅₉ epitope from the vesicular stomatitis virus (RGVYQGL)^[13, 23] also showed significant labeling when modified at the solvent-accessible residues P4 and P7 (Figure 8C). A second disease-relevant viral epitope, Herpes simplex virus (HSV) glycoprotein B₄₉₈₋₅₀₅ (HSV-Gp₄₉₈₋₅₀₅)^[24] also showed reactivity in line with the crystal structure: solvent accessible P4 and P7 could be ligated and solvent inaccessible P2 could not (Figure 9A/D). MHC-affinity of these peptides was identical to the w.t.-HSV-epitope and to SIINFELK (Figure 2C).

With these optimized ligation conditions in hand, a positional scan of cChc-reactivity of all positions in OVA₂₅₇₋₂₆₄ on RMA-S was performed and, again quantified by flow cytometry (Figure 8B). These experiments showed a strong correlation of reactivity with solvent-accessibility (as estimated from the reported crystal structure^[14]; Figure 8): solvent-accessible^[22] positions P4, and P7 showed significant signal-to-noise ratios, whereas P1, P2, P3, P5 and P8 showed no signal over background.

Application to other H2-K^b-binding epitopes

To determine whether the above strategy was restricted only to SIINFELK variants, or whether other H2-K^b-binding epitopes could

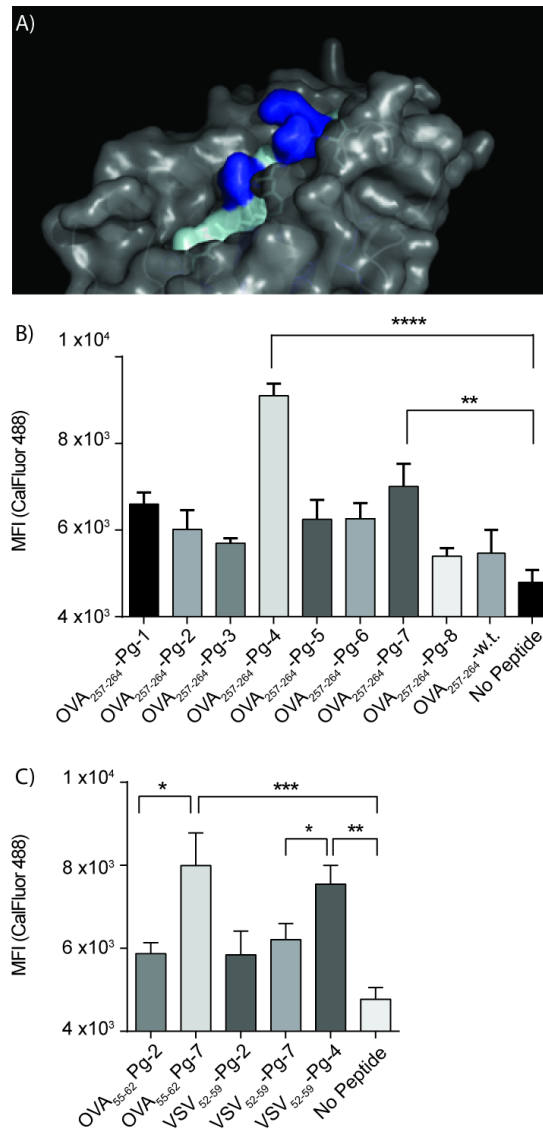


Figure 8. Bioorthogonal modification of peptide-MHC-I complexes. A) Crystal structure of OVA₂₅₇₋₂₆₄ in H2-K^b with solvent accessible positions 4 and 7 highlighted in dark blue and solvent inaccessible positions in light blue. B) Bioorthogonal ligation of each of the positions in the model antigen SIINFEKL substituted with Pg using CalFluor-488^[18]. Solvent accessible positions P4 and P7 gave significant ligations. Solvent inaccessible residues cannot be modified. C) Other epitopes that bind H2-K^b and can be ligated in a cChC-reaction in solvent accessible positions: P7-position of a second H2-K^b-binding ovalbumin, for which no TCR-reagents are available, OVA₅₅₋₆₂, and P4 and P7 position of VSV₅₂₋₅₉ after incubation of RMA-S with 10 μM of the bioorthogonal epitopes. Assays were set up in triplicate with *p ≤ 0.05, **p ≤ 0.01, ***p ≤ 0.001 and ****p ≤ 0.0001. All error bars correspond to SD of the mean.

Finally, it was determined whether the approach could be used to determine MHC-loading of epitopes for which no TCR- or antibody reagents exist. Therefore, another reported H2-K^b binding peptides from OVA, for which no T-cell reagents have been reported, despite a reported affinity^[22] for H2-K^b haplotype MHC-I^[25], namely OVA₅₅₋₆₂

was evaluated. This peptide too showed cHc-reactivity for the predicted solvent accessible modification Pg-7 and not for Pg-2 (Figure 8C).

Due to its robust MHC-I binding, relevance in the immune response against HSV, and robust bioorthogonal labeling, the Pg-7-modified variant of HSV-GpB₄₉₈₋₅₀₅ epitope was explored by performing a serial dilution of HSV-GpB₄₉₈₋₅₀₅-P7 on RMA-S (Figure 9B). A detectable signal over background was still obtained after incubation with 19 nM peptide, which is similar to the sensitivity of detection that can be obtained with a TCR-like antibody^[3] highlighting the power of this research tool for the study of antigen presentation.

However, the sensitivity still does not approach that of T cells. In order for this to become a suitable complementary technique to T cell based reagents this sensitivity should improve to the pM-range at which T cells can detect their cognate peptide antigen.

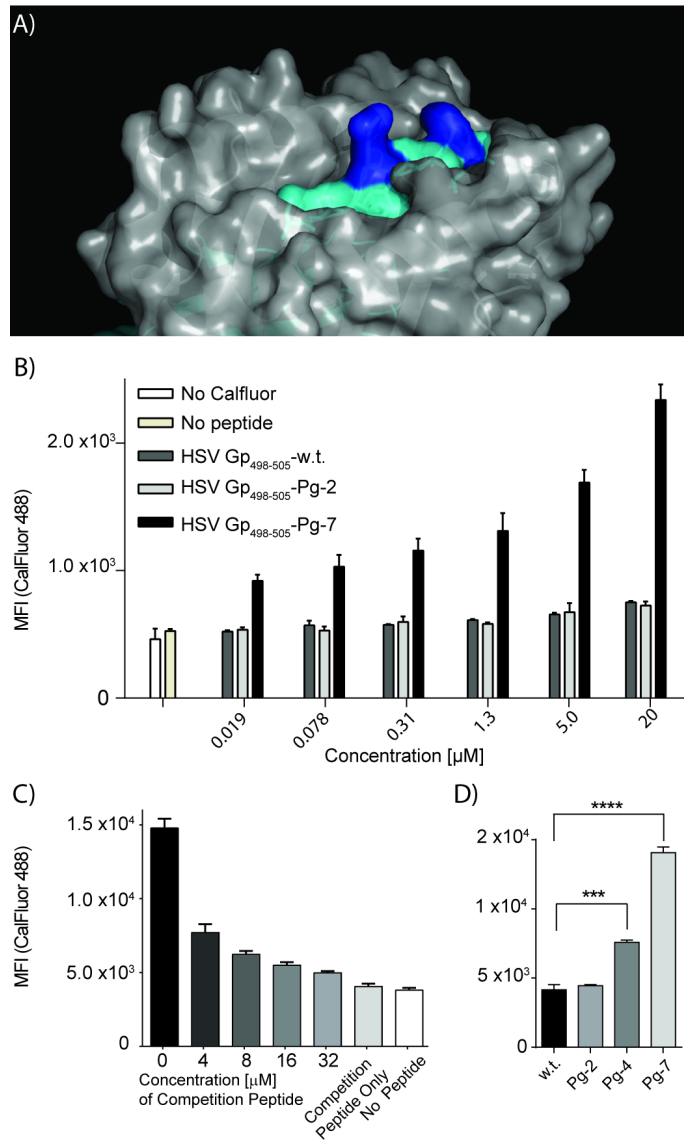


Figure 9. Exploration of the Herpes virus glycoprotein₄₉₈₋₅₀₅ epitope for bioorthogonal ligation. A) Crystal structure of HSV-Gp₄₉₈₋₅₀₅ with solvent accessible positions P4 and P7 shown in blue^[23]. B) Serial dilution of bioorthogonal peptides on RMA-S. Assays were set up in triplicate with $***p \leq 0.001$ and $****p \leq 0.0001$. All error bars correspond to SD of the mean. C) Competition with unlabeled H2-K^b-binding epitope showed that the signal resulting from bioorthogonal ligation is reduced upon increasing concentration of competing peptide. As competing peptide w.t. HSV Gp₄₉₈₋₅₀₅ was used. D) Bioorthogonal modification of the Herpes Virus Gp₄₉₈₋₅₀₅ Epitope: position 7 is most readily reacted in a ligation reaction; Figure S2 shows the raw data for this figure.

To assess the application of the approach to imaging bioorthogonal epitope peptides, the labeling on non-TAP deficient cell lines was attempted. The growth factor dependent dendritic cell line D1^[26] was used as these cells have active TAP-transporter complexes (unlike RMA-S cells); they are loaded with higher affinity

peptides, making the exchange of exogenous peptides proceed with lower efficiency. Despite this limitation, the exchange and ligation of bioorthogonal peptides on these cells could still be detected, albeit with lower signal-to-noise ratios (Figure 10). As for the RMA-S experiments, only peptides modified in solvent-accessible positions once bound to MHC-I showed effective bioorthogonal ligation.

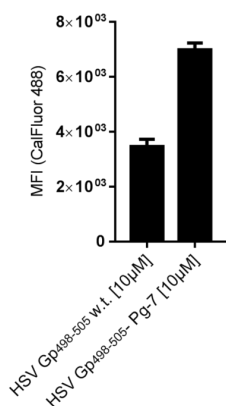


Figure 10. *ccHc* of HSV *Gp*₄₉₈₋₅₀₅-loaded D1-cells. Ligation characteristics were the same as for RMA-S labeling, with HSV *Gp*₄₉₈₋₅₀₅ w.t. control peptide showing minimal labeling, where the solvent exposed P7 labeled strongly. Data obtained from experiments were normalized to the corresponding control of each samples, where the control equals 1. All error bars represent the SD of the mean from 2 independent experiments.

Reactivity of MHC-bound epitopes

To determine what percentage saturation of the 10^5 MHC-I^[27] could be detected, a competition experiment was performed: bioorthogonal peptides were co-incubated with increasing concentrations of unlabeled control peptides (Figure 9C). Bioorthogonal ligation yields indeed showed an inverse correlation with concentration of the unlabeled competition peptide. However, even at a concentration of competing peptide of 32 µM, detectable signal could be observed. Presuming equal affinity of the two peptides for MHC-I, this means that the peptide could be detected at <10% saturation level within the H2-K^b peptide binding groove, suggesting this approach could be used to image 10^4 molecules per cell.

Taken together, the here presented data suggest that bioorthogonal epitopes can bind and be quantified within MHC-complexes at physiologically relevant concentrations and may serve as a useful tool for studying pMHC-I biology on the surface of cells. The requirement is that non-anchor residues in solvent-accessible positions are modified, which results in peptides capable of both binding MHC-I and of being ligated using a fluorogenic *ccHc*-variant.

Super-resolution approaches to visualize bioorthogonal epitopes

A major limitation that was observed for the above approach was that – using the concentrations required to obtain a signal in conventional confocal microscopy – background fluorescence was too high to image peptide appearance. Recent years have seen a surge in the development of diffraction-limit breaking microscopy techniques which use a plethora of elegant physical tricks to break the diffraction barrier^[28] to obtain an image at high resolution and a nanometer localization precision of a single fluorescent molecule^[29]. One of those techniques is a stochastic optical reconstruction microscopy (STORM)^[30] with a resolution of ~20 nm which is

an order of magnitude below the diffraction limit^[31]. The enhanced resolution is achieved through the precise localization of single fluorescent molecules that can be switched on between a fluorescent and a dark state that allow for separating in time the otherwise spatially overlapping light diffractions of the fluorescent molecules^[32]. By repeatedly switching 'on' and 'off' the fluorescent molecules and overlaying the resulting localizations, a super-resolution image can be reconstructed (Figure 11)^[33].

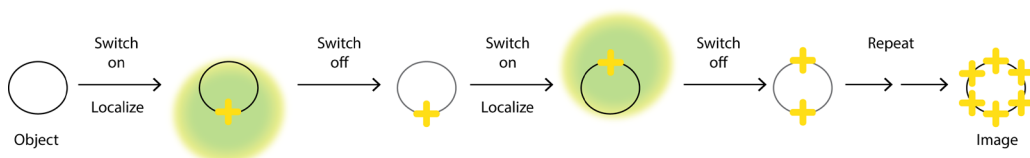


Figure 11. The principle of stochastic optical reconstruction microscopy (STORM). STORM exploits fluorescent dyes that can be switched between fluorescent and dark states which enables for determining their positions with high precision in every snapshot. The process is repeated until all the fluorescent dyes are exhausted due to photo-bleaching. The positions of localized dyes are indicated with yellow crosses. The final super-resolution image is reconstructed from the all measured positions of the fluorescent dyes (Adapted from Dempsey et. al., Nat. Meth. (2011)).

It was thus postulated that STORM-based methods, could improve the signal to noise ratio to allow the detection of peptides using non-fluorogenic, microscopy compatible fluorophores.

However, as it was already found that even the sulfonated Alexa-dyes gave too much background, an approach applied in correlative light-electron microscopy to enhance signal of low numbers of fluorophores was used to isolate surface-signal from intracellular signal^[34]: first all bioorthogonal groups in the cell were modified with a

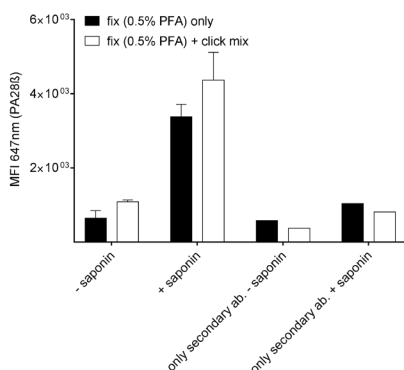


Figure 12. The cHc conditions did not permeabilized the D1 cells to an antibody (~150 kDa), which was assessed by quantifying the mean fluorescence intensity of the cytosolic antibody (PA28β) in the presence and absence of the permeabilizing agent – saponin (0.1 %). Assay was set up in triplicate. All error bars correspond to SD of the mean.

small molecule fluorophore (Alexa Fluor-488) using the cHc-reaction (giving random intracellular labeling). Then, to selectively image the cell-surface population only of the fluorophore, an anti-Alexa-488 antibody to which cells have not become permeable during fixation and cHc was added (Figure 12), which in turn could be visualized using Alexa Fluor-647-conjugated protein A (Figure 13). This latter fluorophore has excellent properties for STORM and in this manner, could not only intracellular background be eliminated, but also an enhancement of the cell surface signal be achieved.

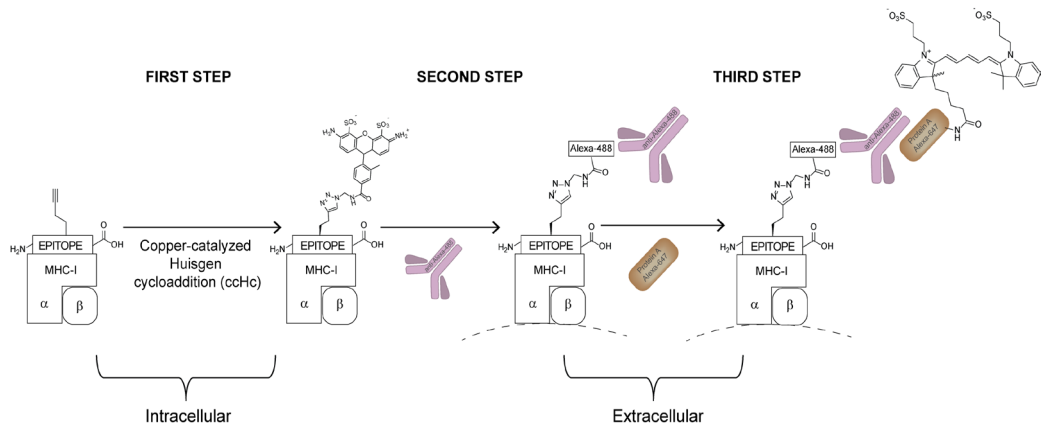


Figure 13. Schematic overview of the technique that allows for imaging both the intracellular and cell-surface pool of antigen in a single experiment. Bioorthogonal labeling was performed using the Alexa Fluor-488 azide in cHc reaction followed by anti-Alexa Fluor-488 antibody binding step and finally by visualizing the antibody with Alexa Fluor-647-conjugated protein A.

To assess whether this three-step labeling could work, the minimal epitopes that showed most robust labeling in the above described CalFluor-FACS-experiments were used for the preliminary STORM imaging experiments. For that the OVA model antigens modified with Propargylglycine (Pg) at position 4 and 7 within the epitope (SIIP**Pg**FEKL and SIINFEP**Pg**L) and the second viral epitope, Herpes simplex virus (HSV) modified with Pg at position 7 (SSIEFAP**Pg**L) were chosen (Table S1). As an initial test to determine whether these minimal epitope peptides could be labeled and selectively imaged at the cell surface, the OVA₂₅₇₋₂₆₄-Pg-4, -Pg-7 and HSV Gp₄₉₈₋₅₀₅-Pg-7 (as well as their non-bioorthogonal controls) were incubated with the C57Bl/6-derived dendritic like cell line DC2.4^[35] at various concentrations for ~1.5h at 37°C followed by wash, fixation and exposure to the cHc labeling using Alexa Fluor-488, followed by anti-Alexa Fluor-488 antibody and finally the Alexa Fluor-647 conjugated protein A. The cells were first imaged on super resolution microscopy using an epi-fluorescence illumination phase (without using quenching-blinking) with a white-light LASER. These images revealed that using this three- step labeling approach, the HSV Gp₄₉₈₋₅₀₅-Pg-7 peptide could be labeled and imaged at the cell surface of the DC2.4 cells with a substantial signal to noise ratio (Figure 14; no significance could be determined as only one biological replicate was performed).

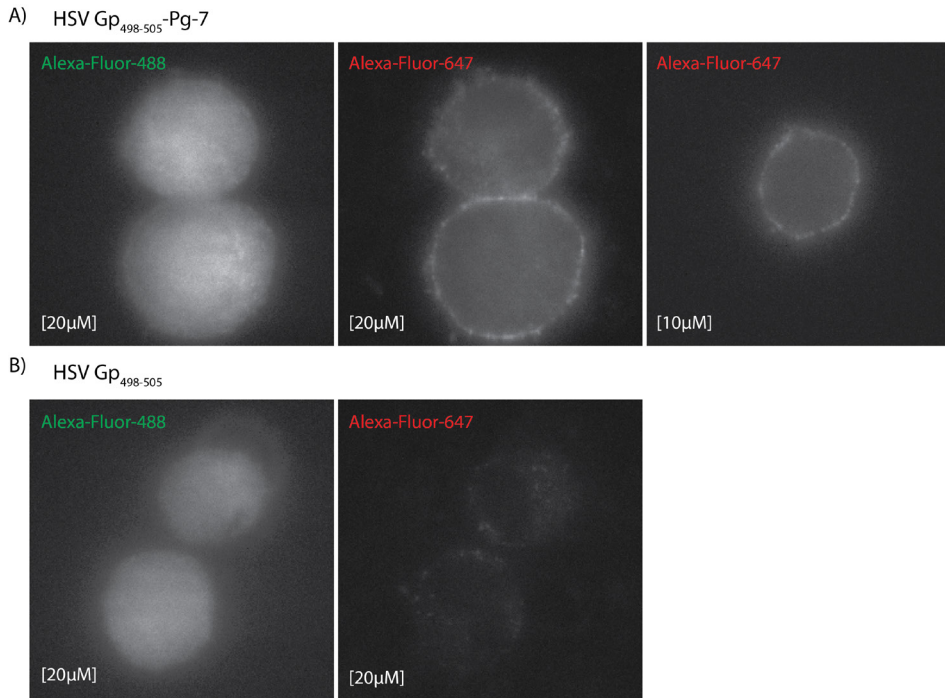


Figure 14. Epi-fluorescence illumination phase with white-light microscopy images of A) HSV Gp₄₉₈₋₅₀₅-Pg-7 at 20 μ M as well as at 10 μ M provided a substantial signal to noise ratio as compared to its non-bioorthogonal control B) DC2.4 were incubated with the indicated peptides for 1.5h followed by wash with medium complete, fixation and exposure to the three- step labeling as described above.

Interestingly, the fluorescence signal obtained from OVA₂₅₇₋₂₆₄-Pg-4 and -Pg-7 was much weaker than that of HSV Gp₄₉₈₋₅₀₅-Pg-7 (Figure S3). The origin of this lack of signal remains unknown, but could be the result of less efficient cChc-labelling of the OVA-peptides (as also observed in the FACS-experiments) perhaps due to diminished accessibility of the side-chains. Alternatively, it can be postulated that the HSV Gp₄₉₈₋₅₀₅-Pg-7 has stronger α -specific cell surface binding, resulting in an inflated signal. This is, however, something that has to be further explored in future experiments.

The successful trial of imaging Gp₄₉₈₋₅₀₅-Pg-7 peptide led to the execution of the super resolution microscopy of the peptide and its non-bioorthogonal control using the blinking properties of Alexa Fluor-647 (Figure 15).

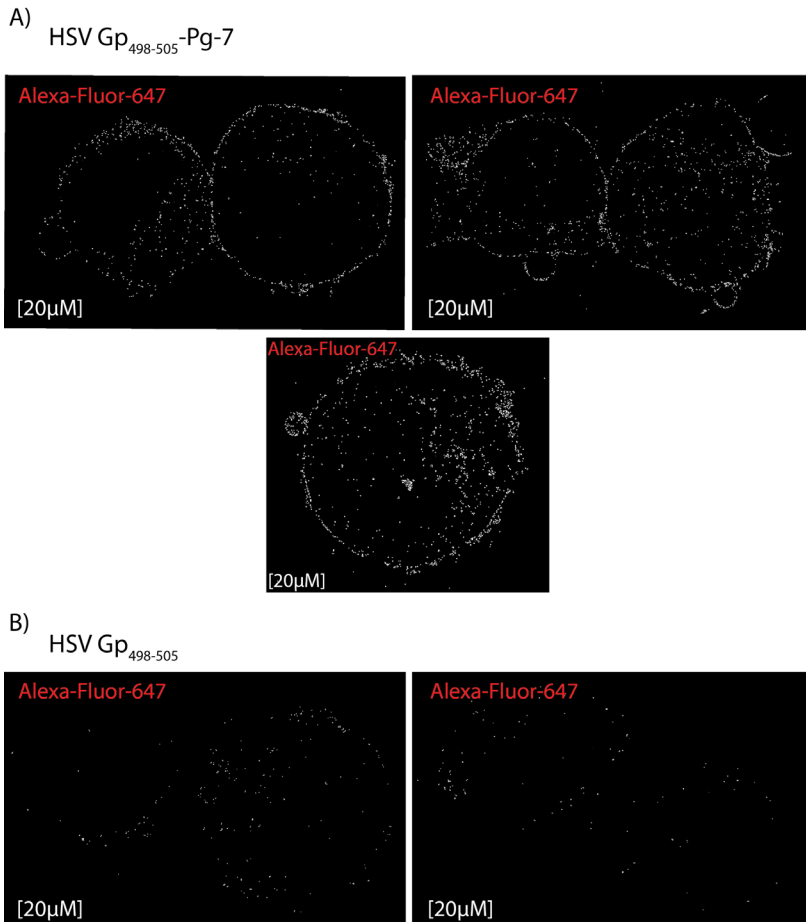


Figure 15. STORM imaging of HSV Gp₄₉₈₋₅₀₅-Pg-7 allowed for visualization of the peptide at the cell surface. DC2.4 were incubated with HSV Gp₄₉₈₋₅₀₅-Pg-7 and w.t. (20μM) for 1.5h followed by wash with medium complete, fixation and exposure to the three- step labeling as described above.

These preliminary results indicate that STORM-imaging of epitopes can in potential result in the localization of individual fluorophores on the cell surface. However, first the lack of broad reactivity in this assay of other epitopes must be explored, as well as the localization within the MHC-I complex confirmed.

3.3 Conclusion

The bioorthogonal ligation using fluorogenic Calfluor-488 in combination with a Cu(I)-catalyzed Huisgen cycloaddition reaction allowed for the bioorthogonal epitopes to be quantified within MHC-complexes at physiologically relevant concentrations. This approach can make the bioorthogonal epitopes a useful addition to the antigen presentation toolkit as quantification of antigenic peptides for which no T cell (or other) reagents are available, such as the H2-K^b-binding peptide OVA₅₅₋₆₂ reported herein. The broad scope of bioorthogonal chemistry^[36] and the breadth of tools

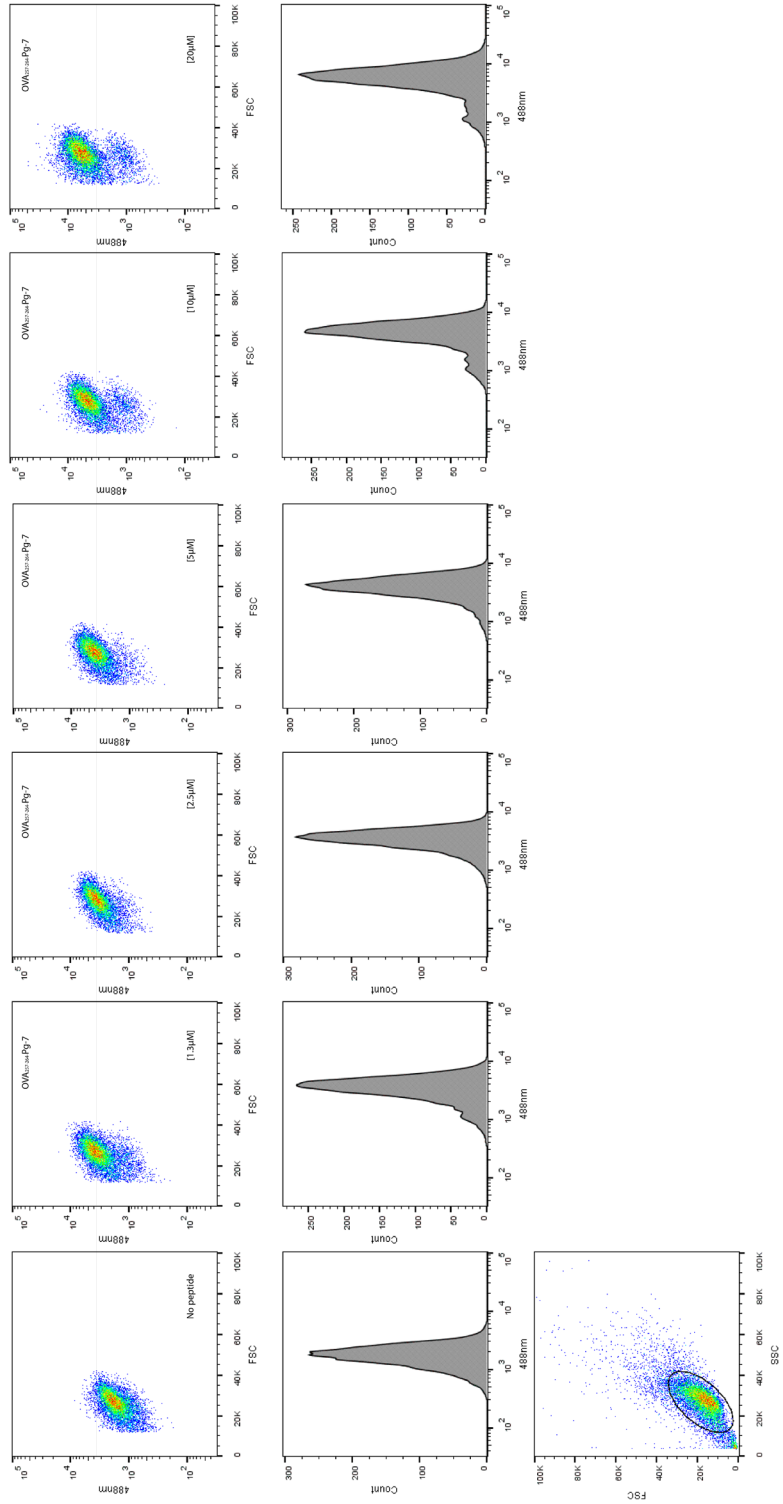
available to incorporate minimal bioorthogonal functionalities into peptides, proteins^[37] from both prokaryotic expression systems^[38], as well as eukaryotic ones^[39], and whole cells^[9a] including various pathogens^[40] suggests that this approach could potentially extend to study the rates at which antigen presenting cells process exogenous antigens for the activation of CTLs – so-called antigen cross-priming. The stability of bioorthogonal groups would be very beneficial here, as antigens encounter some of the harshest conditions known in the human body in the endo-lysosomes of antigen presenting cells, with both strongly oxidizing^[41] and reducing conditions found during cross-presentation^[42].

The preliminary results of the STORM imaging of bioorthogonal epitopes using the three-step labeling revealed a potential to localize and later quantify the epitopes on the cell surface. In the future, this approach can be applied to the synthetic long peptides (SLPs) in order to visualize the intra and extracellular localization of the antigen during antigen cross-presentation.

3.4 Supporting table and figures

<i>Position of Handle</i>	<i>Peptide Sequence</i>	<i>Peptide Name</i>	<i>Source</i>
P1	P gIINFEKL	OVA ₂₅₇₋₂₆₄ -Pg-1	Ovalbumin (<i>Gallus gallus</i>)
P2	S PgIINFEKL	OVA ₂₅₇₋₂₆₄ -Pg-2	Ovalbumin (<i>Gallus gallus</i>)
P3	S I P gNFEKL	OVA ₂₅₇₋₂₆₄ -Pg-3	Ovalbumin (<i>Gallus gallus</i>)
P4	S I I PgFEKL	OVA ₂₅₇₋₂₆₄ -Pg-4	Ovalbumin (<i>Gallus gallus</i>)
P5	S I I N P gEKL	OVA ₂₅₇₋₂₆₄ -Pg-5	Ovalbumin (<i>Gallus gallus</i>)
P6	S I I N F PgKL	OVA ₂₅₇₋₂₆₄ -Pg-6	Ovalbumin (<i>Gallus gallus</i>)
P7	S I I N F E P gL	OVA ₂₅₇₋₂₆₄ -Pg-7	Ovalbumin (<i>Gallus gallus</i>)
P8	S I I N F E K Pg	OVA ₂₅₇₋₂₆₄ -Pg-8	Ovalbumin (<i>Gallus gallus</i>)
P1	A haIINFEKL	OVA ₂₅₇₋₂₆₄ -Aha-1	Ovalbumin (<i>Gallus gallus</i>)
P2	S AhaIINFEKL	OVA ₂₅₇₋₂₆₄ -Aha-2	Ovalbumin (<i>Gallus gallus</i>)
P3	S I A haNFEKL	OVA ₂₅₇₋₂₆₄ -Aha-3	Ovalbumin (<i>Gallus gallus</i>)
P4	S I I AhaFEKL	OVA ₂₅₇₋₂₆₄ -Aha-4	Ovalbumin (<i>Gallus gallus</i>)
P5	S I I N A haEKL	OVA ₂₅₇₋₂₆₄ -Aha-5	Ovalbumin (<i>Gallus gallus</i>)
P6	S I I N F AhaKL	OVA ₂₅₇₋₂₆₄ -Aha-6	Ovalbumin (<i>Gallus gallus</i>)
P7	S I I N F E A haL	OVA ₂₅₇₋₂₆₄ -Aha-7	Ovalbumin (<i>Gallus gallus</i>)
P8	S I I N F E K Aha	OVA ₂₅₇₋₂₆₄ -Aha-8	Ovalbumin (<i>Gallus gallus</i>)
P2	K PgVRFDKL	OVA ₅₅₋₆₂ -Pg-2	Ovalbumin (<i>Gallus gallus</i>)
P7	K VVRFD P gL	OVA ₅₅₋₆₂ -Pg-7	Ovalbumin (<i>Gallus gallus</i>)
P2	R PgYVYQGL	VSV ₅₂₋₅₉ -Pg2	Vesicular Stomatitis Virus Nucleoprotein
P4	R G Y PgGQGL	VSV ₅₂₋₅₉ -Pg4	Vesicular Stomatitis Virus Nucleoprotein
P7	R G Y YQ P gL	VSV ₅₂₋₅₉ -Pg7	Vesicular Stomatitis Virus Nucleoprotein
P2	S PgIEFARL	HSV Gp ₄₉₈₋₅₀₅ -Pg-2	Herpes Simplex Virus GpB
P4	S S I PgFARL	HSV Gp ₄₉₈₋₅₀₅ -Pg-4	Herpes Simplex Virus GpB
P7	S SIEFA P gL	HSV Gp ₄₉₈₋₅₀₅ -Pg-7	Herpes Simplex Virus GpB

Table S1. Overview of all modified epitope peptides used in this study.



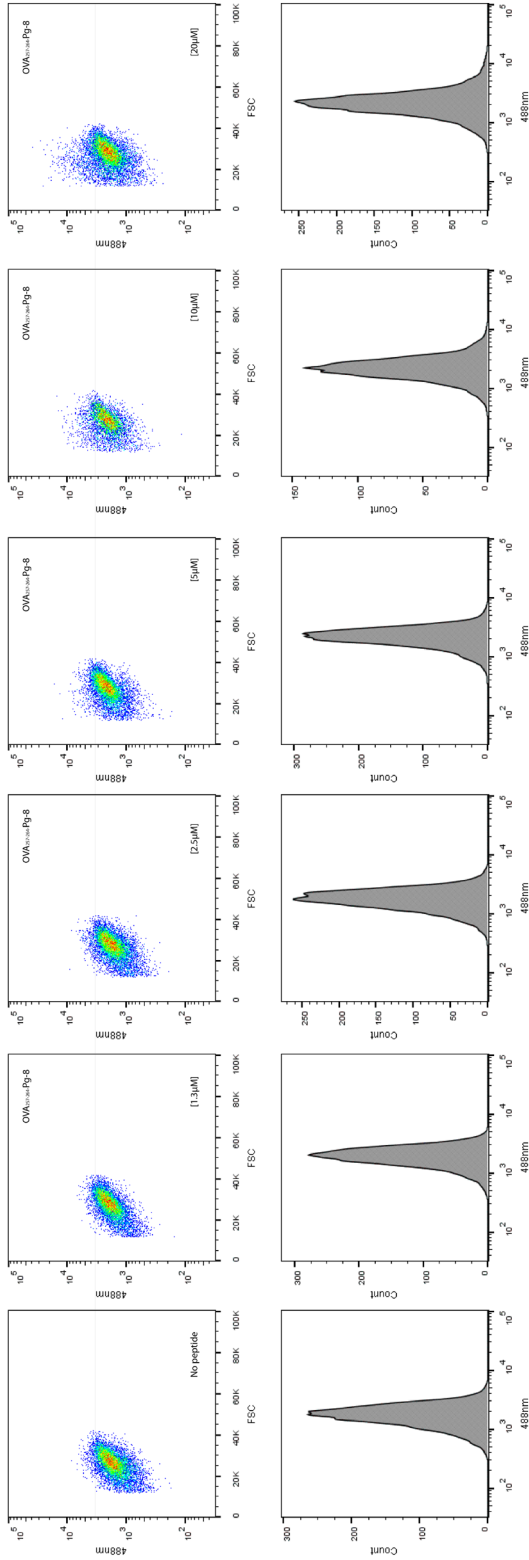


Figure S1: (Previous two pages); Flow cytometry data underpinning Figure 6B: Fluorescence intensity in the FL-1-channel (488 nm) on gated cells was plotted for different peptide concentrations. A) FACS plots of P7-modifications. B) FACS plots of P8-modifications.

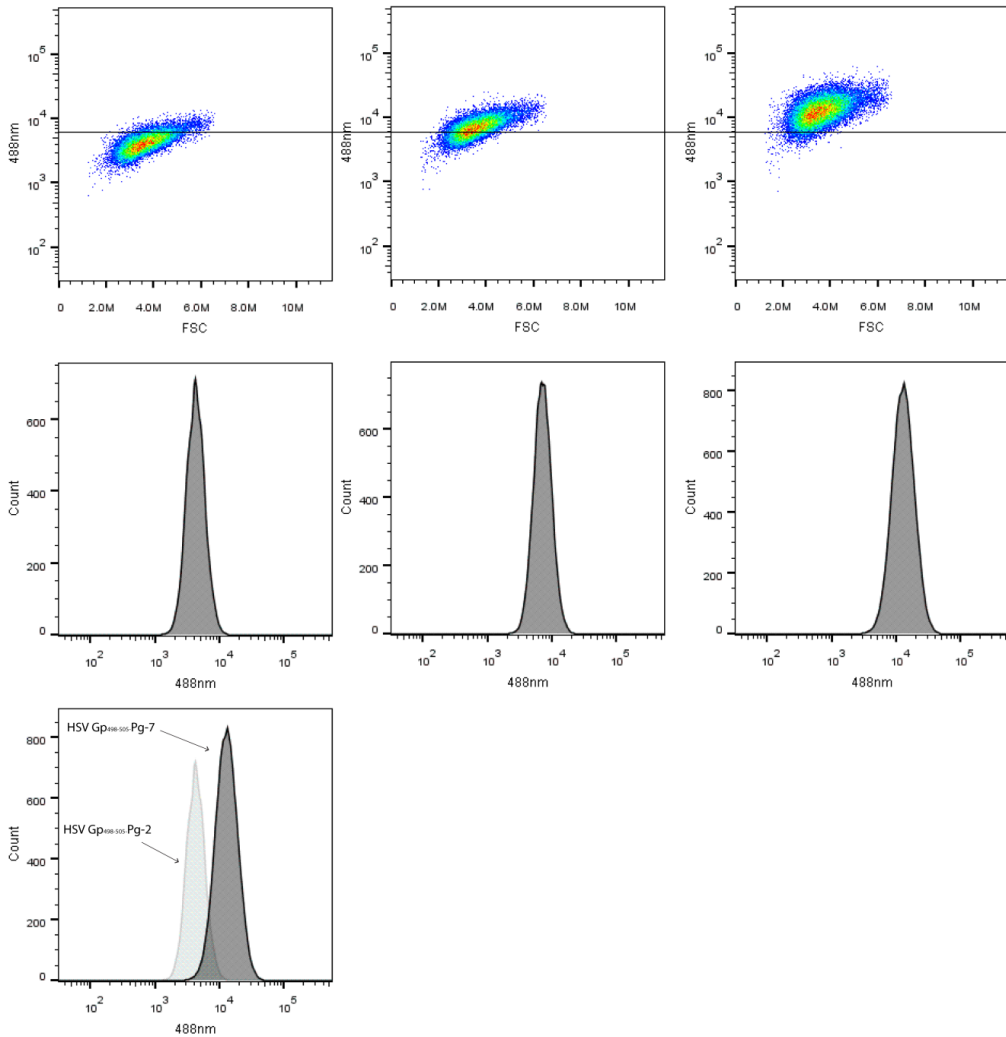
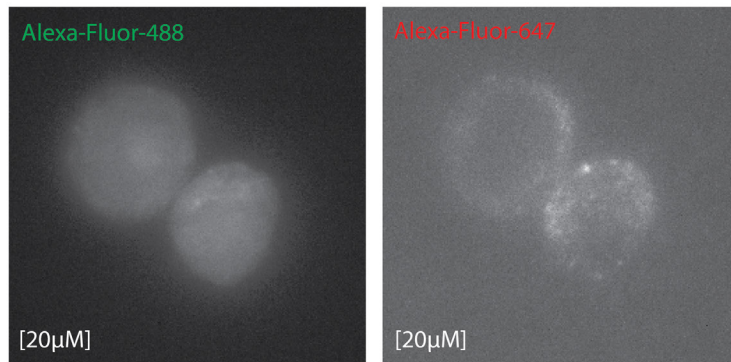
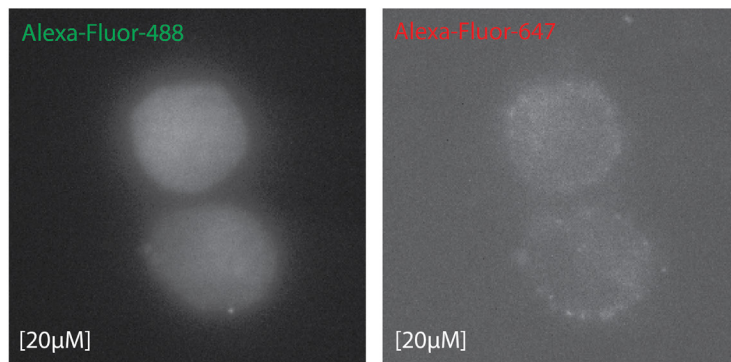


Figure S2. FACS data underpinning Figure 9D. FACS plots and corresponding histograms of HSV Gp₄₉₈₋₅₀₅-Pg-2 (left panel), -Pg-4 (middle panel) and -Pg-7 (right panel).

A) OVA₂₅₇₋₂₆₄-Pg-4



B) OVA₂₅₇₋₂₆₄-Pg-7



C) OVA₂₅₇₋₂₆₄

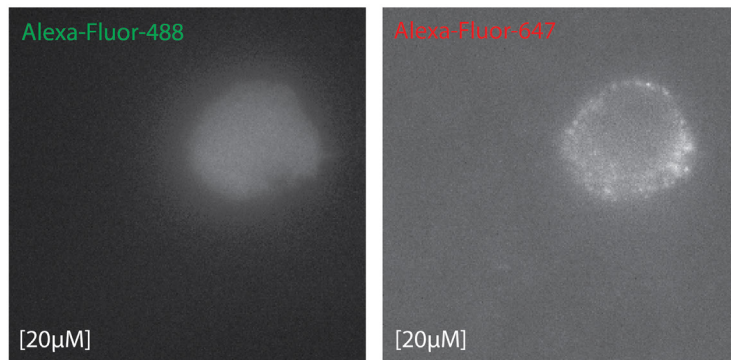


Figure S3. Epi-fluorescence illumination phase with white-light microscopy images of A) OVA₂₅₇₋₂₆₄-Pg-4 at 20 μ M as well as B) OVA₂₅₇₋₂₆₄-Pg-7 at 20 μ M did not show any signal to noise ratio as compared to their non-bioorthogonal control. C) DC2.4 were incubated with the indicated peptides for 1h followed by wash with medium complete, fixation and exposure to the three- step labeling as described above.

3.5 Experimental section

Reagents:

Azidohomoalanine and Propargylglycine-Fmoc were purchased from Anaspec. Tris(3-hydroxypropyl-triazolylmethylamine) (THPTA) was purchased from Sigma-Aldrich, as were all other reagents at the highest available grade. Mouse Anti-Mouse H-2K^b (B8-24-3 clone) was made in-house. 25-D1.16-APC conjugated was purchased from eBioscience (Cat. #: 12-5743-81) (APC conjugated in-house). Secondary antibody (Goat anti-Mouse IgG conjugated to Alexa Fluor-647 (catalogue number: A-21235) was purchased from Thermo Fisher Scientific. All solvents were purchased from Biosolve Ltd. Phosphate buffered saline (PBS) is 5 mM KH₂PO₄, 15 mM Na₂HPO₄, 150 mM NaCl, pH 7.4. Alexa Fluor-488 azide (catalogue number: A10266), AlexaFluor-488 polyclonal antibody (catalogue number: A-11094) and Alexa Fluor-647-conjugated protein A (catalogue number: P21462) as well as donkey anti-goat IgG (H+L) secondary antibody, Alexa Fluor-647 (catalogue number: A-21447) were purchased from Thermo Fisher Scientific. PA28β antibody (catalogue number: SC-23642) was purchased from Santa Cruz biotechnology.

Peptide synthesis:

All peptides were synthesized using standard Fmoc Solid Support Chemistry and purified using high performance liquid chromatography (Prep column Gemini C18 110A 150x21.20 5μm) using 15 to 45 % gradient (A: 0.1% TFA in MilliQ H₂O, B: ACN). LC-MS measurements were done on an API 3000 Alltech 3300 with a Grace Vydac 214TP 4,6 mm x 50 mm C4 column and analyzed by electrospray LC-MS analysis on a PE SCIEX: API 3000 LC/MS/MS system using a Gemini 3u C18 110A analytical column (5μ particle size, flow: 1.0 mL/min), on which the absorbance was also measured at 214 and 254 nm. Solvent system for LC-MS: A: 100% water, B: 100% acetonitrile, C: 1% TFA (aq).

Cell culture:

The D1 cell line, a long-term growth factor-dependent immature myeloid (CD11b⁺, CD8α⁻) DC line of splenic origin, derived from a female C57BL/6 mouse which was provided by M. Camps (Leiden University Medical Center) and was cultured as described previously^[43].

The DC2.4 cell line, an adherent C57BL/6 bone marrow derived DC line was kindly provided by Dr. Kenneth Rock (University of Massachusetts Medical School) and cultured as described previously^[35, 44].

CalFluor-488 synthesis:

CalFluor-488 was synthesized as described previously^[18].

RMA-S MHC I-binding and stability assays:

RMA-S assays were essentially performed as described previously^[12, 45]. Briefly, RMA-S cells were grown and passaged at 37 °C, 5% CO₂ in RPMI-1440 augmented with 10% FCS and antibiotics. Prior to the experiment, the incubation temperature was lowered to 26 °C for 48 hours (10⁶ cells/mL) to ensure metastable MHC-I surface expression. For affinity tests, cells were incubated with rescue peptides in serum free medium at the indicated concentrations for 4 hours and washed in protein blocking agent (PBA: 5% BSA in PBS + 0.1% w/v NaN₃). For MHC-I peptide complex stability assays, 26°C RMA-S cells were pulsed for 1 hour with respective peptides at the indicated concentrations, and washed thoroughly in ice-cold serum free medium, after which they were placed back at 37 °C and chased for the indicated time.

After each timepoint, cells were fixated in 4% fixation buffer (Cat #420801, Biolegend) for 30 minutes. After this time, the cells were washed with PBA. Both assays were subsequently stained with anti-Mouse-H-2K^b (400 ng/mL; >60 μ L/well) in PBA for 30 minutes on ice, prior to washing with PBA twice. Secondary antibody (Goat anti-Mouse IgG conjugated to AlexaFluor-647; 5 μ g/mL) was added and the cells were again incubated on ice for 30 minutes prior to washing twice with PBA before analysis. Analysis was performed on a BD Accuri™ C6 Plus Flow Cytometer. All flow cytometry data was analyzed using FlowJo v10.1 (Miltenyi Biosciences).

25-D1.16-binding of bioorthogonal epitopes:

RMA-S cells were incubated with a serial dilution of peptides as above. After the 4-hour loading period and blocking, cells were incubated with 25-D1.16-APC conjugated antibody (1.3 μ g/mL; >60 μ L/well, conjugated in-house)^[3] in PBA for 30 minutes on ice, prior to washing with PBA twice. Cells were analyzed by flow cytometry as described above. Fluorescence intensity in the APC-channel was plotted against peptide concentration at 1 μ M (as in Figure 4).

Bioorthogonal modification reactions on RMA-S cells:

RMA-S cells were grown and as described above for the binding assay and plated in 96-well v-bottom microtiter plate (4×10^5 cells/well) in serum free medium and incubated for ~1h at 37°C with respective peptides at the indicated concentrations. After the incubation, the cells were washed twice in PBS and subsequently fixed for 1 hour at RT in 0.5% PFA in PBS (Cat #420801, Biolegend; diluted 1:8) and washed twice more with PBS. Cells were then exposed to the bioorthogonal labeling mixture (1 mM CuSO₄, 10 mM sodium ascorbate, 1 mM THPTA ligand, 10 mM aminoguanidine, 100 mM HEPES, pH 8.4, CalFluor-488 10 μ M). After 45 minutes at RT, the reaction mixture was aspirated and the cells were blocked with 1% BSA and 1% fish gelatin before being washed twice with PBS prior to analysis by flow cytometry. Assays were set up in triplicate, unless otherwise indicated. The statistical significance of the indicated differences was analyzed by the two-tailed student's t-test with the significance specified using *p* values with **p* ≤ 0.05, ***p* ≤ 0.01, ****p* ≤ 0.001 and *****p* ≤ 0.0001. All error bars correspond to SD of the mean.

Reactivity of bioorthogonal SIINFEKL peptides in a B3Z T cell assay:

RMA-s cells were grown as described above and plated in 96-well tissue-culture treated microtiter plate (5×10^4 cells/well) and incubated for 1h at 37°C with SIINFEKL modified peptides at the indicated concentrations, followed by a wash with complete IMDM. After the wash, the T cell hybridoma B3Z cells (5×10^4 cells/well) were added. The RMA-S and T cells were co-cultured for 17 h at 37°C. Stimulation of the B3Z hybridoma was measured by a colorimetric assay using CPRG (chlorophenol red- β -D-galactopyranoside) as a substrate as described^[46].

Competition assay with unlabeled peptide:

RMA-S cells were grown and treated as described above for the bindings assay, prior to loading. Incubation of RMA-S cells with HSV-Gp₄₉₈₋₅₀₅-Pg7 epitopes was performed for 4 hours at 4 μ M, in presence of increasing amounts of w.t. HSV-Gp₄₉₈₋₅₀₅ at the indicated concentrations. The amount of peptide in all samples was equalized to 36 μ M by adding the lacking amount of adenoviral H-2D^b binding epitope of the human Adenovirus 5 E1a protein Ad10₂₃₄₋₂₄₃^[47]. Bioorthogonal ligation was subsequently performed as described above.

Permeability assay:

D1s were collected using 2mM EDTA in PBS, fixed in 0.5% PFA in PBS for 1h at RT and exposed to the click cocktail mix (as described previously but without a fluorophore) for 1h at RT. After the wash, cells were permeabilized with 0.1% saponin in 1% BSA in PBS (control cells were incubated without saponin throughout whole experiment) for ~20min at RT followed by incubation with PA28 β antibody (final concentration 2 μ g/mL) in 0.1% saponin in 1% BSA in PBS for 30min on ice followed by wash and incubation with the donkey anti-goat IgG (H+L) secondary antibody (0.5 μ g/mL) in 0.1% saponin in 1% BSA in PBS for 30min on ice followed by wash and analysis by Guava EasyCyteTM flow cytometry (Merck Millipore) and using FlowJo v10.1.

The three- step labeling:

The DC2.4 cells were incubated with respective peptides, at the indicated concentrations and times. After the incubation, the cells were washed ones with medium complete and ones with PBS. The cells were fixed by adding 2% PFA in PBS for 20min at RT followed by double wash with PBS. The fixed DC2.4 were then exposed to the bioorthogonal labeling mixture (1 mM CuSO₄, 10 mM sodium ascorbate, 1 mM THPTA ligand, 10 mM aminoguanidine, 100 mM HEPES, pH 8.4, Alexa Fluor-488-azide 5 μ M). After 1h at RT, the reaction mixture was aspirated and the cells were blocked with 1% BSA and 1% fish gelatin before being washed twice with PBS. Next, the cells were incubated with an Alexa Fluor-488 antibody (final concentration 2 μ g/mL) in 100mM HEPES pH 7.2 supplemented with 1% BSA and 1% fish gelatin for 1h at RT. After the incubation, cells were washed with PBS and blocked with 1% BSA and 1% fish gelatin before being exposed to Alexa Fluor-647-conjugated protein A (final concentration 5 μ g/mL) for 20min at RT followed by PBS wash step and blocking with 1% BSA and 1% fish gelatin.

Stochastic optical reconstruction microscopy and sample preparation:

After the three- step labeling, the samples were exposed to STORM buffer which is composed of 50 mM HEPES buffer (pH=8.5), 1 M NaCl, an oxygen-scavenging system (0.5 mg mL⁻¹ glucose oxidase, 40 μ g mL⁻¹ catalase, 5 wt % glucose) and 200 mM 2-aminoethanethiol.

STORM images were acquired using a Nikon N-STORM system configured for total internal reflection fluorescence (TIRF) imaging. Excitation inclination was tuned to adjust focus and to maximize the signal-to-noise ratio. Alexa Fluor-647 was excited illuminating the sample with the 647 nm (~160 mW) laser line built into the microscope. Fluorescence was collected by means of a Nikon 100x, 1.4NA oil immersion objective and passed through a quad-band-pass dichroic filter (97335 Nikon). 20,000 frames were acquired for the 647 channel and 10,000 frames for the 488 channel (WGA-AF561). Images were recorded onto a 256 \times 256 pixel region (pixel size 160 nm) of a CMOS camera. STORM images were analyzed with the STORM module of the NIS element Nikon software.^[30b]

3.6 References

- [1] J. Karttunen, N. Shastri, *Proc Natl Acad Sci U S A* **1991**, *88*, 3972-3976.
- [2] aB. Laugel, J. M. Boulter, N. Lissin, A. Vuidepot, Y. Li, E. Gostick, L. E. Crotty, D. C. Douek, J. Hemelaar, D. A. Price, B. K. Jakobsen, A. K. Sewell, *J Biol Chem* **2005**, *280*, 1882-1892; bY. Li, R. Moysey, P. E. Molloy, A.-L. Vuidepot, T. Mahon, E. Baston, S. Dunn, N. Liddy, J. Jacob, B. K. Jakobsen, J. M. Boulter, *Nature Biotechnology* **2005**, *23*, 349-354; cW. F. Hoo, M. J. Lacy, L. K. Denzin, E. W. Voss, Jr., K. D. Hardman, D. M. Kranz, *Proc Natl Acad Sci U S A* **1992**, *89*, 4759-4763; dJ. S. Huston, D. Levinson, M. Mudgett-Hunter, M. S. Tai, J. Novotny, M. N. Margolies, R. J. Ridge, R. E. Brucoleri, E. Haber, R. Crea, *Proceedings of the National Academy of Sciences of the United States of America* **1988**, *85*, 5879-5883.
- [3] A. Porgador, J. W. Yewdell, Y. Deng, J. R. Bennink, R. N. Germain, *Immunity* **1997**, *6*, 715-726.
- [4] J. A. Prescher, D. H. Dube, C. R. Bertozzi, *Nature* **2004**, *430*, 873-877.
- [5] W. Ma, Y. Zhang, N. Vigneron, V. Stroobant, K. Thielemans, P. van der Bruggen, B. J. Van den Eynde, *J Immunol* **2016**, *196*, 1711-1720.
- [6] J. W. Yewdell, E. Reits, J. Neefjes, *Nat Rev Immunol* **2003**, *3*, 952-961.
- [7] K. Lang, J. W. Chin, *ACS Chemical Biology* **2014**, *9*, 16-20.
- [8] J. B. Pawlak, G. P. Gentil, T. J. Ruckwardt, J. S. Bremmers, N. J. Meeuwenoord, F. A. Ossendorp, H. S. Overkleeft, D. V. Filippov, S. I. van Kasteren, *Angew Chem Int Ed Engl* **2015**, *54*, 5628-5631.
- [9] aK. L. Kiick, D. A. Tirrell, *Tetrahedron* **2000**, *56*, 9487-9493; bJ. C. M. van Hest, K. L. Kiick, D. A. Tirrell, *Journal of the American Chemical Society* **2000**, *122*, 1282-1288.
- [10] aR. Ekkebus, S. I. van Kasteren, Y. Kulathu, A. Scholten, I. Berlin, P. P. Geurink, A. de Jong, S. Goerdayal, J. Neefjes, A. J. Heck, D. Komander, H. Ovaa, *J Am Chem Soc* **2013**, *135*, 2867-2870; bS. Sommer, N. D. Weikart, U. Linne, H. D. Mootz, *Bioorg Med Chem* **2013**, *21*, 2511-2517.
- [11] P. P. Geurink, L. M. Prely, G. A. van der Marel, R. Bischoff, H. S. Overkleeft, *Top Curr Chem* **2012**, *324*, 85-113.
- [12] H. G. Ljunggren, N. J. Stam, C. Ohlen, J. J. Neefjes, P. Hoglund, M. T. Heemels, J. Bastin, T. N. Schumacher, A. Townsend, K. Karre, et al., *Nature* **1990**, *346*, 476-480.
- [13] D. H. Fremont, M. Matsumura, E. A. Stura, P. A. Peterson, I. A. Wilson, *Science* **1992**, *257*, 919-927.
- [14] D. H. Fremont, E. A. Stura, M. Matsumura, P. A. Peterson, I. A. Wilson, *Proc Natl Acad Sci U S A* **1995**, *92*, 2479-2483.
- [15] K. L. Kiick, R. Weberskirch, D. A. Tirrell, *FEBS Lett* **2001**, *502*, 25-30.
- [16] K. Udaka, K. H. Wiesmuller, S. Kienle, G. Jung, P. Walden, *J Biol Chem* **1995**, *270*, 24130-24134.
- [17] T. Mareeva, E. Martinez-Hackert, Y. Sykulev, *J Biol Chem* **2008**, *283*, 29053-29059.
- [18] P. Shieh, V. T. Dien, B. J. Beahm, J. M. Castellano, T. Wyss-Coray, C. R. Bertozzi, *J Am Chem Soc* **2015**, *137*, 7145-7151.
- [19] J. Mahmoudian, R. Hadavi, M. Jeddi-Tehrani, A. R. Mahmoudi, A. A. Bayat, E. Shaban, M. Vafakhah, M. Darzi, M. Tarahomi, R. Ghods, *Cell Journal (Yakhteh)* **2011**, *13*, 169-172.
- [20] D. H. Fremont, E. A. Stura, M. Matsumura, P. A. Peterson, I. A. Wilson, *Proceedings of the National Academy of Sciences of the United States of America* **1995**, *92*, 2479-2483.

- [21] P. van Endert, *Immunol Rev* **2016**, 272, 80-96.
- [22] S. C. Jameson, M. J. Bevan, *Eur J Immunol* **1992**, 22, 2663-2667.
- [23] A. I. Webb, N. A. Borg, M. A. Dunstone, L. Kjer-Nielsen, T. Beddoe, J. McCluskey, F. R. Carbone, S. P. Bottomley, M.-I. Aguilar, A. W. Purcell, J. Rossjohn, *The Journal of Immunology* **2004**, 173, 402-409.
- [24] M. J. Miley, I. Messaoudi, B. M. Metzner, Y. Wu, J. Nikolich-Zugich, D. H. Fremont, *J Exp Med* **2004**, 200, 1445-1454.
- [25] P. Marrack, R. Shimonkevitz, C. Hannum, K. Haskins, J. Kappler, *The Journal of experimental medicine* **1983**, 158, 1635-1646.
- [26] A. Mortellaro, M. Urbano, S. Citterio, M. Foti, F. Granucci, P. Ricciardi-Castagnoli, *Methods Mol Biol* **2009**, 531, 17-27.
- [27] R. C. Su, R. G. Miller, *Journal of Immunology* **2001**, 167, 4869-4877.
- [28] E. Abbe, *Archiv für mikroskopische Anatomie* **1873**, 9, 413-418.
- [29] aS. van de Linde, M. Heilemann, M. Sauer, *Annu Rev Phys Chem* **2012**, 63, 519-540; bA. Rasmussen, V. Deckert, *Anal Bioanal Chem* **2005**, 381, 165-172.
- [30] aB. Huang, M. Bates, X. Zhuang, *Annu Rev Biochem* **2009**, 78, 993-1016; bD. van der Zwaag, N. Vanparijs, S. Wijnands, R. De Rycke, B. G. De Geest, L. Albertazzi, *ACS Appl Mater Interfaces* **2016**, 8, 6391-6399.
- [31] aL. Albertazzi, D. van der Zwaag, C. M. Leenders, R. Fitzner, R. W. van der Hofstad, E. W. Meijer, *Science* **2014**, 344, 491-495; bR. M. da Silva, D. van der Zwaag, L. Albertazzi, S. S. Lee, E. W. Meijer, S. I. Stupp, *Nat Commun* **2016**, 7, 11561.
- [32] R. Han, Z. Li, Y. Fan, Y. Jiang, *J Genet Genomics* **2013**, 40, 583-595.
- [33] M. J. Rust, M. Bates, X. Zhuang, *Nat Methods* **2006**, 3, 793-795.
- [34] aJ. Herz, J. Pardo, H. Kashkar, M. Schramm, E. Kuzmenkina, E. Bos, K. Wiegmann, R. Wallich, P. J. Peters, S. Herzig, E. Schmelzer, M. Kronke, M. M. Simon, O. Utermohlen, *Nat Immunol* **2009**, 10, 761-768; bD. M. van Elsland, E. Bos, W. de Boer, H. S. Overkleeft, A. J. Koster, S. I. van Kasteren, *Chemical Science* **2016**, 7, 752-758.
- [35] Z. Shen, G. Reznikoff, G. Dranoff, K. L. Rock, *J Immunol* **1997**, 158, 2723-2730.
- [36] C. P. Ramil, Q. Lin, *Chem Commun* **2013**, 49, 11007-11022.
- [37] S. I. van Kasteren, H. B. Kramer, H. H. Jensen, S. J. Campbell, J. Kirkpatrick, N. J. Oldham, D. C. Anthony, B. G. Davis, *Nature* **2007**, 446, 1105-1109.
- [38] J. W. Chin, S. W. Santoro, A. B. Martin, D. S. King, L. Wang, P. G. Schultz, *Journal of the American Chemical Society* **2002**, 124, 9026-9027.
- [39] aA. Deiters, T. A. Cropp, M. Mukherji, J. W. Chin, J. C. Anderson, P. G. Schultz, *Journal of the American Chemical Society* **2003**, 125, 11782-11783; bW. Liu, A. Brock, S. Chen, S. Chen, P. G. Schultz, *Nature Methods* **2007**, 4, 239-244.
- [40] M. S. Siegrist, S. Whiteside, J. C. Jewett, A. Aditham, F. Cava, C. R. Bertozzi, *ACS chemical biology* **2012**, 8, 500-505.
- [41] F. Kotsias, E. Hoffmann, S. Amigorena, A. Savina, *Antioxidants & redox signaling* **2013**, 18, 714-729.
- [42] R. Singh, P. Cresswell, *Science* **2010**, 328, 1394-1398.
- [43] aD. H. Schuurhuis, S. Laban, R. E. M. Toes, P. Ricciardi-Castagnoli, M. J. Kleijmeer, E. I. H. van der Voort, D. Rea, R. Offringa, H. J. Geuze, C. J. M. Melief, F. Ossendorp, *The Journal of Experimental Medicine* **2000**, 192, 145-150; bC. Winzler, P. Rovere, M. Rescigno, F. Granucci, G. Penna, L. Adorini, V. S. Zimmermann, J. Davoust, P. Ricciardi-Castagnoli, *The Journal of Experimental Medicine* **1997**, 185, 317-328.
- [44] A. Rhule, B. Rase, J. R. Smith, D. M. Shepherd, *J Ethnopharmacol* **2008**, 116, 179-186.

- [45] M. C. Feltkamp, H. L. Smits, M. P. Vierboom, R. P. Minnaar, B. M. de Jongh, J. W. Drijfhout, J. ter Schegget, C. J. Melief, W. M. Kast, *European Journal of Immunology* **1993**, *23*, 2242-2249.
- [46] S. Khan, M. S. Bijker, J. J. Weterings, H. J. Tanke, G. J. Adema, T. van Hall, J. W. Drijfhout, C. J. M. Melief, H. S. Overkleeft, G. A. van der Marel, D. V. Filippov, S. H. van der Burg, F. A. Ossendorp, *J. Biol. Chem.* **2007**, M701705200.
- [47] A. Neisig, J. Roelse, A. J. Sijts, F. Ossendorp, M. C. Feltkamp, W. M. Kast, C. J. Melief, J. J. Neefjes, *J Immunol* **1995**, *154*, 1273-1279.

4

Towards imaging of bioorthogonal antigens throughout antigen cross-presentation

Joanna B. Pawlak, Daphne M. van Elsland, Anouk M.F. van der Gracht, Silvia Pujals Riatos, Nico J. Meeuwenoord, Marcel Camps, Colin Watts, Dmitri V. Filippov, Lorenzo Albertazzi, Herman S. Overkleef, Ferry A. Ossendorp and Sander I. van Kasteren contributed to the work described in this chapter.

4.1 Introduction

The activation of cytotoxic T cells (CTLs) is one of the key events in adaptive immunity and essential for the clearance of viruses and cancers^[1]. CTLs are activated by antigen presenting cells (APCs) in a process called antigen cross-presentation^[2]. Cross-presentation involves uptake of antigen, followed by routing to a compartment where it can be loaded onto MHC-I^[3]. During this routing, the antigen is proteolytically processed to liberate epitope peptides that are loaded onto MHC-I^[4].

The use of traditional reporter strategies to study intracellular antigen routing has some limitations: the requirement of proteolysis for liberation of epitope peptides means that any amide-linked reporters must be disconnected from the peptide somewhere during routing. Furthermore, the chemical modification of sidechains with fluorophores can alter protease specificity, membrane crossing ability and solubility of the antigen^[5]. In chapter 3 of this thesis bioorthogonal antigens were explored in their ability to determine surface levels of epitope peptides. To this end, minimal epitopes (which essentially do not require processing prior to loading and can be loaded by surface exchange^[6]) were exchanged on cells and the modification chemistry to label these peptides was optimized.

This chapter describes the further exploration of these bioorthogonal antigens as reagents to study cross-presentation itself. In theory, their properties allow the unbiased imaging throughout the cross-presentation process: from uptake all the way through to the on-surface appearance of the epitope. Not only can they be loaded into the MHC-IIs and can the fluorophores be ligated following the loading (see Chapter 3), but the chemical stability of (at least some) bioorthogonal functionalities^[7] could prevent their sequestration after uptake: fluorescence quenching due to the oxidative^[8], reductive^[9] and acidic conditions^[10] found during antigen cross-presentation does not occur if the fluorophore is introduced after fixation. Secondly, their incorporation as sidechains of single amino acids would keep them intact even during the proteolytic degradation that degrades/disconnects other amide-based reporters.

A third property that was hypothesized to be favorable for the study of antigen processing and presentation was that the bioorthogonal groups are very small compared to fluorophores and can be incorporated isosterically and isocoulombically: the similar size and identical charge compared to natural amino acids results in minimal structural interference. This is postulated to minimize the effect on the rate of proteolysis. This is unlike, for example modification of lysines with small molecule fluorophores which alters the charge of the protein, the lipophilicity and subsequent rates of proteolysis^[11].

4.2 Results and discussion

The aim of the work in this chapter was to therefore explore whether the bioorthogonal epitopes could be used in the context of longer antigens as reagents to study the intracellular mechanisms of cross-presentation and finally the on-surface appearance.

Design of the bioorthogonal antigens

The aim was to use antigens with only a single bioorthogonal group at defined positions within the epitope, analogous to the minimal bioorthogonal epitopes used in chapter 3 of this thesis. The ideal reagent for this work would be a whole, folded protein antigen carrying a single modification at a controllable position within the epitope peptide (or elsewhere in the protein) for which here are two approaches available to obtain it: amber codon suppression^[12] and methionine removal combined with auxotrophic methionine analogue incorporation^[13].

The first approach makes use of an expanded genetic code, whereby *E.coli* cells are transformed with a tRNA capable of recognizing the amber stop-codon and a tRNA-synthetase capable of loading this tRNA with an amino acid containing a bioorthogonally-modified amino acid. The second approach makes use of the fact

that certain strains of *E. coli* are auxotrophic for methionine, that is they do not biosynthesize their own methionine^[14]. Depleting these cells of methionine allowed the replacement with a structural analogue of methionine^[15]. Early examples of this use were the incorporation of heavy atoms (selenium) for crystallization^[16], or other non-natural sidechains^[13b, 17] as well as bioorthogonal methionine analogues azidohomolalanine (AHA) and homopropargylglycine (HPG)^[18]. Davis and co-workers used this approach in combination with isosteric amino acid substitution (Met → Ile) to site-selectively modify proteins with single bioorthogonal groups and quantitatively ligating these using the same copper-catalyzed Huisgen reaction as described in chapter 3^[13a, 19].

However, for the initial exploration of bioorthogonal antigens for cross-presentation studies, a simpler, more versatile, approach was chosen: solid-phase synthesis^[20] that would allow the rapid production of differentially modified antigens. The advantage of this method over the above approaches is the ease with which diversity can be introduced, due to the rapid rate at which these peptides can be synthesized. The downside is that the peptides likely lack secondary/tertiary structures. However, they have been shown to be relevant for immune system studies. Synthetic long peptide (SLP) antigens – as the ones proposed for use in this chapter – are making strong headway in the clinic for use in anti-cancer vaccines^[21]. They are also potent activators of CD8 CTLs, which highlights their ability to be cross-presented^[22]. A series of SLPs carrying bioorthogonal groups within their epitopes were thus designed to explore the use of these bioorthogonal antigens in this complex setting of cross-presentation.

In chapter 3 it was shown that the ligation reaction of a Propargylglycine (Pg) modified HSV-Gp₄₉₈₋₅₀₅ peptide resulted in the most significant signal to noise ratio compared to other peptides tested. Therefore it was decided to synthesize a series of HSV-Gp synthetic long peptides. The sequence of these SLPs was designed based on the flanking regions of this minimal epitope^[23]. Two variants were made based on long peptides that had previously been shown to show robust cross-presentation *in vitro*^[22]. The first of these was an N-terminally extended peptide with the C-terminus being the end of the epitope as this peptide does not require processing by the proteasome (which is responsible for C-terminal liberation^[24]) (Table 1, entry 1). The second peptide that was synthesized did carry a C-terminal extension (A₅K), which has been used in previous work by Khan *et al.*^[22]. This peptide does require proteasomal processing to release the epitope (Table 1, entry 2).

These wild type peptides were also substituted with Pg-residues at position P4 or P7 within the epitope (Table 1, entries 3, 4 and 5) since these were shown in chapter 3 to be the most ligatable positions within this epitope.

Entry	Peptide Sequence	Peptide Name	Based on ovalbumin model peptide sequence
1	NASVERIKTTSSIEFARL	HSV-Gp ₄₈₈₋₅₀₅	DEVSGLEQLESIIINFEKL (OVA ₂₄₇₋₂₆₄)
2	NASVERIKTTSSIEFARLAAAAAK	HSV-Gp ₄₈₈₋₅₀₅ A ₅ K	DEVSGLEQLESIIINFEKLAAAAAK (OVA ₂₄₇₋₂₆₄ A ₅ K)
3	NASVERIKTTSSIEFAPgL	HSV-Gp ₄₈₈₋₅₀₅ -Pg-7	
4	NASVERIKTTSSIPgFARLAAAAAK	HSV-Gp ₄₈₈₋₅₀₅ A ₅ K-Pg-4	
5	NASVERIKTTSSIEFAPgLAAAAAK	HSV-Gp ₄₈₈₋₅₀₅ A ₅ K-Pg-7	

Table 1. Overview of HSV-Gp synthetic long peptides used in this study.

T cell activation of HSV synthetic long peptides

The first aspect of these HSV-SLPs that was assessed was the ability of the non-bioorthogonal parent sequences to activate the HSV-Gp₄₉₈₋₅₀₅-specific, *LacZ*-inducible T cell hybridoma HSV2.3.2E2^[25]. This was to confirm that these peptides were indeed cross-presented and would thus serve as suitable models for the imaging of routing inside APCs. T cell activation of the non-bioorthogonal peptides as well as their Pg-modified variants was examined through monitoring of the β -galactosidase-mediated conversion of a fluorogenic substrate^[22, 26] (Figure 1).

The first of these T cell activation assays were performed in the laboratory of Prof. Colin Watts at the University of Dundee (by Prof. Watts himself; Figure 1). There, bone marrow-derived dendritic cells^[27] were incubated with the HSV-Gp₄₈₈₋₅₀₅ and -Pg-7 synthetic long peptides at the indicated concentrations followed by wash with medium and finally by addition of the HSV-specific T cell hybridomas^[22]. Both the minimal epitope (HSV-Gp₄₉₈₋₅₀₅) as control and C-terminally extended peptide (HSV-Gp₄₈₈₋₅₀₅) could activate the T cell clone, proving this peptide to be suitable to study cross-presentation. The propargylated epitope did not activate the HSV2.3.2E2-clone at any of the tested concentrations (Figure 1).

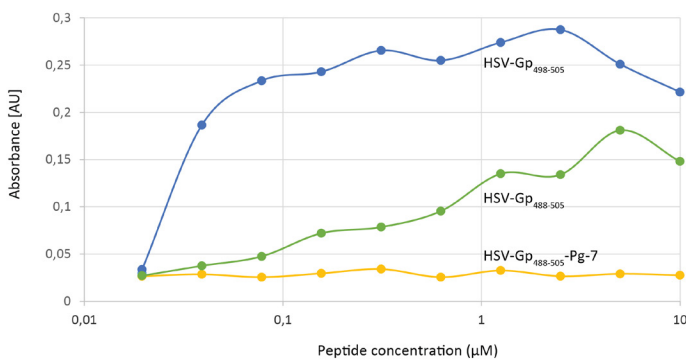


Figure 1. Reactivity of the HSV peptides with the SSIEFARL-specific T cell clone HSV2.3.2E2. Only the non bioorthogonal controls - the HSV-Gp₄₉₈₋₅₀₅ and HSV-Gp₄₈₈₋₅₀₅ were recognized by the T cells.

Cellular uptake of bioorthogonal synthetic long peptides

As the bioorthogonal variant of HSV-Gp₄₈₈₋₅₀₅ was not recognized by the cognate T cells, its suitability for studying cellular uptake was instead assessed using ccHc-ligation reaction. The uptake of HSV-Gp₄₈₈₋₅₀₅-Pg-7 was measured using Alexa Fluor-488 azide in ccHc-ligation conditions (as optimized in Chapter 3) after cells were fixed (Figure 3A). A pulse chase experiment using flow cytometry was conducted first: HSV-Gp₄₈₈₋₅₀₅-Pg-7 as well as its non-bioorthogonal control were incubated with the dendritic-cell line D1^[28] for a fixed pulse (1h) followed by different chase periods. At the end of each chase period, the cells were fixed and exposed to ligation using AF-488 azide (Figure 3B). Use of a permeabilizing agent (saponin) proved unnecessary as cells became permeable to ccHc-reagents and Alexa Fluor-488 azide after fixation (Figure 2).

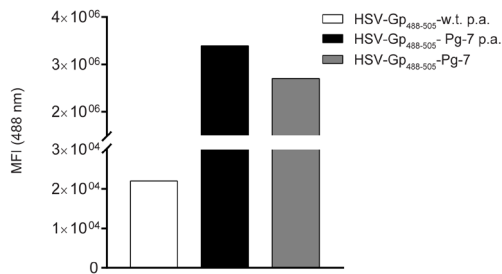


Figure 2. D1s were pulsed for 5h with HSV-Gp₄₈₈₋₅₀₅ w.t. and HSV-Gp₄₈₈₋₅₀₅-Pg-7 (both 50 μM). ccHc was performed after fixation and permeabilization using permeabilizing agent (p.a.) - saponin (0.1 %). No significant improvement of the fluorescent signal was observed after addition of p.a. The fluorescent signal of AF-488 was assessed by quantification of the mean fluorescence intensity (MFI) at 488 nm using flow cytometry.

As depicted in figure 3B, the fluorescent signal obtained from AF-488 azide peaked after the 1-hour pulse and showed time-dependent decay afterwards.

As a second assay to determine whether 1 hour was the optimal pulse-length for uptake, confocal microscopy was used to image this event. D1 cells were incubated with HSV-Gp₄₈₈₋₅₀₅-Pg-7 (50μM) for different time periods, both short (5, 15, 30, 45 minutes and 1 h; Figure 3C) and longer (1h, 3h, 5h, 8h; Figure 3D), then the cells were washed,

fixed and reacted with AF-488 azide. Confocal images revealed a non-homogeneous fluorescent signal detectable from one hour onwards.

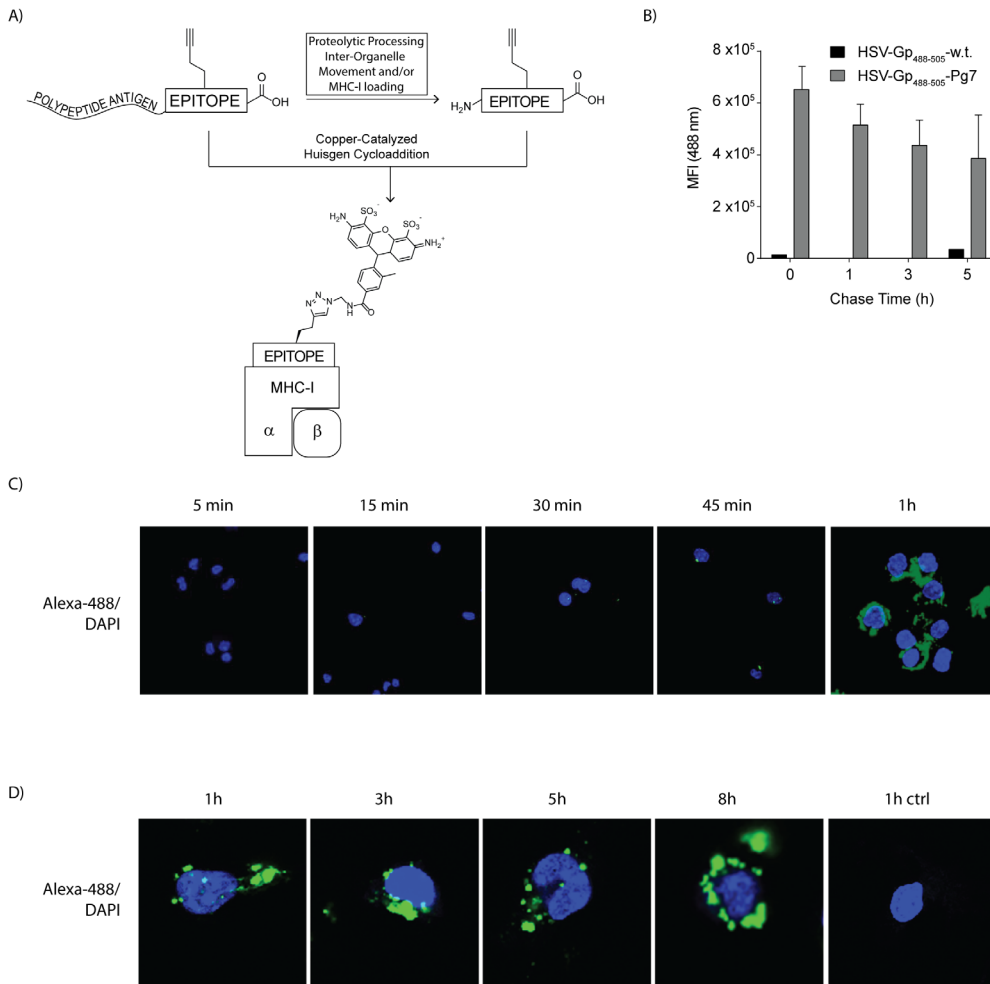


Figure 3. Cellular uptake of the bioorthogonal synthetic long peptide (HSV-Gp₄₈₈₋₅₀₅-Pg-7). A) Overview of the approach: synthetic long peptides carrying bioorthogonal handles within their epitope are incubated with the D1-dendritic cell-line. At the end of the pulse chase experiments the cells are fixed and exposed to the bioorthogonal ligation reaction using AF-488. B) Flow cytometry of a pulse-chase experiment using HSV-Gp₄₈₈₋₅₀₅-Pg-7 (50 μ M) showed the uptake followed by a slow decay over time. Assay was set up in triplicate. All error bars correspond to SD of the mean. C) Confocal images revealed no fluorescent signal detectable after incubation shorter than one hour. D) Incubation at longer time periods resulted in the presence of a non-homogeneous fluorescent signal.

To provide further insights into the uptake of this peptide, bioorthogonal correlative-light electron microscopy (CLEM)^[29] imaging was performed. D1 cells were pulsed with HSV-Gp₄₈₈₋₅₀₅-Pg-7 (50 μ M) for 5 hours followed by wash and fixation. Subsequently, these samples were labeled with Alexa Fluor-488-azide. After the labeling, the samples were cryo-sectioned then transferred to an EM grid and finally imaged using confocal microscopy. After confocal imaging, sections were embedded in methyl cellulose with uranyl acetate and subjected to EM imaging. Images were correlated and morphological information obtained from the EM images has revealed

a patchy pattern of fluorescent signal located largely at or near the plasma membrane of the cells (Figure 4).

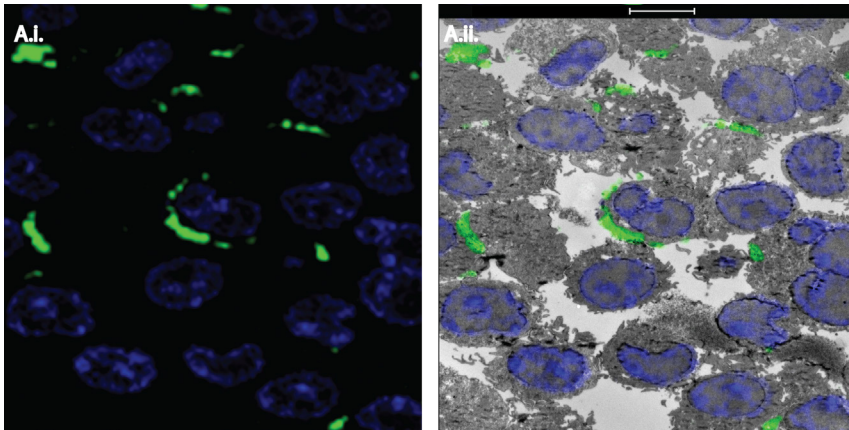


Figure 4. CLEM imaging of the D1s cells incubated with HSV-Gp₄₈₈₋₅₀₅-Pg-7 (50 μ M) followed by wash with medium complete and PBS. Cells were fixed and labeled with Alexa Fluor-488-azide using cChC-conditions (green). DAPI (blue) staining was used for correlation purposes; Samples were subjected to Tokuyasu sample preparation and cryosectioned into 75 nm sections^[29]. A.i.) High magnification confocal image (green channel; AF-488). A.ii.) CLEM image of A.i. correlated with EM image; Scale bar 5 μ m.

In order to determine more accurate location of the fluorescent signal, CLEM imaging at higher magnification was performed. The images have shown presence of large aggregates of the fluorescent signal located predominantly at or near the plasma membrane (Figure 5).

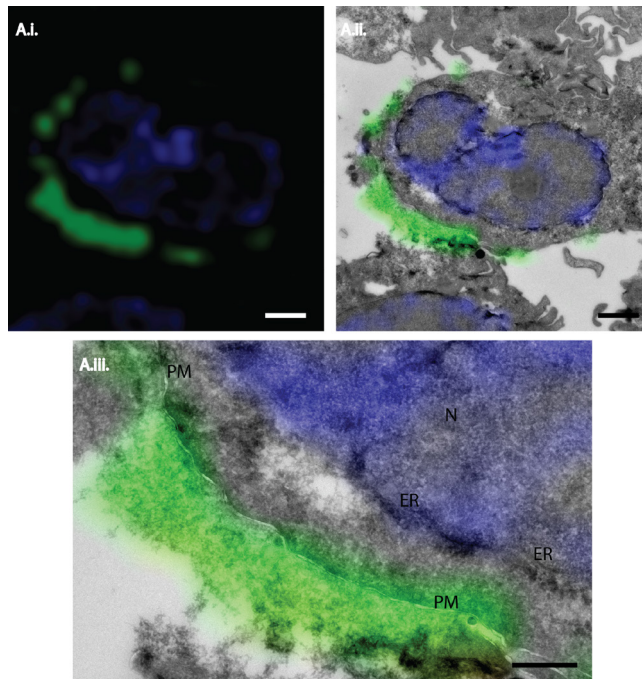


Figure 5. CLEM imaging of the D1s cells incubated with HSV-Gp₄₈₈₋₅₀₅-Pg-7 (50 μ M) followed by wash with medium complete and PBS. Cells were fixed and labeled with Alexa Fluor-488-azide using cChC-conditions (green). DAPI (blue) staining was used for correlation purposes; Samples were subjected to Tokuyasu sample preparation and cryosectioned into 75 nm sections^[29]. A.i.) High magnification confocal image of AF-488 (green channel); Scale bar 1 μ m. A.ii.) CLEM image of A.i. correlated with EM image; Scale bar 1 μ m. A.iii.) Detail of A.ii. PM=plasma membrane, ER= endoplasmic reticulum, N=nucleus. Scale bar 500nm.

These experiments have led to a hypothesis that HSV-Gp₄₈₈₋₅₀₅-Pg-7 aggregates and that these aggregates are either slowly internalized, perhaps serving as an antigen depot^[30] or are not internalized at all. More research is needed to fully elucidate the behavior of these peptides in regard to solubility and T cell activation.

Taken together, these preliminary results demonstrate a potential of bioorthogonal SLPs as a tool to study cellular uptake using Alexa Fluor-488 azide in the cChC reaction. However, an optimal bioorthogonal SLP model should first be synthesized and assessed and perhaps the switch to intact, folded, soluble bioorthogonal proteins should be made.

Selective cell surface labeling of bioorthogonal synthetic long peptides

After establishing the use of bioorthogonal antigens to image uptake, it was next attempted to use the approach to selectively ligate the processed peptide appearing on the cell surface. As fixing rendered the cells permeable to cHc-reagents, the three-step labeling approach outlined in the latter part of Chapter 3 was explored to see whether it was sufficiently cell-surface restricted to only label this pool of the peptide (which is vastly smaller than the total intracellular pool).

To prevent labeling of cell-surface bound aggregates (which would give false positives), the switch was made to the more soluble SLP (Table 1, entry 2) carrying a C-terminal extension of 5 alanines and a lysine residue, which was less prone to aggregation than peptide (Table 1, entry 3). This extension had previously been shown to enhance solubility of other epitopes^[22, 31]. HSV-Gp₄₈₈₋₅₀₅A₅K-Pg-4 and -Pg-7 (Table 1, entries 4 and 5 respectively) were thus used as bioorthogonal substitutes for the poorly soluble HSV-Gp₄₈₈₋₅₀₅-Pg-7 (Table 1, entry 3). The T cell assays of these

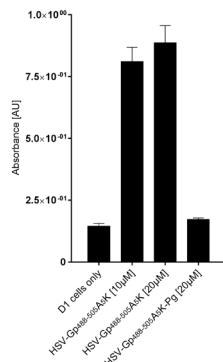


Figure 6. Reactivity of the HSV peptides with the SSIEFARL-specific T cell clone HSV2.3.2E2. Only the non bioorthogonal control - the HSV-Gp₄₈₈₋₅₀₅A₅K was recognized by the T cells.

doubly extended peptides showed the wild-type to be efficiently cross-presented (and again the bioorthogonal variant failed to induce T cell activation) (Figure 6).

The same bioorthogonal three-step labeling protocol as outlined in chapter 3 was applied to these two bioorthogonal SLPs to determine whether they could be labeled on-surface only in this case using an epi-fluorescence microscopy and flow cytometry. For the microscopy imaging, DC2.4 cells were incubated with the HSV-Gp₄₈₈₋₅₀₅A₅K-Pg-4 and -Pg-7 and with their non-bioorthogonal control for ~5 hours after which the cells were washed with medium, fixed and subjected to the three- step labeling. The images revealed an intracellular fluorescent signal obtained from Alexa Fluor-488 (Figure 7).

Unfortunately, the Alexa Fluor-647 (from the three-step protocol) was not exclusively located at the cell surface. The bulk of the material showed non-homogeneous punctate staining that overlapped in part with the Alexa Fluor-488 intracellular stain. This suggested that for these experiments where the bulk of the peptide resided within the cell, even three-step labelling was insufficient to selectively label the extracellular pool.

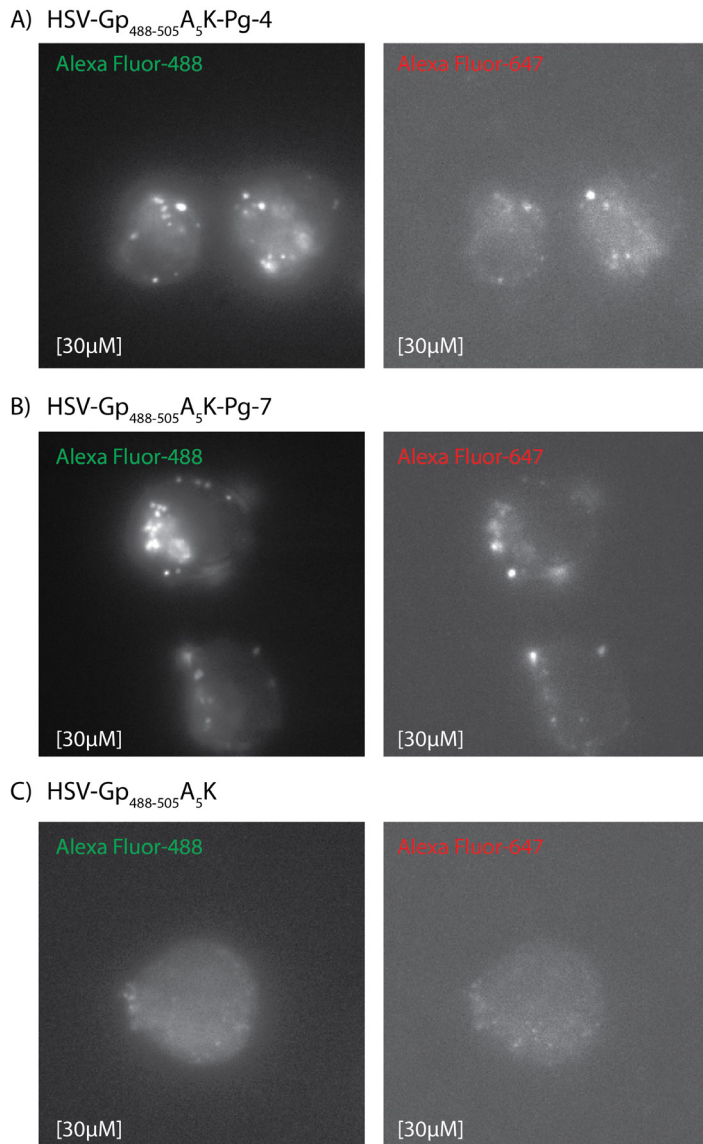


Figure 7. Epi-fluorescence illumination phase with white-light microscopy images of A) HSV-Gp₄₈₈₋₅₀₅A₅K-Pg-4 at 30µM as well as B) HSV-Gp₄₈₈₋₅₀₅A₅K-Pg-7 at 30µM showed not-substantial but visible signal to noise ratio as compared to their C) non-bioorthogonal control. DC2.4 were incubated with the indicated peptides for ~5h followed by wash with medium complete, fixation and exposure to the three- step labeling as described above.

To assess whether the punctate staining was actually intracellular, an acid-strip experiment was performed whereby MHC-bound peptides are removed from the cell surface of the APC with mild acid^[32]. If the signal from the Alexa Fluor-647 disappears after this acid strip, this would indicate that the observed peptide was indeed extracellular.

First, the completeness of the acid strip experiments was assessed using the T cell against the HSV-Gp₄₉₈₋₅₀₅-epitope. D1 cells were incubated with the HSV-Gp₄₈₈₋₅₀₅A₅K-

Pg-7 (20 μ M final concentration) and without the peptide (control) for 1,5h at 37°C. Followed the incubation, D1 cells were either washed with medium or gently fixed to prevent further processing and possible reuptake of the peptides. Alternatively, the peptides were exposed to mild acid elution, which results in the removal of cell surface proteins. After acid elution cells were either left to recover for ~5h at 37 °C to regenerate their peptide MHC-I complexes^[33] or gently fixed. After the recovery time, the cells were mildly fixed and the SSIEFARL specific and MHC-I restricted cognate T cell clone (HSV2.3.2E2)^[26] was added to all D1 cells. As a control to check whether the D1 cells after recovery were able to regenerate the MHC-I molecules, a MHC-I specific epitope SSIEFARL and no epitope (control) was added to these cells.

Next day, the epitopes were quantified by measuring the HSV T cell response as described above. T cell responses were observed in cells incubated with HSV-Gp₄₈₈₋₅₀₅A₅K as well as after recovery (Figure 8A), but no T cell responses were observed in the D1 cells fixed directly after acid strip. Controls (T cell only as well as T cell only after incubation with the minimal epitope sample) were also negative (Figure 8B). These results strongly imply that the signal of presented epitope from HSV-Gp₄₈₈₋₅₀₅A₅K can be abolished.

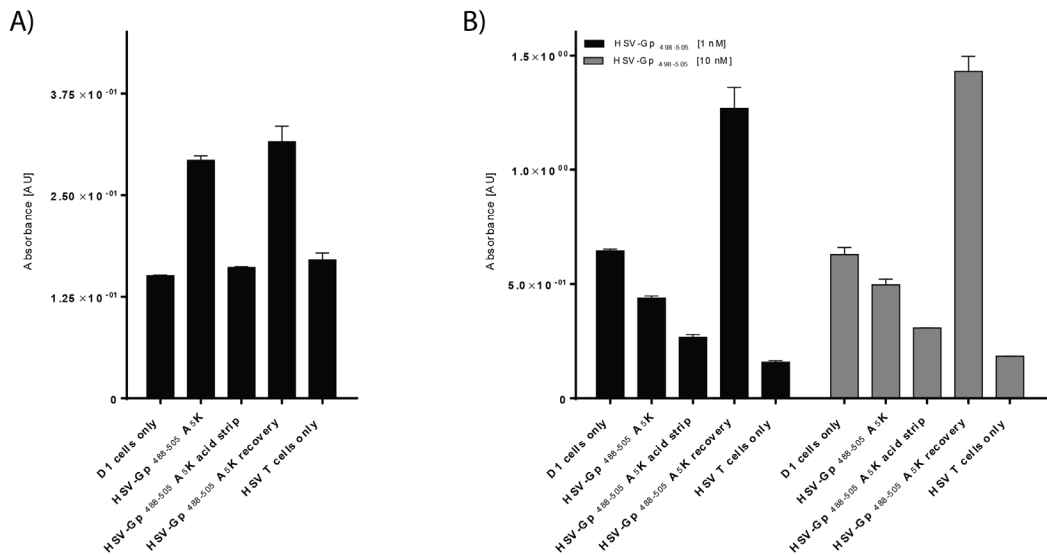


Figure 8. Reactivity of the HSV-A₅K peptide in acid elution treated and untreated D1 cells with the SSIEFARL-specific T cell clone HSV2.3.2E2. A) Acid strip treatment abolished T cell response which can be rescued after recovery time of approximately 5h at 37°C. B) T cell response after recovery and in the presence of the minimal epitope (SSIEFARL) is increased as compared to incubation with HSV-A₅K only in the presence of SSIEFARL. Assay was set up in triplicate. All error bars correspond to SD of the mean.

Interestingly, T cell reactivity was not only rescued after the recovery period, but it was increased after the addition of the epitope as compared to incubation with HSV-Gp₄₈₈₋₅₀₅A₅K only after addition of the epitope (Figure 8B). This phenomenon could be explained by the reported enhancement of MHC-I regeneration after cell recovery in the presence of the minimal epitopes^[34].

With this suitable stripping protocol in hand, it was checked whether the Alexa-647 signal in Figure 7 resulted exclusively from the cell surface pool of peptide, or whether some of the signal was background resulting from background permeation of the antibody and protein A.

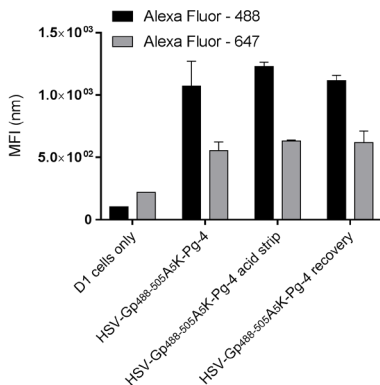


Figure 9. Mean fluorescence intensity of Alexa Fluor-488 and -647 in acid elution treated and untreated D1 cells exposed to the three- step labeling. A substantial signal to noise ratio was not only observed in acid elution untreated cells and after recovery but also after acid strip treatment. Assay was set up in triplicate. All error bars correspond to SD of the mean.

To assess this by flow cytometry, the D1s were incubated with HSV-Gp₄₈₈₋₅₀₅A₅K-Pg-4 and exposed to acid elution treatment as described above. The fluorescent signal of Alexa Fluor-488 and Alexa Fluor-647 was measured in acid elution treated and untreated cells. A substantial signal was observed in non-acid treated cells after recovery but also in acid elution treated cells (Figure 9).

The experiments in chapter 3 (Figure 12) showed that – despite an increase in small molecule penetrance, the cell’s permeability to antibodies was not significantly affected after fixation and cChc conditions. The data from Figure 9, however, indicate that the conditions of acid-strip, fixation followed by

the cChc-reaction could render the cells permeable to antibodies.

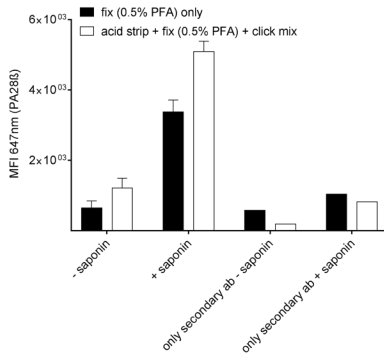


Figure 10. The combination of exposure to acid strip treatment and cChc conditions did permeabilized the D1 cells to antibody, which was assessed by quantifying the mean fluorescence intensity of the cytosolic antibody (PA288) in the presence and absence of the permeabilizing agent – saponin (0.1%). Assay was set up in triplicate. All error bars correspond to SD of the mean.

bioorthogonal long peptides are taken up by the APCs, a fluorescent signal (obtained from three- step labeling) will be expected in cells that were incubated with long peptides prior to the gentle fixation and not in cells that were incubated with long peptides after they were mildly fixed. If this however is not the case it would be an indication for an specific adhesion of the peptides to the cell surface.

4.3 Conclusion

Bioorthogonal antigens are useful reagents to track the uptake of antigens. The one-step labeling approach indicates that the fed antigen is only minimally altered compared to wild-type antigens. This means there is less chance of artifacts stemming from other labeling techniques.

The three-step labeling presents a promising approach to selectively label the intracellular and extracellular pool of the bioorthogonal synthetic long peptides in a single experiment. However, the cell surface labeling still needs further research as it cannot be determined with these experiments whether the antigen labeled by the three-step approach is actually on the cell surface and loaded in an MHC-complex. In the future, using CLEM, intracellular (for example LAMP1 – lysosomal marker) and extracellular (for example MHC-I) markers should be combined with the three- step labeling method in order to provide an accurate antigen localization at a given time during cross-presentation process. This would also mean that (by studying co-localization with organelle markers), the relative contribution of the different proposed cross-presentation routes could be quantified in an unbiased manner, shedding light on this controversial and complex pathway^[1, 3, 35].

This was next assessed by quantifying the mean fluorescence intensity of an antibody targeting a cytosolic region of the proteasomal protein (PA28 β) in presence and absence of saponin. This was done for both acid stripped cells, as well as untreated cells. Indeed, it was observed that in the presence of both, acid elution and click mixture, the cells became partly permeable to the antibody (Figure 10).

These results excluded the use of acid strip-based protocols in combination with three-step labeling. Instead, in future, cells should either be incubated with bioorthogonal long peptides or gently fixed prior incubation to prevent peptide uptake and processing. If the

4.4 Experimental section

Reagents:

Alexa Fluor-488 azide (catalogue number: A10266), Alexa Fluor-488 polyclonal antibody (catalogue number: A-11094) and Alexa Fluor-647-conjugated protein A (catalogue number: P21462) as well as donkey anti-goat IgG (H+L) secondary antibody, Alexa Fluor-647 (catalogue number: A-21447) were purchased from Thermo Fisher Scientific. PA28 β antibody (catalogue number: SC-23642) was purchased from Santa Cruz biotechnology. Propargylglycine-Fmoc was purchased from Anaspec. Tris(3-hydroxypropyl-triazolylmethylamine) (THPTA) was purchased from Sigma-Aldrich, as were all other reagents at the highest available grade.

Peptide synthesis:

All peptides were synthesized using standard Fmoc Solid Support Chemistry and purified using high performance liquid chromatography (Prep column Gemini C18 110A 150x21.20 5 μ m) using 15 to 45 % gradient (A: 0.1% TFA in MilliQ H₂O, B: ACN). LC-MS measurements were done on an API 3000 Alltech 3300 with a Grace Vydac 214TP 4,6 mm x 50 mm C4 column and analyzed by electrospray LC-MS analysis on a PE SCIEX: API 3000 LC/MS/MS system using a Gemini 3u C18 110A analytical column (5 μ particle size, flow: 1.0 ml/min), on which the absorbance was also measured at 214 and 254 nm. Solvent system for LC-MS: A: 100% water, B: 100% acetonitrile, C: 1% TFA (aq).

Cell culture:

The D1 cell line, a long-term growth factor-dependent immature myeloid (CD11b⁺, CD8 α ⁻) DC line of splenic origin, derived from a female C57BL/6 mouse was provided by M. Camps (Leiden University Medical Center) and was cultured as described previously^[36]. When necessary, full maturation was achieved by adding Escherichia coli-derived LPS (serotype 026.B6; Sigma Aldrich) to the culture medium for 12h (final concentration 5 μ g/mL).

The DC2.4 cell line, an adherent C57BL/6 bone marrow derived DC line was kindly provided by Dr. Kenneth Rock (University of Massachusetts Medical School) and cultured as described previously^[37].

Mild acid stripping and HSV T cell assay:

The D1s cells were incubated with respective peptides, at the indicated concentrations and times. After the incubation the cells were washed once with medium complete and twice with PBS. The cells were either immediately fixed by adding 0.2% PFA in PBS for 15min at RT followed by double wash with PBS or mild acid treated essentially as described by Storkus *et. al*^[32]. With the exception that D1 cell pellet was resuspended followed by addition of elution buffer (0.131 M Citric acid monohydrate, 0.061 M Na₂HPO₄·2H₂O pH=3.3 adjusted with 5N NaOH or 5N HCl) for 60s at RT followed by addition of ice-cold medium complete. Cell suspension was then pelleted and washed with ice-cold PBS and either left at 37°C for ~5h in medium complete to recover or immediately fixed by adding 0.2% PFA in PBS for 15min at RT followed by double wash with PBS. At the end all D1 cells were plated in 96-well tissue-culture treated microtiter plate (5x10⁴ cells/well) and HSV2.3.2E2 T cells (5x10⁴ cells/well) were co-incubated for ~17h at 37°C. Stimulation of the HSV hybridoma was measured by a colorimetric assay using CPRG (chlorophenol red- β -D-galactopyranoside) as a substrate as described^[22].

Bioorthogonal ligation reaction using Alexa Fluor-488:

Flow cytometry:

D1s were plated in 24-well tissue-culture treated plate (5×10^5 cells/well) and allowed to adhere for 1h at 37°C. The cells were incubated with respective peptides, at the indicated concentrations (usually 50µM) and times. After the incubation the cells were collected using 2mM EDTA in PBS, washed ones with medium complete and ones with PBS and transferred to Greiner v-bottom 96-well plate. The D1s were fixed by adding 50µl/well of 0.5% PFA in PBS for 1h at RT followed by double wash with PBS. The fixed D1s were then exposed to the bioorthogonal labeling mixture (1 mM CuSO₄, 10 mM sodium ascorbate, 1 mM THPTA ligand, 10 mM aminoguanidine, 100 mM HEPES, pH 8.4, Alexa Fluor-488-azide 5µM). After 1h at RT, the reaction mixture was aspirated and the cells were blocked with 1% BSA and 1% fish gelatin before being washed twice with PBS and analysis by guava easyCyte™ flow cytometry (Merck Millipore) and using FlowJo v10.1.

Confocal microscopy:

D1s were seeded (7×10^4) on a 12-well removable chamber slide (Ibidi) and allowed to adhere for ~1h at 37°C. The cells were incubated with respective peptides, at the indicated concentrations (usually 50µM) and times. After the incubation the cells were washed ones with medium complete and ones with PBS. The D1s were fixed by adding ~150µl/well of 0.5% PFA in PBS for 1h at RT followed by double wash with PBS. The fixed D1s were then exposed to the bioorthogonal labeling mixture (1 mM CuSO₄, 10 mM sodium ascorbate, 1 mM THPTA ligand, 10 mM aminoguanidine, 100 mM HEPES, pH 8.4, Alexa Fluor-488-azide 5µM). After 1h at RT, the reaction mixture was aspirated and the cells were blocked with 1% BSA and 1% fish gelatin before being washed twice with PBS and DAPI stained for 5min at RT (final concentration 2µg/mL). After the staining procedures chambers were removed and cells were covered with a small drop of 50% glycerol after which a coverslip was mounted over the grid. Coverslips were fixed using Scotch Pressure Sensitive Tape. Samples were imaged with a Leica TCS SP8 confocal microscope (63x oil lens, N.A.=1.4).

Correlation of light-electron microscopy (CLEM)

The CLEM approach was adapted from van Elsland^[29] *et. al.* Samples were prepared for cryosectioning as described elsewhere^[38]. D1 cells were incubated with respective peptides, at the indicated concentrations (usually 50µM) and times. After the incubation the cells were washed ones with medium complete and ones with PBS. Cells were fixed and subjected to the bioorthogonal labeling as for confocal microscopy. After the labeling, cells were washed with PBS (3x) and were then fixed for 24h in freshly prepared 2% PFA in 0.1 M phosphate buffer. Fixed cells were embedded in 12% gelatin (type A, bloom 300, Sigma) and cut with a razor blade into 0.5 mm³ cubes. The sample blocks were infiltrated in phosphate buffer containing 2.3 M sucrose for 3h. Sucrose-infiltrated sample blocks were mounted on aluminum pins and plunged in liquid nitrogen. The frozen samples were stored under liquid nitrogen.

Ultrathin cell sections of 75 nm were obtained as described elsewhere^[29]. Briefly, the frozen sample was mounted in a cryo-ultramicrotome (Leica). The sample was trimmed to yield a squared block with a front face of about 300 x 250 µm (Diatome trimming tool). Using a diamond knife (Diatome) and antistatic devise (Leica) a ribbon of 75 nm thick sections was produced that was retrieved from the cryo-chamber with a droplet of 2.3 M sucrose. Obtained sections were transferred to a specimen grid previously coated with formvar and carbon grids were additionally coated with 100 nm FluoroSpheres (blue) carboxylate-modified (350/440) (Life Technologies).

Grids containing the thawed cryosections were left for 30 minutes on the surface of 2% gelatin in phosphate buffer at 37 °C. Grids were then washed with PBS, labeled with DAPI (final concentration 2µg/mL), and additionally washed with PBS and aquadest. Subsequently grids were washed with 50% glycerol and placed on a glass slides (pre- cleaned with 100% ethanol). Grids were then covered with a small drop of 50% glycerol after which a coverslip was mounted over the grid. Coverslips were fixed using Scotch Pressure Sensitive Tape. Samples were imaged with a Leica TCS SP8 confocal microscope (63x oil lens, N.A.=1.4).

After confocal microscopy the EM grid with the sections was remove from the glass slide, rinsed in distilled water and incubated for 5min on droplets of uranylacetate/methylcellulose. Excess of uranylacetate/methylcellulose was blotted away and grids were air-dried. EM imaging was performed with a Tecnai 12 Biotwin transmission electron microscope (FEI) at 120 kV acceleration voltages. Correlation of confocal and EM images was performed in Adobe Photoshop CS6. In Adobe Photoshop, the LM image was copied as a layer into the EM image and made 50 % transparent. Transformation of the LM image was necessary to match it to the larger scale of the EM image. This was performed via isotropic scaling and rotation. Interpolation settings; bicubic smoother. Alignment at low magnification was carried out with the aid of nuclear DAPI staining in combination with the shape of the cells; at high magnification alignment was performed using the fiducial beads.

Permeability assay:

D1s were collected using 2mM EDTA in PBS, fixed in 0.5% PFA in PBS for 1h at RT and exposed to the click cocktail mix (as described previously but without a fluorophore) for 1h at RT. After the wash, cells were permeabilized with 0.1% saponin in 1% BSA in PBS (control cells were incubated without saponin throughout whole experiment) for ~20min at RT followed by incubation with PA28β antibody (final concentration 2µg/mL) in 0.1% saponin in 1% BSA in PBS for 30min on ice followed by wash and incubation with the donkey anti-goat IgG (H+L) secondary antibody (0.5µg/mL) in 0.1% saponin in 1% BSA in PBS for 30min on ice followed by wash and analysis by Guava EasyCyte™ flow cytometry (Merck Millipore) and using FlowJo v10.1.

The three- step labeling:

The DC2.4 cells were incubated with respective peptides, at the indicated concentrations and times. After the incubation the cells were washed ones with medium complete and ones with PBS. The cells were fixed by adding 2% PFA in PBS for 20min at RT followed by double wash with PBS. The fixed DC2.4 were then exposed to the bioorthogonal labeling mixture (1 mM CuSO₄, 10 mM sodium ascorbate, 1 mM THPTA ligand, 10 mM aminoguanidine, 100 mM HEPES, pH 8.4, Alexa Fluor-488-azide 5µM). After 1h at RT, the reaction mixture was aspirated and the cells were blocked with 1% BSA and 1% fish gelatin before being washed twice with PBS. Next, the cells were incubated with an Alexa Fluor-488 antibody (final concentration 2µg/mL) in 100mM HEPES pH 7.2 supplemented with 1% BSA and 1% fish gelatin for 1h at RT. After the incubation, cells were washed with PBS and blocked with 1% BSA and 1% fish gelatin before being exposed to Alexa Fluor-647-conjugated protein A (final concentration 5µg/mL) for 20min at RT followed by PBS wash step and blocking with 1% BSA and 1% fish gelatin.

4.5 References

- [1] J. Neefjes, M. L. Jongsma, P. Paul, O. Bakke, *Nat Rev Immunol* **2011**, *11*, 823-836.
- [2] aO. P. Joffre, E. Segura, A. Savina, S. Amigorena, *Nat Rev Immunol* **2012**, *12*, 557-569; bM. J. Bevan, *The Journal of experimental medicine* **1976**, *143*, 1283-1288.
- [3] J. S. Blum, P. A. Wearsch, P. Cresswell, *Annu Rev Immunol* **2013**, *31*, 443-473.
- [4] K. L. Rock, D. J. Farfan-Arribas, L. Shen, *J Immunol* **2010**, *184*, 9-15.
- [5] aM. Grammel, H. C. Hang, *Nat Chem Biol* **2013**, *9*, 475-484; bL. D. Hughes, R. J. Rawle, S. G. Boxer, *PLoS One* **2014**, *9*, e87649.
- [6] J. B. Pawlak, B. J. Hos, M. J. van de Graaff, O. A. Megantari, N. Meeuwenoord, H. S. Overkleeft, D. V. Filippov, F. Ossendorp, S. I. van Kasteren, *ACS chemical biology* **2016**, *11*, 3172-3178.
- [7] J. A. Prescher, C. R. Bertozzi, *Nat Chem Biol* **2005**, *1*, 13-21.
- [8] in *Principles of Fluorescence Spectroscopy* (Ed.: J. R. Lakowicz), Springer US, Boston, MA, **2006**, pp. 277-330.
- [9] S. Prashanthi, P. H. Kumar, L. Wang, A. K. Perepogu, P. R. Bangal, *Journal of fluorescence* **2010**, *20*, 571-580.
- [10] J. Feitelson, *The Journal of Physical Chemistry* **1964**, *68*, 391-397.
- [11] aC. P. Toseland, *Journal of Chemical Biology* **2013**, *6*, 85-95; bS. T. Larda, D. Pichugin, R. S. Prosser, *Bioconjug Chem* **2015**, *26*, 2376-2383.
- [12] J. Normanly, L. G. Kleina, J. M. Masson, J. Abelson, J. H. Miller, *J Mol Biol* **1990**, *213*, 719-726.
- [13] aS. I. van Kasteren, H. B. Kramer, H. H. Jensen, S. J. Campbell, J. Kirkpatrick, N. J. Oldham, D. C. Anthony, B. G. Davis, *Nature* **2007**, *446*, 1105-1109; bK. L. Kiick, D. A. Tirrell, *Tetrahedron* **2000**, *56*, 9487-9493.
- [14] A. J. Doherty, S. R. Ashford, J. A. Brannigan, D. B. Wigley, *Nucleic Acids Res* **1995**, *23*, 2074-2075.
- [15] Y. Ma, H. Biava, R. Contestabile, N. Budisa, M. L. di Salvo, *Molecules (Basel, Switzerland)* **2014**, *19*, 1004-1022.
- [16] aH. Walden, *Acta Crystallographica Section D: Biological Crystallography* **2010**, *66*, 352-357; bJ. Sheng, Z. Huang, *International Journal of Molecular Sciences* **2008**, *9*, 258-271.
- [17] aK. L. Kiick, R. Weberskirch, D. A. Tirrell, *FEBS Letters* **2001**, *502*, 25-30; bJ. C. M. Van Hest, K. L. Kiick, D. A. Tirrell, *Journal of the American Chemical Society* **2000**, *122*, 1282-1288.
- [18] aA. J. Link, D. A. Tirrell, *Journal of the American Chemical Society* **2003**, *125*, 11164-11165; bK. L. Kiick, E. Saxon, D. A. Tirrell, C. R. Bertozzi, *Proceedings of the National Academy of Sciences of the United States of America* **2002**, *99*, 19-24.
- [19] S. I. Van Kasteren, H. B. Kramer, D. P. Gamblin, B. G. Davis, *Nature Protocols* **2007**, *2*, 3185-3194.
- [20] R. A. Houghten, *Proc Natl Acad Sci U S A* **1985**, *82*, 5131-5135.
- [21] aG. G. Zom, D. V. Filippov, G. A. van der Marel, H. S. Overkleeft, C. J. Melief, F. Ossendorp, *Oncoimmunology* **2014**, *3*, e947892; bC. J. Melief, S. H. van der Burg, *Nature reviews. Cancer* **2008**, *8*, 351-360; c*Molecular Therapy* **2004**, *9*, 102.
- [22] S. Khan, M. S. Bijker, J. J. Weterings, H. J. Tanke, G. J. Adema, T. van Hall, J. W. Drijfhout, C. J. Melief, H. S. Overkleeft, G. A. van der Marel, D. V. Filippov, S. H. van der Burg, F. Ossendorp, *J Biol Chem* **2007**, *282*, 21145-21159.

- [23] M. J. Miley, I. Messaoudi, B. M. Metzner, Y. Wu, J. Nikolich-Zugich, D. H. Fremont, *J Exp Med* **2004**, *200*, 1445-1454.
- [24] C. C. Oliveira, T. van Hall, *Frontiers in Immunology* **2015**, *6*, 298.
- [25] S. Sanderson, N. Shastri, *Int Immunol* **1994**, *6*, 369-376.
- [26] S. N. Mueller, C. M. Jones, C. M. Smith, W. R. Heath, F. R. Carbone, *J Exp Med* **2002**, *195*, 651-656.
- [27] M. B. Lutz, N. Kukutsch, A. L. Ogilvie, S. Rossner, F. Koch, N. Romani, G. Schuler, *J Immunol Methods* **1999**, *223*, 77-92.
- [28] C. Winzler, P. Rovere, M. Rescigno, F. Granucci, G. Penna, L. Adorini, V. S. Zimmermann, J. Davoust, P. Ricciardi-Castagnoli, *J Exp Med* **1997**, *185*, 317-328.
- [29] D. M. van Elsland, E. Bos, W. de Boer, H. S. Overkleeft, A. J. Koster, S. I. van Kasteren, *Chemical Science* **2016**, *7*, 752-758.
- [30] N. van Montfoort, M. G. Camps, S. Khan, D. V. Filippov, J. J. Weterings, J. M. Griffith, H. J. Geuze, T. van Hall, J. S. Verbeek, C. J. Melief, F. Ossendorp, *Proceedings of the National Academy of Sciences of the United States of America* **2009**, *106*, 6730-6735.
- [31] J. L. Meek, *Proc Natl Acad Sci U S A* **1980**, *77*, 1632-1636.
- [32] W. J. Storkus, H. J. Zeh, 3rd, R. D. Salter, M. T. Lotze, *J Immunother Emphasis Tumor Immunol* **1993**, *14*, 94-103.
- [33] M. H. Fortier, E. Caron, M. P. Hardy, G. Voisin, S. Lemieux, C. Perreault, P. Thibault, *J Exp Med* **2008**, *205*, 595-610.
- [34] aC. C. Oliveira, B. Querido, M. Sluijter, A. F. de Groot, R. van der Zee, M. J. Rabelink, R. C. Hoeben, F. Ossendorp, S. H. van der Burg, T. van Hall, *J Immunol* **2013**, *191*, 4020-4028; bE. D. Cram, R. S. Simmons, A. L. Palmer, W. H. Hildebrand, D. D. Rockey, B. P. Dolan, *Infect Immun* **2015**, *84*, 480-490.
- [35] J. M. Vyas, A. G. Van der Veen, H. L. Ploegh, *Nat Rev Immunol* **2008**, *8*, 607-618.
- [36] aD. H. Schuurhuis, S. Laban, R. E. M. Toes, P. Ricciardi-Castagnoli, M. J. Kleijmeer, E. I. H. van der Voort, D. Rea, R. Offringa, H. J. Geuze, C. J. M. Melief, F. Ossendorp, *The Journal of Experimental Medicine* **2000**, *192*, 145-150; bC. Winzler, P. Rovere, M. Rescigno, F. Granucci, G. Penna, L. Adorini, V. S. Zimmermann, J. Davoust, P. Ricciardi-Castagnoli, *The Journal of Experimental Medicine* **1997**, *185*, 317-328.
- [37] aZ. Shen, G. Reznikoff, G. Dranoff, K. L. Rock, *J Immunol* **1997**, *158*, 2723-2730; bA. Rhule, B. Rase, J. R. Smith, D. M. Shepherd, *J Ethnopharmacol* **2008**, *116*, 179-186.
- [38] P. J. Peters, in *Current Protocols in Cell Biology*, John Wiley & Sons, Inc., **2001**.

Bioorthogonal deprotection on the dendritic cell surface allows chemical control of antigen cross-presentation

Published as part of: Joanna B. Pawlak, Geoffroy P. Gential, Tracy J. Ruckwardt, Jessica S. Bremmers, Nico J. Meeuwenoord, Ferry A. Ossendorp, Herman S. Overkleeft, Dmitri V. Filippov and Sander I. van Kasteren
Angewandte Chemie International Edition. Hot Paper. **2015**, 54(19): 5628-31.

5.1 Introduction

In the process of antigen cross-presentation^[1], long polypeptides are taken up by phago-^[2], endo-^[3], or macropinocytosis^[4] and proteolytically degraded inside the cell to octamer or nonamer peptides by a host of different proteases^[5]. During processing, the polypeptides pass through a series of organelles^[1] to end up loaded on major histocompatibility complex class I (MHC-I) receptors for immune surveillance by CD8⁺ T cells^[6] (Figure 1A). This process is essential for both self-tolerance and priming of CD8⁺ T cells against virus-infected and malignantly transformed self-cells^[7] and is therefore of pivotal importance, for example, in cancer immunotherapy^[8]. The biochemistry of antigen cross-presentation is complex^[1]: different organelles, channels, and chaperones have been implicated in the routing of the antigen, and many proteases are involved in the proteolytic liberation of the epitope peptides during this routing^[9] (see chapter 2). This chapter concerns the development of a new method for studying this process that would allow chemical control over the final activation step while causing only minimal structural alteration of the epitope^[10]. Organic azides are the most extensively used bioorthogonal group^[11]. They have been incorporated into glycoproteins^[12], polypeptides^[13], and lipids^[14] in bacteria^[15], eukaryotes^[16], and metazoans^[17]. Azides are readily incorporated by hijacking the

cell's biosynthetic machinery^[18] with minimal structural perturbation to the biomolecule and minimal cytotoxicity. Three different bioorthogonal reactions exist for ligating this handle: Staudinger–Bertozzi ligation^[12], copper-catalyzed [3+2] Huisgen cycloaddition (cChC)^[19], and strain-promoted [3+2] cycloaddition (SPC) reactions^[20]. Owing to their versatility, stability, and ease of use, azides have become the functional group of choice for *in vivo* bioorthogonal chemistry^[21]. However, one aspect of the azide that has been relatively underexplored to date is its function as a bioorthogonal protecting group for amines. Here a different use of the azide is described: not for ligation, but instead as a bioorthogonal protecting group to mask the amine groups in a CD8⁺ T cell epitope and render it unrecognized by its cognate T cell. Combining this “latent epitope” with on-surface deprotection chemistry would liberate the native epitope and thus activate the T cell (Figure 1B). This approach offers advantages over existing methods that employ photocaged epitopes^[22] as very low conversions into the native antigen are observed in this approach^[22b]. Furthermore, photocaged epitopes have not been shown to be compatible with intracellular processing and routing. This study herein reports that masked epitopes bearing organic azides are 1) cross-presented by antigen-presenting cells (APCs) with near-equal efficiency compared to their native counterparts, and 2) are unmasked with high efficiency by a Staudinger reduction to yield a fully operational MHC-I/peptide epitope complex.

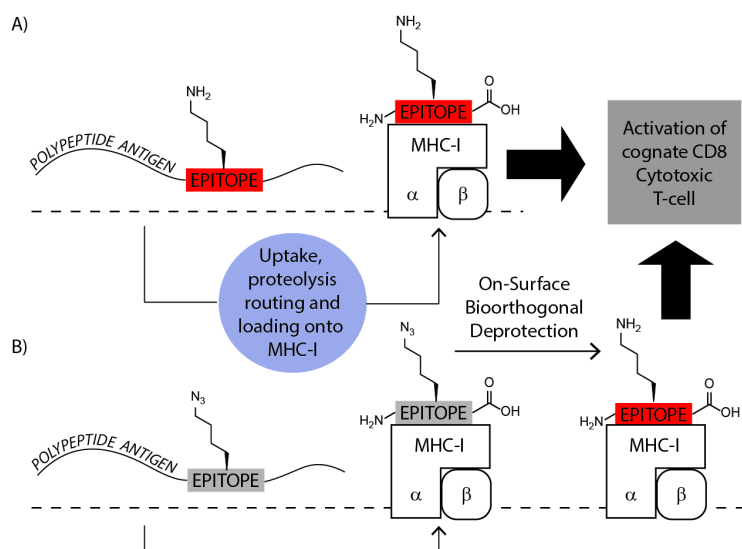


Figure 1. A) Cross-presentation of a polypeptide antigen. During this process the polypeptide is taken up and routed to the MHC-I loading complex. Meanwhile the polypeptide is degraded to liberate an 8-9-mer epitope peptide that is loaded. B) Processing and presentation of azide-protected latent epitopes. Azido-antigens are processed and presented on MHC-I as normal, but not recognized by the epitope-specific cognate T cell clone. Only after an on-cell deprotection is the native epitope liberated and the T cell activated.

5.2 Results and discussion

The H2-K^b-restricted immunodominant epitope from chicken egg white ovalbumin OVA₂₅₇₋₂₆₄ (OT-I, SIINFEKL; Figure 2A) was chosen as a starting epitope for modification.

This extensively studied epitope has three residues that mediate the interaction with its cognate TCR^[23]: P4, P6, and P7. Four other residues ensure MHC-I anchoring^[24]: P2, P3, P5, and P8. It can be thus anticipated that a chemical mutation of Lys₂₆₃ (P7) to an azidonorleucine (ANL; Figure 2B) would strongly reduce T cell recognition while minimally affecting MHC-I binding. Mutation of this residue to alanine had a minor effect on peptide/MHC-I stability, but reduced T cell recognition of cognate clones by a factor of 100–1000^[24]. The OT-I epitope peptide and a variant peptide bearing a Lys to ANL substitution (OT-Az; Figure 2B) was synthesized and the recognition of this epitope by an OT-I- specific T cell was assessed. Further the fact that high-affinity epitopes can be loaded onto receptive MHC-I complexes on the surface of APCs by simple co-incubation was exploited^[25] and the antigenicity of the OT-I and OT-Az peptides using the immortal LacZ-containing reporter T cell line, B3Z^[26] was measured. This T cell line allows the quantitation of T cell activation through monitoring of the β -galactosidase- mediated conversion of a fluorogenic substrate^[27]. H2-K^b-positive bone-marrow- derived dendritic cells (BMDCs) were used as the APCs^[28]. After peptide loading and overnight incubation with B3Z, no T cell activation by OT-Az at concentrations as high as 10 μ M (Figure 2C) was observed. This represents a reduction in T cell activation by more than five orders of magnitude, which underscores the key role of the lysine ϵ -amino group for OT-I recognition by the T cell.

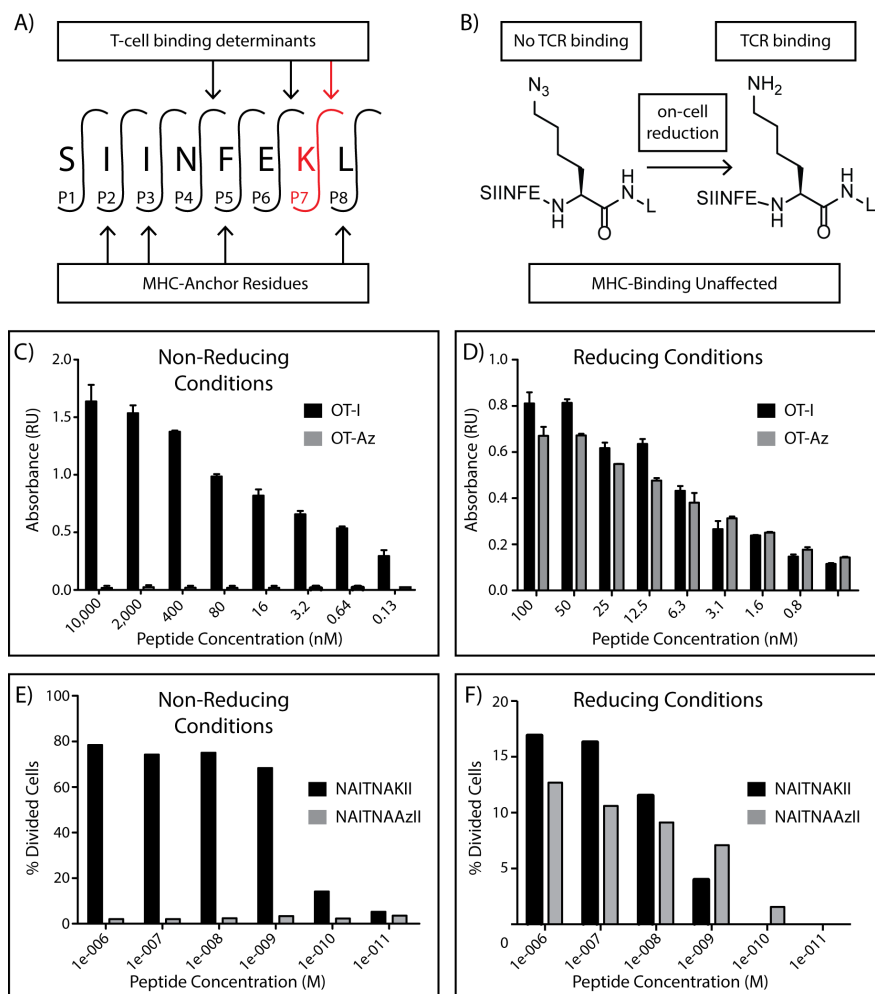


Figure 2. Chemical unmasking of azido epitopes restored T cell activation. *A)* Certain residues are key for anchoring to MHC-I and others are key T cell recognition determinants. *B)* Lysine at P7 was chosen as the target residue for masking; converting the cognate epitope OT-I into the azido analogue OT-Az was postulated to prevent T cell recognition while minimally affecting MHC-I binding. *C)* OT-Az is indeed not recognized by B3Z T cells. *D)* Upon reduction with TCEP (100 mM), OT-Az is converted into an epitope that is recognized by B3Z. *E)* The activation of D^bM₁₈₇₋₁₉₅-specific transgenic CD8⁺ T cells by NAITNAKII or NAITNAAZII follows a similar trend: Azido epitopes were not recognized. *F)* After reduction as above, the recognition of NAITNAAZII was restored.

To assess the potential of the azide moiety as a bioorthogonal protecting group, the Staudinger reduction—the aqueous reduction of azides by trivalent phosphorus species was explored as a possible bioorthogonal deprotection reaction^[29]. The biocompatibility of this reaction was established by the group of Bertozzi, who showed that tris(2-carboxyethyl) phosphine hydrochloride (TCEP) partially reduces azido groups on mammalian cell surfaces^[12]. A series of phosphorus reagents were screened for their ability to reduce azides (Supporting Table 1 (S1)). Interestingly, when the phosphine-mediated reduction of the azide with TCEP was monitored

(Figure S1A), the azide was observed to disappear almost completely within the first 20 minutes. Alongside the formation of the expected OT-I epitope, the conversion of the azide into the primary alcohol was also observed by NMR spectroscopy. Its formation may be due to nucleophilic substitution of the intermediate iminophosphorane group by water. The formation of a small amount of alkene, as detected by LC-MS, is consistent with the idea that the iminophosphorane can also serve as a leaving group. Treatment of OT-Az with bulkier and less nucleophilic triphenylphosphine-3,3',3''-trisulfonic acid proceeded sluggishly (Figure S1B) and did not yield any OT-I; instead, an approximately 2:1 mixture of OT-OH and the alkene was formed. In future, the study of more reactive water-soluble phosphines, such as those containing alkyl sulfonates, PEGylated variants as well as other azide reducing agents might be considered. Finally the on-cell TCEP-mediated unmasking of the OT-Az epitope on BMDCs was performed. It has been found that 100 mM TCEP resulted in optimal on-surface deprotection (Figure 3A). Unmasking appeared to be complete within a reaction time of 15 minutes (Figure 3B).

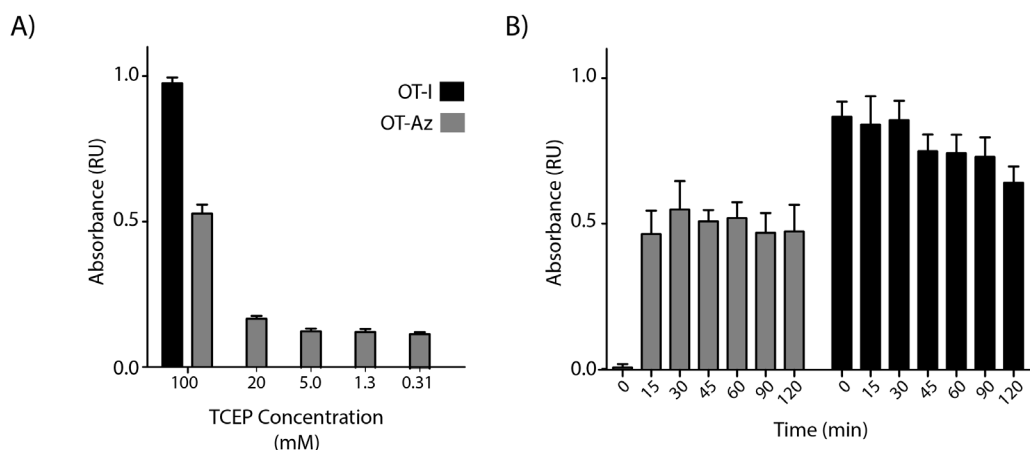


Figure 3. A) B3Z T cells response to OT-I (10 nM) and OT-Az (10 nM) in presence of the reducing agent TCEP for 30 minutes at the indicated concentrations. B) reduction of OT-Az and OT-I (10 nM) with TCEP (100 mM) for indicated time periods. Reduction was complete within 15 minutes.

Under these conditions (100 mM TCEP, 30 min), the T cell reactivity on the cell surface of BMDCs was fully rescued at dose-limiting peptide concentrations. At high concentrations, partial rescue was observed (>80%, Figure 2D), which could be due to inefficient conversion at these concentrations or competition of the aforementioned side reactions, which leads to unrecognized side products. Effects that are due to toxicity were ruled out (Table S1) as pH-adjusted TCEP was found to be non-toxic to BMDCs at the concentrations and reaction times required for on-surface unmasking (viability >98%; Table S1). To exclude artifacts stemming from the specific epitope

(OT-I) and the specific MHC-I haplotype (H2-K^b), a second epitope and MHC-I haplotype was also tested: the D^bM₁₈₇₋₁₉₅ epitope from respiratory syncytial virus (RSV)^[30]. RSV is the main causative agent of respiratory failure in infants, and the role of CD8⁺ mediated T cell immunity remains somewhat controversial. D^bM₁₈₇₋₁₉₅ is a dominant epitope in C57BL/6 mice^[31] and a highly functional subdominant epitope in CB6F1 mice^[30]. The D^b-binding NAITNAKII nonamer is critically dependent on Lys₁₉₃ for T cell recognition^[32], thus masking of this residue would presumably ablate T cell recognition similarly to the OT-I epitope. Residue 193 was therefore subjected to a chemical mutation from Lys to ANL (NAITNAAzII). Masking successfully prevented recognition of the ANL-variant peptide by T cell receptor transgenic CD8⁺ T cells specific for the D^bM₁₈₇₋₁₉₅ epitope, even at high peptide concentrations (up to 1 μM tested, Figure 2E). Upon addition of TCEP, T cell recognition was restored to a similar extent as for OT-Az/OT-I (Figure 2F). These results indicate that the azide group can indeed be used to generate masked epitopes and that the unmasking reaction can be chemically controlled and proceeds with good yields. However, the pivotal aim was to develop a reagent that could be used to unmask antigens after intracellular processing, to allow the separation of intracellular cross-presentation kinetics and on-cell pMHC dynamics. To study whether this approach was compatible with the biochemistry that an antigen encounters during cross-presentation, long peptides containing either the OT-I or OT-Az epitopes (LP-I and LP-Az; Figure 4A) were synthesized. Subsequently, these long peptides were added to BMDCs and after 3 hours, they were subjected to a reduction with TCEP. The cells were washed prior to addition of B3Z T cells for immune surveillance. No intracellular reduction of the azide to the corresponding amine was observed during cross-presentation (Figure 4B). When TCEP was added after the addition of one of the peptides, full T cell reactivity against OT-I could be recovered at low peptide concentrations (Figure 4C). A marked reduction in rescue was observed (>50% rescue) at higher peptide concentrations, which could in part be explained as before, and in part be due to minor differences in processing efficiency resulting from the amine-to-azide modification.

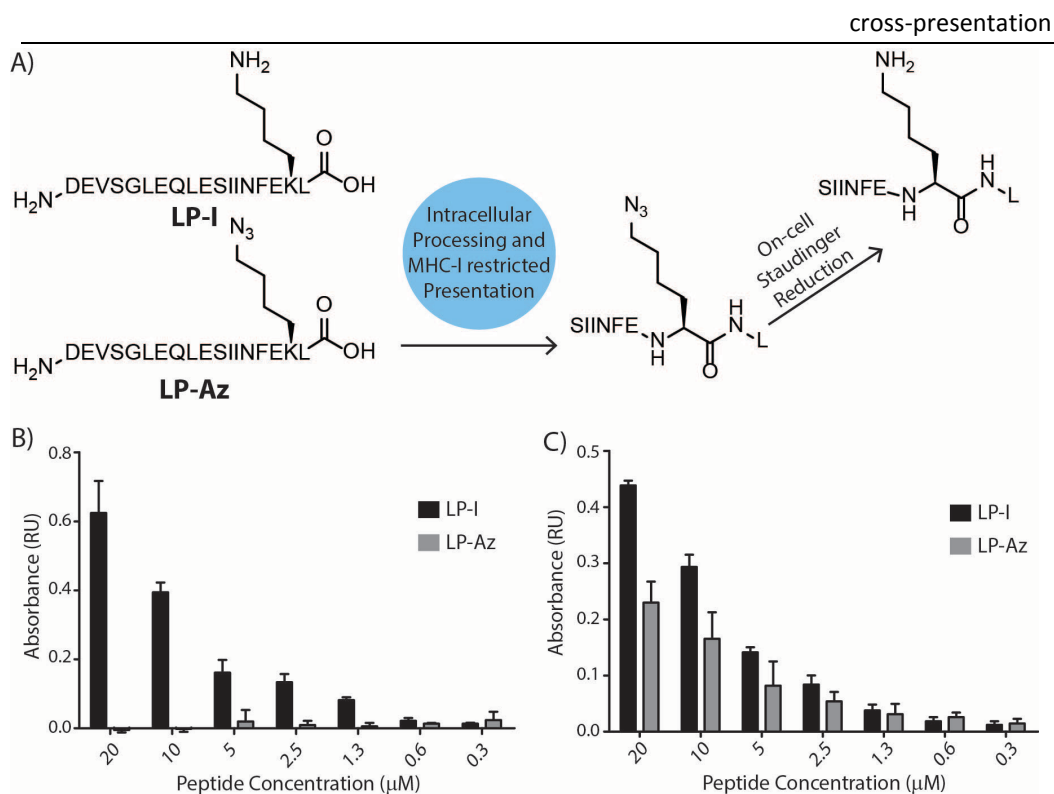


Figure 4. Presentation of long peptides to B3Z-hybridoma. A) Design of long peptides for studying the suitability of azido epitopes as latent antigens for intracellular routing. B) Intracellular routing of LP-Az resulted in no activation of the OT-I cognate B3Z T cell clone. C) Reduction with TCEP three hours after the initial peptide addition resulted in partial recovery of T cell activation.

In summary, the results have demonstrated that organic azides are not only valuable bioorthogonal ligation handles, but are equally applicable to bioorthogonal protection. This phenomenon was exploited to produce latent epitopes that enabled the controlled activation of epitopes on the surface of APCs after uptake, intracellular routing, and proteolysis for the first time. Azide-masked epitopes represent a powerful new approach for the study of antigen cross-presentation. They are mutually orthogonal to photocaged epitopes^[22b, 33]. Applying this approach to whole protein antigens would also offer an interesting comparison of the presentation kinetics of these different antigen classes. The chemical unmasking of a bioorthogonal group using a Diels–Alder reaction on a whole protein can be envisaged to be of use to this approach^[34], although—like the photocaging reaction—it employs a bulky protecting group, which may preclude normal intracellular routing and proteolytic processing. The main limitation of this approach is that it is currently limited to epitopes with lysine at key positions for T cell recognition. The application of other bioorthogonal reactions to mask other natural epitopes would broaden the scope of this approach and offer even further additions to the immunologist’s toolkit, as it

allows the separation of early and late-appearing antigens for the first time, which would allow the determination of the contribution of such populations to the overall immune response.

Despite the above application of this reagent for studying for example early appearing antigen, the importance laid in the interest in the study of later-appearing peptide-MHC-I complexes. Therefore a reaction that could permanently block the latent epitopes early in the immune response was sought. For this, other azide chemistry, namely the biocompatible strain-promoted alkyne-azide [3+2] cycloaddition reactions (SPAAC)^[20] was applied. These reactions (Figure 5A) can selectively form a new triazolyl-species in a bioorthogonal fashion at the cell surface^[21]. The potential of the SPAAC-reaction was studied by incubating OT-Az-pulsed BMDCs with bicyclo[6.1.0]non-4-yn-9-ylmethanol (BCN-NH₂)^[35], as this strained alkyne has the most favorable properties with respect to aspecific binding^[27]. First, the BMDCs were OT-Az pulsed for 1 hour followed by reaction with BCN-NH₂. After subsequent reduction with TCEP, it was found that BCN-NH₂ prevented uncloning by TCEP (Figure 5B). Antigen presentation of OT-I peptide-pulsed BM-DCs treated under these same conditions was unaffected. Next this sequence was applied to the study of long peptide antigen processing. BMDCs were pulsed for 3 hours with LP-1 or LP-Az, followed by a blocking with BCN-NH₂ at the end of this 3 hour pulse period followed by a reduction (Figure 5C). This sequence showed that presentation of OT-Az could be blocked by this reagent without affecting routing and presentation of LP-Az.

To test whether this reaction could be used to isolate the contribution of late appearing antigen during the immune response against the OVA-long peptide, the BMDCs were first pulsed for 3 hours (no immune responses were observed with shorter pulses of LP-I) followed by the blocking step with BCN-NH₂. Reductions were then performed at different time points after this initial blocking step (Figure 5D). Strikingly, no new antigen appeared after the initial 3 hour block, suggesting a rapid burst in processing kinetics.

5.3 Conclusion

These results demonstrate that azide-modified epitopes are a powerful new class of reagents for the study of antigen cross-presentation. Not only can they be uncloaked in robust yields on the surface of cells to reveal lysines, they can also be used to visualize the presence of peptide MHC-I on the cell surface. In the future, it would be exciting to use these peptides with the previously reported photocaged epitopes^[22a], if an increase in on-cell uncaging yields can be achieved for this approach^[22b]. Also, the incorporation of these handles into protein antigens, or the combination with the recently reported chemical uncloaking of a bioorthogonal handle that was incorporated into a whole protein^[36] would allow further expansion of this approach.

5.4 Supporting table and figure

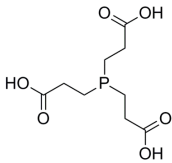
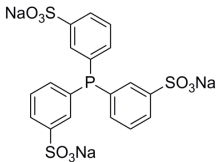
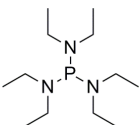
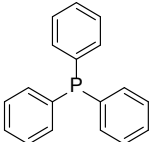
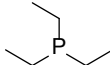
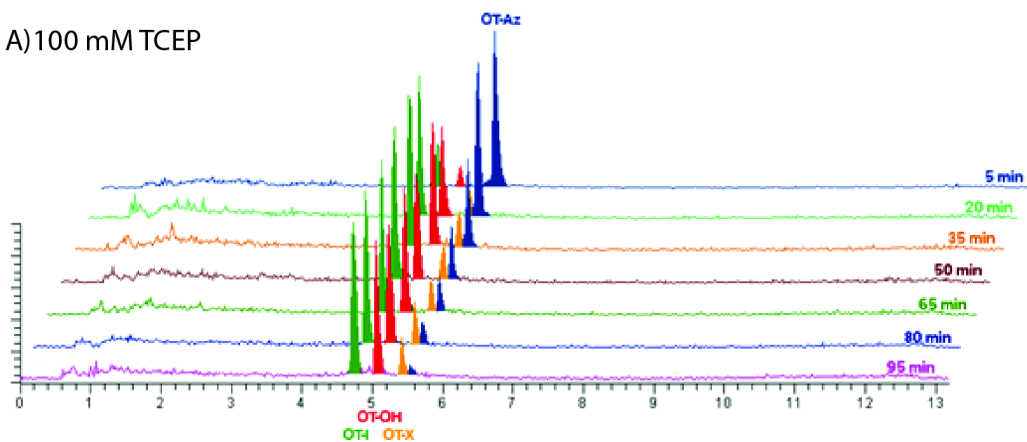
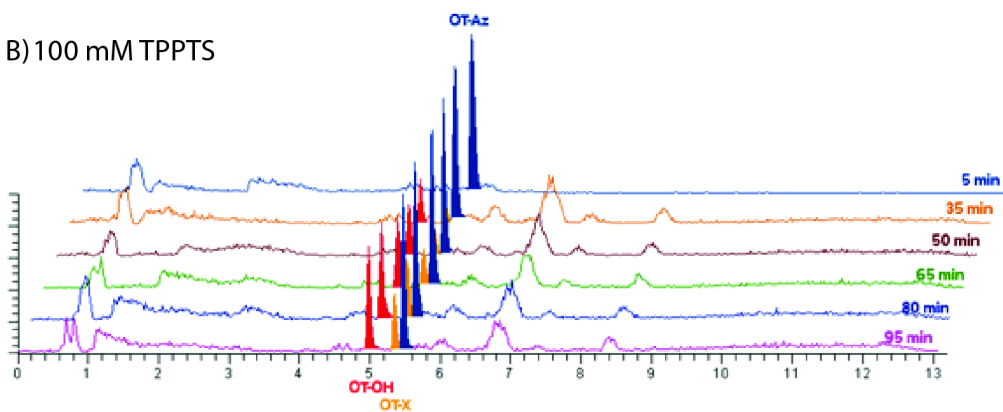
Name	Structure	Solubility in PBS			Incubation Time (h)	Percentage viable Cells			
		500 mM	100 mM	10 mM		100 mM	10 mM	1 mM	0 mM
Tris-(2-carboxyethyl) phosphine (TCEP)		500 mM	100 mM	10 mM		100 mM	10 mM	1 mM	0 mM
		Yes	Yes	Yes	0.5	98	94	96	94
					1.0	94	93	94	98
					1.5	57	89	95	99
					2.0	1	89	93	97
Triphenyl-phosphine-3,3',3''-trisulfonic acid (TPPTS)		500 mM	100 mM	10 mM		100 mM	10 mM	1 mM	
		Yes	Yes	Yes	0.5	98	91	99	
					1.0	98	99	98	
					1.5	87	99	99	
					2.0	0	99	99	
Sodium hypophosphite (SHP)		500 mM	100 mM	10 mM		100 mM	10 mM	1 mM	
		Yes	Yes	Yes	0.5	97	99	93	
					1.0	100	98	99	
					1.5	97	99	99	
					2.0	97	99	99	
Insoluble phosphine also tested									
Tris-(diethyl amino)-phosphine (TDAP)		Triphenyl Phosphine (TPP)				Triethyl Phosphine (TEP)			

Table S1. Overview of all phosphines tested in this study.

A) 100 mM TCEP



B) 100 mM TPPTS



C) 100 mM SHP

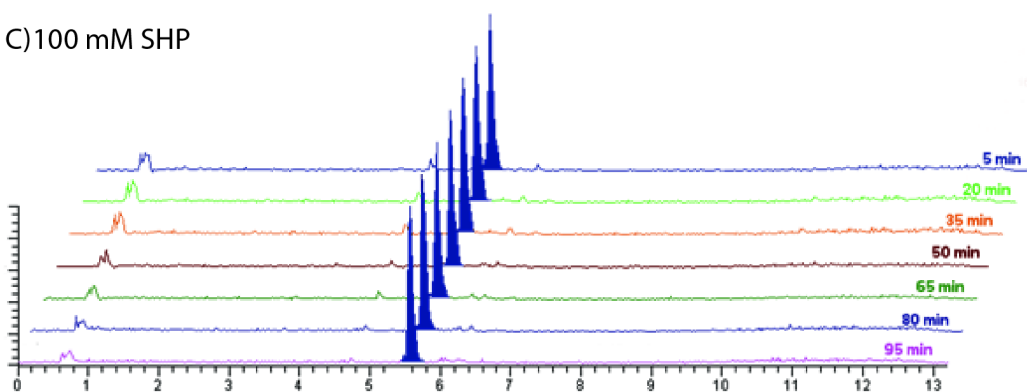


Figure S1. 0.1mM OT-Az solution (in PBS) was reduced with 100 mM of phosphines. The reaction was performed at room temperature and monitored every 15 minutes using LCMS. A) Reduction with 100 mM TCEP. B) Reduction with 100 mM TPPTS. C) Reduction with SHP. LCMS indicated the formation of 2 major side products: OT-OH – the ϵ -hydroxylysine - and OT-X – the δ - ϵ -alkene, the result of elimination via an E2 mechanism.

5.5 Experimental section

Reagents:

Solvents used for column chromatography were of technical grade from Sigma Aldrich and used directly. Chemicals tris(2-carboxyethyl)phosphine, triphenyl-phosphine-3,3',3''-trisulfonic acid, sodium hypophosphite, tris-(diethylamino)-phosphine, streptomycin, chlorophenol red- β -D-galactopyranoside, IMDM-medium were purchased from Sigma Aldrich and used without further purifications. OT-I was purchased from Invivogen. Endotoxin-free PBS was Gibco-brand purchased from Life Technologies. GM-CSF was purchased from ImmunoTools and hygromycin B from AG technologies.

HPLC kinetics:

In 700 μ L of PBS was added 100 μ L of 1mM SIINFEAZL solution in PBS. Then 200 μ L of 0.5M solution of desired phosphine and the reaction was performed at room temperature without stirring. Monitoring the reaction was done using LCMS every 15 min. For LC-MS analysis a JASCO HPLC-system (detection simultaneously at 214 and 254 nm) equipped with an analytical C18 column (4.6 mmD \times 50 mL, 3 μ particle size) in combination with buffers A: H₂O, B: MeCN and C: 0.5% aq. TFA and coupled to a PE/SCIEX API 165 single quadruple mass spectrometer (Perkin-Elmer) was used.

Bone marrow derived dendritic cells:

BMDCs were generated from B57BL/6 mice bone marrow essentially as described^[37] with some modifications. Briefly, bone marrow was flushed from femurs and tibia and cells were cultured in IMDM supplemented with 8% heat-inactivated fetal calf serum, 2mM glutamax, 20 μ M 2-Mercaptoethanol, penicillin 100 I.U./mL and streptomycin 50 μ g/mL in the presence of 20ng/mL GM-CSF. Medium was replaced on day 3 and 7 of culture and the cells were generally used between days 10 and 13.

B3Z-hybridoma culturing: The OVA₂₅₇₋₂₆₄-specific, H-2K^b-restricted CTL hybridoma, B3Z^[26] was cultured in IMDM medium supplemented with 10% FCS, 2mM glutamax, 0.25mM 2-Mercaptoethanol, penicillin 100 I.U./mL and streptomycin 50 μ g/mL in the presence of hygromycin B (500 μ g/mL)^[38].

Antigen presentation assays:

BMDCs were plated in 96-well tissue-culture treated microtiterplates (5 \times 10⁴ cells/well) for 1h and allowed to adhere at 37 °C for 1 h prior the addition of peptides at the indicated concentrations. BMDCs were incubated with the peptides for the indicated times (usually 1h for minimal epitopes and 3h for SLPs), followed by a wash with complete IMDM. Peptide-pulsed BMDCs were then treated with 100 mM TCEP in 1% fetal calf serum for 1h at 37°C. After removal of the reduction medium, the cells were washed with complete IMDM and resuspended in 100 μ L/well cIMDM before the addition of the T cell hybridoma B3Z cells (5 \times 10⁴ cells/well). The BMDCs and T cells were co-cultured for 17 h at 37°C. Stimulation of the B3Z hybridoma was

measured by a colorimetric assay using CPRG (chlorophenol red- β -D-galactopyranoside) as a substrate as described^[39].

Mixed splenocyte T cell activation assay:

To assess the ability of T cells to respond to the natural Db-binding NAITNAKII peptide of RSV or the chemically-modified NAITNAAzII peptide, splenocytes were isolated from CB6F1 (Db-bearing) mice using Fico/Lite-LM. Following isolation, splenocytes were incubated with the indicated concentrations of the natural or modified peptide for one hour at 37°C in R-10 (RPMI supplemented with 10% fetal bovine serum, 2mM L-Glutamine, 1mM sodium pyruvate, non-essential amino acids, 25mM HEPES, 5x10⁻⁵M β -mercaptoethanol and pen/strep antibiotics) prior to washing and incubating in either PBS with 1% serum (control), or 100mM TCEP in PBS/1% serum. After an additional hour at 37°C, the splenocytes were washed with media, and cocultured with CFSE-labeled D^bM₁₈₇₋₁₉₅-specific transgenic CD8⁺ T cells isolated using an untouched CD8 α ⁺ T cell isolation kit (MiltenyiBiotec) as previously described^[40]. Following three days of culture, samples were stained for CD8⁺, CD3⁺, and viability as previously described^[40], and the percent of the labeled transgenic CD8⁺ T cell population that divided was determined using the proliferation module of FlowJo 9.7.4.

Cell viability assay:

BMDCs were plated into 24-well tissue-culture treated flat bottom transparent plate (3x10⁵ cells/well) and allowed to adhere for 1 hour at 37°C. The cells were incubated with different phosphines at the indicated concentration and time (½ hour, 1h, 1½ hour and 2h) in 1% fetal calf serum in PBS at 37°C. After removal of the phosphine solutions, the cells were washed with cIMDM and incubated for 2h at 37°C before the addition of propidium iodide (2 μ g/mL) and Hoechst 33258 (2 μ g/mL) and incubation for 15min at RT. The cells were imaged on Olympus IX81 using 4x objective. 10 images were collected per condition and counted for Hoechst 33258 and propidium iodide analyzed with LASAF software and live-dead cell counting was performed automatically using the particle counting functionality in the ImageJ analysis software.

Peptide synthesis:

Peptides were synthesized using standard Fmoc Solid Support Chemistry and purified using high performance liquid chromatography (Prep column Gemini C18 110A 150x21.20 5 μ m) using 15 to 45 % gradient (A: 0.1% TFA in MilliQH2O, B: ACN). LC-MS measurements were done on an API 3000 Alltech 3300 with a Grace Vydac 214TP 4,6 mm x 50 mm C4 column.

5.6 References

- [1] O. P. Joffre, E. Segura, A. Savina, S. Amigorena, *Nat Rev Immunol* **2012**, *12*, 557-569.
- [2] M. Kovacovics-Bankowski, K. L. Rock, *Science* **1995**, *267*, 243-246.
- [3] K. L. Rock, K. Clark, *J Immunol* **1996**, *156*, 3721-3726.
- [4] C. C. Norbury, L. J. Hewlett, A. R. Prescott, N. Shastri, C. Watts, *Immunity* **1995**, *3*, 783-791.
- [5] aJ. M. Vyas, A. G. Van der Veen, H. L. Ploegh, *Nat Rev Immunol* **2008**, *8*, 607-618; bK. L. Rock, L. Shen, *Immunol Rev* **2005**, *207*, 166-183; cT. Serwold, F. Gonzalez, J. Kim, R. Jacob, N. Shastri, *Nature* **2002**, *419*, 480-483.
- [6] J. Neefjes, M. L. Jongsma, P. Paul, O. Bakke, *Nat Rev Immunol* **2011**, *11*, 823-836.
- [7] A. Lanzavecchia, *Nature* **1998**, *393*, 413-414.
- [8] D. S. Chen, I. Mellman, *Immunity* **2013**, *39*, 1-10.
- [9] I. A. York, A. L. Goldberg, X. Y. Mo, K. L. Rock, *Immunol Rev* **1999**, *172*, 49-66.
- [10] L. Schmitt, R. Tampe, *Chembiochem* **2000**, *1*, 16-35.
- [11] E. M. Sletten, C. R. Bertozzi, *Acc Chem Res* **2011**, *44*, 666-676.
- [12] E. Saxon, C. R. Bertozzi, *Science* **2000**, *287*, 2007-2010.
- [13] K. L. Kiick, E. Saxon, D. A. Tirrell, C. R. Bertozzi, *Proc Natl Acad Sci U S A* **2002**, *99*, 19-24.
- [14] H. C. Hang, J. P. Wilson, G. Charron, *Acc Chem Res* **2011**, *44*, 699-708.
- [15] R. Hatzenpichler, S. Scheller, P. L. Tavormina, B. M. Babin, D. A. Tirrell, V. J. Orphan, *Environ Microbiol* **2014**, *16*, 2568-2590.
- [16] D. C. Dieterich, J. J. Lee, A. J. Link, J. Graumann, D. A. Tirrell, E. M. Schuman, *Nat Protoc* **2007**, *2*, 532-540.
- [17] aS. T. Laughlin, J. M. Baskin, S. L. Amacher, C. R. Bertozzi, *Science* **2008**, *320*, 664-667; bP. V. Chang, J. A. Prescher, E. M. Sletten, J. M. Baskin, I. A. Miller, N. J. Agard, A. Lo, C. R. Bertozzi, *Proc Natl Acad Sci U S A* **2010**, *107*, 1821-1826.
- [18] K. L. Kiick, D. A. Tirrell, *Tetrahedron* **2000**, *56*, 9487-9493.
- [19] C. W. Tornoe, C. Christensen, M. Meldal, *J Org Chem* **2002**, *67*, 3057-3064.
- [20] N. J. Agard, J. A. Prescher, C. R. Bertozzi, *J Am Chem Soc* **2004**, *126*, 15046-15047.
- [21] D. M. Patterson, L. A. Nazarova, J. A. Prescher, *ACS Chem Biol* **2014**, *9*, 592-605.
- [22] aM. Huse, *Immunology* **2010**, *130*, 151-157; bM. Huse, L. O. Klein, A. T. Girvin, J. M. Faraj, Q. J. Li, M. S. Kuhns, M. M. Davis, *Immunity* **2007**, *27*, 76-88.
- [23] aO. Rotzschke, K. Falk, S. Stevanovic, G. Jung, P. Walden, H. G. Rammensee, *Eur J Immunol* **1991**, *21*, 2891-2894; bS. Malarkannan, S. Goth, D. R. Buchholz, N. Shastri, *J Immunol* **1995**, *154*, 585-598.
- [24] S. C. Jameson, M. J. Bevan, *Eur J Immunol* **1992**, *22*, 2663-2667.
- [25] N. Shastri, F. Gonzalez, *J Immunol* **1993**, *150*, 2724-2736.
- [26] J. Karttunen, N. Shastri, *Proc Natl Acad Sci U S A* **1991**, *88*, 3972-3976.
- [27] M. M. Willems, G. G. Zom, N. Meeuwenoord, F. A. Ossendorp, H. S. Overkleeft, G. A. van der Marel, J. D. Codee, D. V. Filippov, *Beilstein J Org Chem* **2014**, *10*, 1445-1453.
- [28] M. B. Lutz, N. Kukutsch, A. L. Ogilvie, S. Rossner, F. Koch, N. Romani, G. Schuler, *J Immunol Methods* **1999**, *223*, 77-92.
- [29] aH. Staudinger, J. Meyer, *Helvetica Chimica Acta* **1919**, *2*, 635-646; bY. G. Gololobov, L. F. Kasukhin, *Tetrahedron* **1992**, *48*, 1353-1406.
- [30] T. J. Ruckwardt, C. Luongo, A. M. Malloy, J. Liu, M. Chen, P. L. Collins, B. S. Graham, *J Immunol* **2010**, *185*, 4673-4680.

- [31] J. A. Rutigliano, M. T. Rock, A. K. Johnson, J. E. Crowe Jr, B. S. Graham, *Virology* **2005**, 337, 335-343.
- [32] P. Billam, K. L. Bonaparte, J. Liu, T. J. Ruckwardt, M. Chen, A. B. Ryder, R. Wang, P. Dash, P. G. Thomas, B. S. Graham, *J Biol Chem* **2011**, 286, 4829-4841.
- [33] A. L. DeMond, T. Starr, M. L. Dustin, J. T. Groves, *J Am Chem Soc* **2006**, 128, 15354-15355.
- [34] R. M. Versteegen, R. Rossin, W. ten Hoeve, H. M. Janssen, M. S. Robillard, *Angew Chem Int Ed Engl* **2013**, 52, 14112-14116.
- [35] J. Dommerholt, S. Schmidt, R. Temming, L. J. Hendriks, F. P. Rutjes, J. C. van Hest, D. J. Lefeber, P. Friedl, F. L. van Delft, *Angew Chem Int Ed Engl* **2010**, 49, 9422-9425.
- [36] J. Li, S. Jia, P. R. Chen, *Nat Chem Biol* **2014**, 10, 1003-1005.
- [37] S. Hoogendoorn, G. H. van Puijvelde, J. Kuiper, G. A. van der Marel, H. S. Overkleeft, *Angew Chem Int Ed Engl* **2014**, 53, 10975-10978.
- [38] G. Cafri, A. Sharbi-Yunger, E. Tzehoval, L. Eisenbach, *PLoS ONE* **2013**, 8, e55583.
- [39] S. Khan, M. S. Bijker, J. J. Weterings, H. J. Tanke, G. J. Adema, T. van Hall, J. W. Drijfhout, C. J. M. Melief, H. S. Overkleeft, G. A. van der Marel, D. V. Filippov, S. H. van der Burg, F. A. Ossendorp, *J. Biol. Chem.* **2007**.
- [40] T. J. Ruckwardt, A. M. Malloy, K. M. Morabito, B. S. Graham, *PLoS Pathog* **2014**, 10, e1003934.



Summary and future prospects

The research described in this thesis offers an initial exploration of bioorthogonal chemistry as a tool to study antigen cross-presentation. Furthering the understanding of this process is crucial as it is an important mechanism to elicit specific cytotoxic T cell response necessary for clearance of cancers and pathogenic infections. It is also crucial regarding vaccinations with protein antigens as the aim is to apply the knowledge obtained here to the design of new peptides for anti-cancer vaccines.

In **chapter 1**, the general principles of antigen processing and presentation in MHC-I, -II, as well as the rudimentary details of cross-presentation are described. Antigen cross-presentation pathways are central to the work described in this thesis. Therefore, **Chapter 2** presents an overview of the various antigen cross-presentation pathways as well as molecular approaches for studying them. A few examples of the current methods are described in detail together with their limitations and potential applications. Also, bioorthogonal antigens as novel tools to study cross-presentation process are introduced in this chapter.

The initial development of a new strategy to quantify specific peptide–MHC-I complexes (pMHC-I) on cell surface using bioorthogonal chemistry is described in **chapter 3**: A library of peptides containing different bioorthogonal handles (azides and alkynes) within the epitope were synthesized and the MHC-I binding^[1] and stability of these modified peptides in the RMA-S cell line assay^[2] were optimized. In

order to obtain the most efficient bioorthogonal ligation reaction, various types of bioorthogonal ligation reactions were tested and assessed. The most optimal condition, type of fluorophore and bioorthogonal ligation reaction^[3] were established. The requirement for the most efficient epitope quantification is the alkyne modification in non-anchor residues in solvent-accessible epitope positions using CalFluor-488 in combination with a Cu(I)-catalyzed Huisgen cycloaddition reaction (Figure 1).

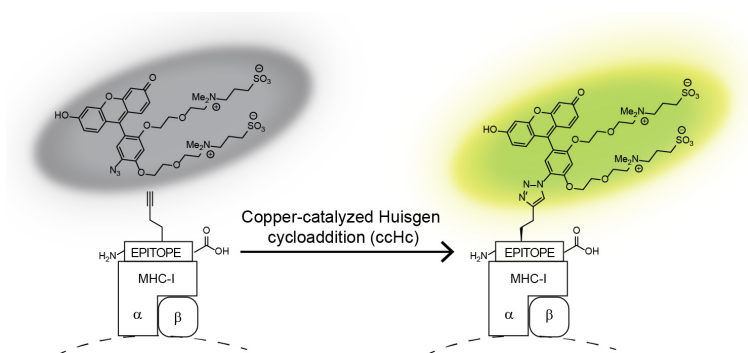


Figure 1. Schematic representation of the bioorthogonal ligation strategy using CalFluor-488 in cHc reaction.

The major limitation of this approach is the requirement of copper in the cHc reaction. Alternative to this approach, the use of click chemistries not requiring catalysis could be applied. For example, the inverse electron-demand Diels-Alder (IEDDA) reaction (Figure 2) between cyclopropene as a dienophile and tetrazine as a diene can, in principle, allow *in vivo* labeling without the need of copper and fixation^[4]. However, the background reactivity of this chemistry has not been fully explored in a system as stringent as antigen presentation.

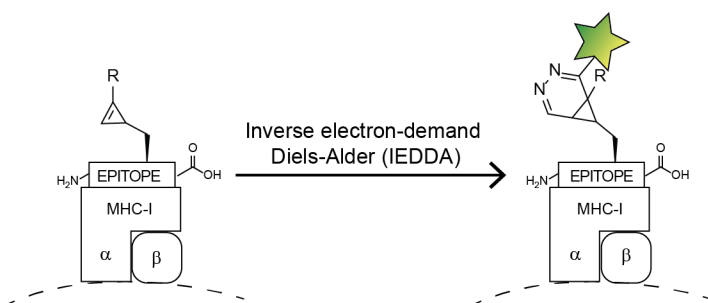


Figure 2. Proposed schematic representation of the bioorthogonal ligation strategy using tetrazine-fluorophore in IEDDA reaction.

When studying antigen processing and presentation, techniques that can label the cell surface in isolation would be very valuable. Hence, such a method was developed based on a three- step labeling procedure. To circumvent the permeability to small molecules caused by the use of copper, a three step labeling approach was developed in the second part of **chapter 3**. This three-step labeling consists of three labeling steps: first step is accomplished by modifying all bioorthogonal groups with Alexa Fluor 488 in the ccHc reaction, the second step is executed by applying the anti-Alexa Fluor 488 antibody and the final third step by applying protein A conjugated to Alexa Fluor 647 (Figure 3). The steric bulk of the antibody minimizes intracellular labeling to allow imaging of the surface pool of the bioorthogonal epitope.

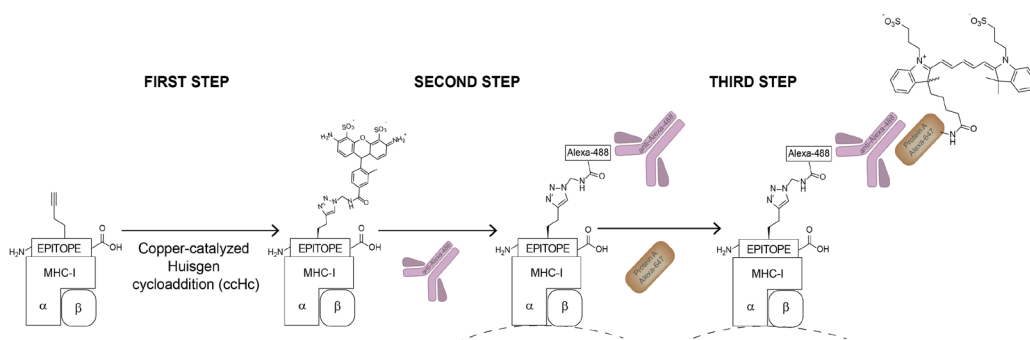


Figure 3. Schematic representation of the three-step labeling.

This three step labeling protocol was used to perform a super resolution (stochastic optical resolution microscopy or STORM^[5]) imaging experiments of peptides in MHC-complexes. The preliminary results of the STORM imaging of bioorthogonal epitopes using the three-step labeling revealed a potential to localize and later quantify the epitopes on the cell surface. In the future, this approach could be applied to quantify the number of epitopes per cell and – once T cells against bioorthogonal groups become available – to quantify the correlation of surface peptide quantity to T cell response strength.

Chapter 4 describes the exploration of bioorthogonal chemistry to the study of longer antigens that – unlike the minimal epitopes of chapter 3 – do require intracellular processing prior to their presentation. A series of bioorthogonal synthetic long peptides (SLPs) were designed and the use of click chemistry to study their uptake, routing and surface presentation was assessed. The labeling and imaging of a herpes virus vaccine candidate HSV-Gp₄₈₈₋₅₀₅-Pg-7 with Alexa Fluor-488 azide revealed a patchy pattern of fluorescent signal on the cell membrane indicating that the peptide aggregated and that these aggregates are either slowly internalized or not at all. This was confirmed using correlative-light electron microscopy (CLEM)^[6] of the bioorthogonally introduced fluorophores. Due that reason to selectively label

epitopes on the cell surface, the switch was made to a more soluble SLP that requires proteasome-dependent processing on both the *N* and *C*-terminus (HSV-Gp₄₈₈₋₅₀₅A₅K-Pg-7)^[7].

The rate of uptake of this HSV-Gp₄₈₈₋₅₀₅A₅K-Pg-7 was assessed using click chemistry and it was attempted to use the three-step labeling described in chapter 3 to quantify the cell surface appearance of the processed epitope. The quantification turned out to be troublesome. The weak extracellular signal (due to only a small fraction of the bioorthogonal SLP reaching the surface for MHC-loading and instead mostly remaining in endo-lysosomal^[8] like compartments) prevented robust labeling. Even the use of the three-step labeling approach did not give enough signal over background.

In summary, the use of the three-step labeling in combination with a Cu(I)-catalyzed Huisgen cycloaddition reaction for the bioorthogonal long peptides allowed for imaging of the cellular uptake however the cell surface labeling still requires further research.

A possible alternative approach to achieve this would require live-cell compatible chemistry and/or a signal enhancement step. For example one alternative could be the recently reported 'DNA-click-PAINT' method^[9]. Here an azide or tetrazine moiety can be attached to a single-stranded DNA and used in a click reaction (ccHc or IEDDA). A complementary DNA strand equipped with a fluorophore can be annealed to the docking DNA strand. This approach has as the advantage that the fluorophore is more water soluble reducing background signal. Mismatching of the two strands can also be used to induce fluorophore blinking (Figure 4), where a correctly chosen DNA strand can give on/off rates optimal for STORM imaging^[10].

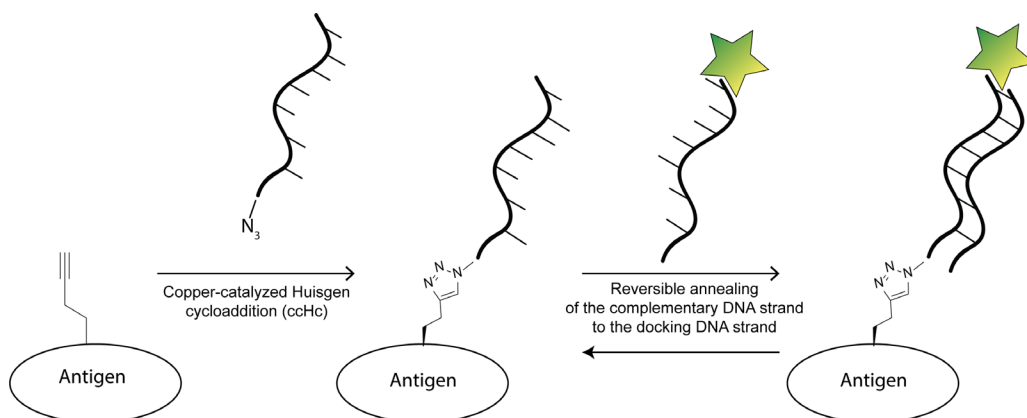


Figure 4. Schematic representation of the 'DNA-click-PAINT' method. The fluorescently labeled complementary DNA strand (imager strand) anneals to the 'docking' DNA strand inducing fluorophore blinking needed for high-precision single-molecule localization.

However, still only a single fluorophore per bioorthogonal handle is introduced which can impinge on the signal to noise ratios of this approach. To increase the signal-to-noise ratios a technique called rolling circle amplification (RCA) could be applied^[11]. RCA is an efficient isothermal enzymatic process conducted at a constant temperature where a short DNA or RNA primer in the presence of fluorophore conjugated nucleoside triphosphates containing deoxyribose (dNTPs), is amplified using a circular DNA template and DNA or RNA polymerases to form a long single stranded DNA or RNA containing multiple fluorophores^[12]. Antigens functionalized with complementary DNA sequences and equipped with the fluorophore could be potentially visualized by docking to the long single stranded DNA at various locations resulting in a presence of multiple fluorophores and thus an enhanced signal-to-noise^[13].

Chapter 5 focused on different uses of bioorthogonal antigens. During the work leading to chapters 3 and 4, it was discovered that the 2-3 atom alterations of the epitope obliterated recognition by the cognate T cells. This led to the development of a new method that allowed for chemical control over T cell activation^[14]. The chemical deprotection strategy was used to study the activation of cytotoxic T cells by antigen presenting cells: by substituting the key lysine in the H2-K^b-restricted epitope SIINFEKL for an azidonorleucine, the peptide was rendered unresponsive to its cognate T cell. By then performing a Staudinger reduction^[15] (from the azidonorleucine back to a lysine) on the surface of the cell, more than 80% of the original T cell reactivity was recovered^[16] (Figure 5A).

The chemical uncaging strategy worked well *in vitro*, but the required reaction conditions were not compatible with *in vivo* use. In the future the IEDDA-based elimination reaction could serve as an *in vivo*-compatible deprotection reaction. In this reaction a strained alpha-substituted trans-cyclooctene^[17] (TCO)-modified antigen reacts with certain tetrazines to result in the elimination of the alpha-positioned substitute.^[17-18] This reaction has been used *in vivo* for the release of drugs from antibodies^[19] and the unblocking of enzyme active sites^[20]. In the context of these experiments, it would allow for deprotection and chemical control over T cell activation *in vivo* (Figure 5B), which in turn would allow the study of T cell activation kinetics and the role they have on their activation.

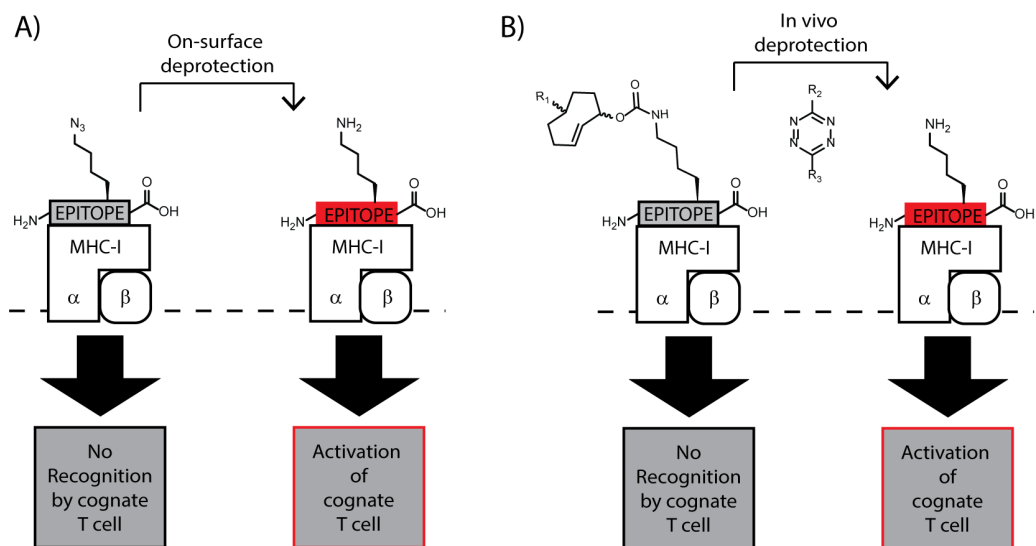


Figure 5. A) Schematic representation of the on-surface deprotection using Staudinger reduction reaction. B) Proposed schematic representation of the in vivo deprotection using trans-cyclooctene-modified epitope and tetrazine as a reaction partner in inverse electron-demand Diels-Alder reaction.

In conclusion, the results from this thesis show that bioorthogonal antigens exhibit potential as reagents for the study of antigen cross-presentation. However, limitations with regards to signal-to-noise and the use of metal-based catalysts need to be addressed to truly allow them to fulfill their potential.

References

- [1] A. Porgador, J. W. Yewdell, Y. Deng, J. R. Bennink, R. N. Germain, *Immunity* **1997**, *6*, 715-726.
- [2] aH. G. Ljunggren, N. J. Stam, C. Ohlen, J. J. Neefjes, P. Hoglund, M. T. Heemels, J. Bastin, T. N. Schumacher, A. Townsend, K. Karre, et al., *Nature* **1990**, *346*, 476-480; bM. C. Feltkamp, H. L. Smits, M. P. Vierboom, R. P. Minnaar, B. M. de Jongh, J. W. Drijfhout, J. ter Schegget, C. J. Melief, W. M. Kast, *Eur J Immunol* **1993**, *23*, 2242-2249.
- [3] aC. R. Bertozzi, *Acc Chem Res* **2011**, *44*, 651-653; bJ. Li, P. R. Chen, *Nat Chem Biol* **2016**, *12*, 129-137.
- [4] K. Lang, L. Davis, J. Torres-Kolbus, C. Chou, A. Deiters, J. W. Chin, *Nat Chem* **2012**, *4*, 298-304.
- [5] D. van der Zwaag, N. Vanparijs, S. Wijnands, R. De Rycke, B. G. De Geest, L. Albertazzi, *ACS Appl Mater Interfaces* **2016**, *8*, 6391-6399.
- [6] D. M. van Elsland, E. Bos, W. de Boer, H. S. Overkleeft, A. J. Koster, S. I. van Kasteren, *Chemical Science* **2016**, *7*, 752-758.
- [7] S. Khan, M. S. Bijker, J. J. Weterings, H. J. Tanke, G. J. Adema, T. van Hall, J. W. Drijfhout, C. J. Melief, H. S. Overkleeft, G. A. van der Marel, D. V. Filippov, S. H. van der Burg, F. Ossendorp, *J Biol Chem* **2007**, *282*, 21145-21159.
- [8] aO. P. Joffre, E. Segura, A. Savina, S. Amigorena, *Nat Rev Immunol* **2012**, *12*, 557-569; bJ. W. Yewdell, E. Reits, J. Neefjes, *Nat Rev Immunol* **2003**, *3*, 952-961.
- [9] aR. Jungmann, M. S. Avendano, J. B. Woehrstein, M. Dai, W. M. Shih, P. Yin, *Nat Methods* **2014**, *11*, 313-318; bI. Nikic, G. Estrada Girona, J. H. Kang, G. Paci, S. Mikhaleva, C. Koehler, N. V. Shymanska, C. Ventura Santos, D. Spitz, E. A. Lemke, *Angew Chem Int Ed Engl* **2016**, *55*, 16172-16176.
- [10] J. Enderlein, *Nat Nanotechnol* **2016**, *11*, 737-738.
- [11] C. M. Clausson, L. Arngarden, O. Ishaq, A. Klaesson, M. Kuhnemund, K. Grannas, B. Koos, X. Qian, P. Ranefall, T. Krzywkowski, H. Brismar, M. Nilsson, C. Wahlby, O. Soderberg, *Sci Rep* **2015**, *5*, 12317.
- [12] aM. Nilsson, M. Gullberg, F. Dahl, K. Szuhai, A. K. Raap, *Nucleic Acids Res* **2002**, *30*, e66; bM. Kuhnemund, I. Hernandez-Neuta, M. I. Sharif, M. Cornaglia, M. A. Gijs, M. Nilsson, *Nucleic Acids Res* **2017**.
- [13] aM. M. Ali, F. Li, Z. Zhang, K. Zhang, D. K. Kang, J. A. Ankrum, X. C. Le, W. Zhao, *Chem Soc Rev* **2014**, *43*, 3324-3341; bX. Zhang, R. Li, Y. Chen, S. Zhang, W. Wang, F. Li, *Chemical Science* **2016**, *7*, 6182-6189.
- [14] L. Schmitt, R. Tampe, *Chembiochem* **2000**, *1*, 16-35.
- [15] aH. Staudinger, J. Meyer, *Helvetica Chimica Acta* **1919**, *2*, 635-646; bY. G. Gololobov, L. F. Kasukhin, *Tetrahedron* **1992**, *48*, 1353-1406.
- [16] J. B. Pawlak, G. P. Gentile, T. J. Ruckwardt, J. S. Bremmers, N. J. Meeuwenoord, F. A. Ossendorp, H. S. Overkleeft, D. V. Filippov, S. I. van Kasteren, *Angewandte Chemie (International ed. in English)* **2015**, *54*, 5628-5631.
- [17] M. L. Blackman, M. Royzen, J. M. Fox, *J Am Chem Soc* **2008**, *130*, 13518-13519.
- [18] N. K. Devaraj, R. Weissleder, S. A. Hilderbrand, *Bioconjugate Chemistry* **2008**, *19*, 2297-2299.
- [19] R. Rossin, S. M. van Duijnhoven, W. Ten Hoeve, H. M. Janssen, L. H. Kleijn, F. J. Hoeben, R. M. Versteegen, M. S. Robillard, *Bioconjug Chem* **2016**, *27*, 1697-1706.
- [20] G. Zhang, J. Li, R. Xie, X. Fan, Y. Liu, S. Zheng, Y. Ge, P. R. Chen, *ACS Central Science* **2016**, *2*, 325-331.

Bioortogonalne Antygeny

Badania opisane w tej pracy wykorzystują bioortogonalną chemię jako narzędzie do badania krzyżowej prezentacji antygeny. Dalsze zrozumienie tego procesu ma zasadnicze znaczenie, ponieważ jest to główny mechanizm wywołujący specyficzną cytotoksyczną odpowiedź komórek zwanych limfocyty T, niezbędną do usunięcia raka i patogennych infekcji, jak również w szczepionkach z antygenami białka, gdyż głównym celem jest zastosowanie tej wiedzy do opracowywania nowych peptydów do szczepionek przeciwrakowych. Proces prezentacji krzyżowej antygeny jest głównym tematem opisanym w niniejszej pracy. Powyższy proces ma miejsce gdy wirusy, bakterie lub komórki rakowe są pochłonięte, następnie przetworzone i ich fragmenty (peptydy) są prezentowane przez komórki prezentujące antygen (APC), głównie dendrytyczne, na cząsteczkach głównego układu zgodności tkankowej (MHC-I). Taki kompleks MHC klasy I z peptydem może być rozpoznany przez limfocyt T zwany $CD8^+$. Gdy taki kompleks zostanie rozpoznany jako obcy dla organizmu, $CD8^+$ T limfocyty są zdolne do wyeliminowania komórek posiadających taki kompleks. W **rozdziale 1** opisano ogólne zasady przetwarzania i prezentacji antygeny na cząsteczkach głównego układu zgodności tkankowej (MHC-I, -II i prezentacji krzyżowej). **Rozdział 2** przedstawia przegląd różnych molekularnych metod do badania pochłaniania, przetwarzania i prezentacji antygeny przez komórki prezentujące antygen na cząsteczkach MHC-I. Kilka przykładów obecnych metod zostało opisanych szczegółowo wraz z ich ograniczeniami i potencjalnym zastosowaniem antygenów bioortogonalnych jako nowych narzędzi do badania procesu prezentacji krzyżowej.

Wstępny rozwój nowej strategii do ilościowego oznaczania specyficznych kompleksów peptydowo-MHC-I (pMHC-I) na powierzchni komórkowej przy użyciu bioortogonalnej chemii został opisany w **rozdziale 3**. Biblioteka peptydów zawierających różne uchwyty bioortogonalne (azydki i alkyny) w obrębie epitopu (fragment antygeny łączący się bezpośrednio z receptorem limfocyty T) została zsyntetyzowana. Stabilność tych zmodyfikowanych peptydów jak i wiązanie się ich z MHC-I kompleksami została zoptymalizowana używając linii komórkowej RMA-S. W celu uzyskania najskuteczniejszej reakcji bioortogonalnej ligacji, testowano i oceniono różne typy reakcji "kliknięcia" (ang. "click"). Ustalono najbardziej optymalny rodzaj fluoroforu i

warunki ligacji bioortogonalnej. Wymóg dotyczący najbardziej efektywnego oznaczania ilościowego epitopu polega na modyfikacji alkinu w pozycjach dostępnych dla rozpuszczalnika w obrębie epitopów, stosując sondę CalFluor-488 w połączeniu z reakcją cykloaddycji Huisgena katalizowaną przez Cu (I) (ang. ccHc reaction). Głównym ograniczeniem tego podejścia jest wymóg miedzi w reakcji ccHc. Alternatywą dla tego podejścia może być zastosowanie reakcji kliknięcia nie wymagających katalizy. Na przykład, retro reakcja Dielsa-Aldera (IEDDA) pomiędzy cyklopropenem i tetrazyną nie wymaga stosowania miedzi i może zasadniczo umożliwić oznaczanie pMHC-I *in vivo*. Jednak reaktywność tej reakcji pod względem stosunku sygnału do szumu nie została w pełni zbadana w systemie tak rygorystycznym, jak krzyżowa prezentacja antygeny. Przy badaniu procesu przetwarzania i prezentacji antygeny, techniki, które mogą selektywnie oznaczać antygeny na powierzchni komórki byłyby bardzo cenne. Stąd taka metoda została opracowana na podstawie trzyetapowej procedury znakowania. Aby obejść przepuszczalność komórkową małych cząsteczek (spowodowanej obecnością miedzi), w drugiej części **rozdziału 3** opracowano trzyetapowe podejście do selektywnego znakowania antygenów na powierzchni komórki. To trzyetapowe oznakowanie składa się z trzech etapów: pierwszy krok można osiągnąć modyfikując wszystkie znajdujące się w antygenie grupy bioortogonalne z Alexa Fluor 488 w reakcji ccHc, drugi etap przeprowadza się stosując przeciwciało anti-Alexa Fluor 488 i końcowy trzeci etap, stosując białko A skoniugowane z Alexa Fluor 647. Steryczna objętość przeciwciała minimalizuje wewnątrzkomórkowe oznakowanie i pozwala umożliwić oznakowanie puli epitopu bioortogonalnego na powierzchni komórki. Ten trzyetapowy protokół znakowania został użyty do wykonania wysokorozdzielczych obrazów peptydów w kompleksach MHC na powierzchni komórki przy użyciu mikroskopii stochastycznej rekonstrukcji optycznej (ang. STORM). Wstępne wyniki obrazowania epitopów bioortogonalnych metodą STORM przy użyciu trzyetapowej procedury ujawniły potencjał do zlokalizowania i późniejszego oznaczenia ilościowego tych epitopów na powierzchni komórki. W przyszłości takie podejście można zastosować do oznaczenia ilości epitopów przypadających na komórkę, a kiedy tylko limfocyty T przeciwko grupom bioortogonalnym staną się dostępne - do ilościowego określania korelacji ilościowej peptydu powierzchniowego do siły odpowiedzi limfocytów T.

Rozdział 4 opisuje zastosowanie bioortogonalnej chemii w badaniach dłuższych antygenów, które w przeciwieństwie do minimalnych epitopów z rozdziału 3 wymagają przetwarzania wewnątrzkomórkowego przed ich prezentacją. Stąd zaprojektowano serię bioortogonalnych syntetycznych długich peptydów (ang. SLPs) i wykorzystano chemię typu "click" w celu zbadania ich pochłaniania, przetwarzania i prezentacji na powierzchni komórki. Oznaczanie i obrazowanie kandydata na

szczepionkę przeciwko wirusowi opryszczki, peptydu HSV-Gp₄₈₈₋₅₀₅-Pg-7 z azydkiem Alexa Fluor-488 wykazało niejednorodny wzór sygnału fluorescencyjnego na błonie komórkowej wskazujący, że peptyd agreguje się i że te agregaty są albo powoli albo wcale nie internalizowane przez komórki. Potwierdzono to stosując korelacyjną mikroskopię świetlną-elektronową (ang. CLEM) na bioortogonalnie wprowadzonych fluoroforach. Z tego względu aby selektywnie oznaczyć epitopy na powierzchni komórek, postanowiono zastosować bardziej rozpuszczalny SLP, który wymaga przetwarzania zależnego od proteasomu zarówno na końcu jak i początku peptydu (HSV-Gp₄₈₈₋₅₀₅A5K-Pg-7).

Szybkość prezentacji tego HSV-Gp₄₈₈₋₅₀₅A5K-Pg-7 została oceniona za pomocą chemii "kliknięcia" i stosując trzyetapowe oznakowanie opisane w rozdziale 3 w celu ilościowego określenia przetworzonego epitopu na powierzchni komórki. Kwantyfikacja jednak okazała się kłopotliwa. Słaby sygnał na powierzchni komórki (spowodowany niewielką częścią SLP docierającą do powierzchni w celu załadunku na MHC, a zamiast tego głównie pozostającą w częściach wewnątrzkomórkowych) zapobiegł silnemu oznakowaniu. Nawet użycie podejścia opartego na trzech etapach nie dało wystarczającego sygnału do szumu.

Podsumowując, zastosowanie trzyetapowego znakowania w połączeniu z reakcją cycoaddycji Huisgena katalizowanej przez Cu (I) na bioortogonalnych długich peptydach pozwoliło na obrazowanie wewnątrzkomórkowe, ale oznakowanie peptydów na powierzchni komórek nadal wymaga dalszych badań.

Rozdział 5 dotyczył różnych zastosowań antygenów bioortogonalnych. Podczas prac prowadzących do rozdziałów 3 i 4, odkryto, że zmiany 2-3 atomów epitopu zacierają rozpoznawanie przez specyficzne limfocyty T. Doprowadziło to do opracowania nowej metody pozwalającej na chemiczną kontrolę nad aktywacją limfocytów T. Strategię odbezpieczenia chemicznego zastosowano do badania aktywacji cytotoksycznych limfocytów T przez komórki prezentujące antygen: przez zastąpienie kluczowej lizyny w epitopie SIINFEKL na azydo-norleucynę, cytotoksyczna reakcja rozpoznania peptydu na powierzchni komórek dendrytycznych przez komórki T została zahamowana. Następnie przeprowadzając redukcję Staudingera (z azydo-norleucyny z powrotem do lizyny) na powierzchni komórki, odzyskano ponad 80% pierwotnej reaktywności limfocytów T.

Ostatni **rozdział 6** przedstawia podsumowanie tej tezy oraz przyszłe zastosowania, strategie i wskazówki dotyczące obrazowania (wizualizacji) całego procesu prezentacji krzyżowej antygeny.

List of Publications

- 1. Trans-cyclooctene-modified epitopes allow chemical control over T cell activation *in vivo*.** van der Gracht A.M.F., de Geus M.A.R., Camps M.G., Ruckwardt T.J., Bremmers J., Maurits E.J., Pawlak J.B., Posthoorn M.M., Bongers K.M., Filippov D.V., Overkleef H.S., Robillard M.S., Ossendorp F.A., van Kasteren S.I. **2017**, *Manuscript submitted*.
- 2. Antigen processing and cross-presentation.**
Pawlak J.B., van Kasteren S.I. *eLS*. **2017**, *in press*.
- 3. Correlative light and electron microscopy reveals discrepancy between gold and fluorescence labeling.**
van Elsland D.M., Bos E., Pawlak J.B., Overkleef H.S., van Kasteren S.I., Koster A.J. *J. Microsc.* **2017**, 267(3):309-317.
- 4. The optimization of bioorthogonal epitope ligation within MHC-I complexes.**
Pawlak J.B., Hos B.J., van de Graaff M.J., Megantari O.A., Meeuwenoord N., Overkleef H.S., Filippov D.V., Ossendorp F.A., van Kasteren S.I. *ACS Chem. Biol.* **2016**, 11(11):3172-3178.
- 5. Bioorthogonal deprotection on the dendritic cell surface for chemical control of antigen cross-presentation.**
Pawlak, J.B., Gential G.P., Ruckwardt T.J., Bremmers J.S., Meeuwenoord N.J., Ossendorp F.A., Overkleef H.S., Filippov D.V., van Kasteren S.I. *Angew. Chem. Int. Ed. Engl. Hot Paper*. **2015**, 54(19):5628-31.

Curriculum Vitae

English

Joanna B. Pawlak was born on January 24th 1983 in Olsztyn, Poland. She obtained her high school diploma at the III lyceum ogólnokształcące in Olsztyn (major in Life Science) in 2002 and moved to the Netherlands in 2003 where she subsequently started with the Nederlands als tweede Taal (Dutch as a Second Language) course at the University of Amsterdam (UvA). In 2005 she obtained her NT2 diploma and then started with her bachelor's program in Biomedical Sciences at the University of Amsterdam, quickly followed by the master's program in Biomedical Sciences (track oncology) at the same university. During her master's program, she performed two major internships. The first at the Academic Medical Center (AMC) in Amsterdam in the group of Prof. J.P. Medema – part of the Center of Experimental and Molecular Medicine (CEMM). The research performed at the AMC aimed to determine what properties were responsible for making stem cells resistant to radiotherapy. Her second internship took place at the Netherlands Cancer Institute (NKI) in the group of Prof. J. Neefjes then a member of the cell biology division. The research performed at the NKI under the supervision of Dr. Ilana Berlin aimed to study the deubiquitinating enzyme AMSH and its function in endocytosis. Joanna obtained her master's degree in 2012 and started with her PhD in the same year under the supervision of Prof. dr. H.S. Overkleeft and Dr. S.I. van Kasteren in the Bio-organic group at the Leiden University. Part of the research described in her thesis was conducted at the Leiden University Medical Center in the Immunohematology and blood transfusion group of Prof. dr. F.A. Ossendrop and at the Institute for Bioengineering of Catalonia (IBEC) in the Nanoscopy for nanomedicine group of Dr. L. Albertazzi in Spain. Posters as part of her PhD research were presented at various national and international conferences. Oral presentations were given at the Leiden Chemical Biology departmental lecture (2015), Dutch Peptide Symposium (Nijmegen, the Netherlands, 2015), CHAINS (Veldhoven, the Netherlands, 2015) and at the American Association of Immunologists (AAI) annual meeting (Seattle, WA, USA, 2016) and was awarded with the Trainee Abstract Award.

In April, 2017 she was awarded the NWO Rubicon grant and in the fall will start her postdoctoral research as a Rubicon fellow in the group of Prof. dr. P. Cresswell at the Yale University School of Medicine, USA.

Curriculum Vitae

Polish

Joanna B. Pawlak urodziła się 24-tego stycznia 1983 roku w Olsztynie, Polsce. Maturę uzyskała w III liceum ogólnokształcącym w Olsztynie (o profilu biologiczno-chemicznym) w 2002 roku. W 2003 roku przeniosiła się do Holandii, gdzie następnie rozpoczęła kurs języka holenderskiego na Uniwersytecie w Amsterdamie (UvA). W 2005 roku zdała egzamin państwowy z języka holenderskiego a następnie rozpoczęła program licencjacki - Biomedycyna (Biomedical Sciences) na Uniwersytecie w Amsterdamie, a później program magisterski (Biomedycyna ze specjalizacją w onkologii) na tym samym uniwersytecie. Podczas programu magisterskiego przeprowadziła dwie główne praktyki. Pierwsza z nich miała miejsce w Akademickim Centrum Medycznym (AMC) w Amsterdamie w grupie Prof. J.P. Medema na oddziale Centrum Medycyny Doświadczalnej i Molekularnej (CEMM). Badania przeprowadzone w AMC miały na celu ustalenie, jakie właściwości są odpowiedzialne za odporność komórek macierzystych na radioterapię. Jej drugi staż odbył się w Holenderskim Centrum Raka (NKI) w grupie Prof. J. Neefjes wtedy członka oddziału biologii komórki. Badania przeprowadzone w NKI odbyły się pod opieką Dr. Ilany Berlin i ich celem było zbadanie enzymu AMSH i jego funkcji w endocytozie. Joanna zdobyła tytuł magistra w 2012 roku i zaczęła studia doktoranckie w tym samym roku pod opieką Prof. H.S. Overkleeft i Dr. S.I. van Kasteren w grupie Bio-organicznej na Uniwersytecie w Leiden. Podczas badań doktoranckich uzyskała dyplom umożliwiający pracę ze zwierzętami laboratoryjnymi (laboratory animal handling diploma) na Uniwersyteckim Centrum Medycznym (LUMC) w Leiden w 2013 roku. Część badań opisanych w niniejszej pracy doktoranckiej zostały przeprowadzone w LUMC w grupie Immunohematologii i transfuzji krwi u Prof. F.A. Ossendorp oraz w Katalońskim Instytucie Bio-inżynierii (IBEC) w grupie Dr. L. Albertazzi (Nanosocopia dla nanomedycyny) w Barcelonie, Hiszpanii. Plakaty w ramach badań doktoranckich były prezentowane na wielu konferencjach krajowych i międzynarodowych. Prezentacje ustne zostały podane na biologiczno-chemicznym wykładzie oddziałowym w Leiden (2015), holenderskim Peptide Symposium (Nijmegen, Holandia, 2015), CHAINS (Veldhoven, Holandia, 2015) oraz na corocznym spotkaniu American Association of Immunologists (AAI) (Seattle, Waszyngton, USA, 2016) gdzie Joanna została wyróżniona nagrodą Trainee Abstract Award.

W kwietniu 2017 roku Joanna została nagrodzona grantem Rubicon i w jesieni tego samego roku rozpocznie habilitację w grupie Prof. P. Cresswell na wydziale immunobiologii na Uniwersytecie Medycznym Yale, w Stanach Zjednoczonych Ameryki.